

Use of Piperazine Ligands for Bleaching and Epoxidation Catalysis

A thesis submitted for the degree of Doctor of Philosophy

Farid Uddin

© Farid Uddin, 2010. The copyright of this thesis rests with the author and no quotation from it or information derived from it may be published without the prior written consent of the author.

Table of Contents	Page
Declaration	5
Acknowledgements	6
Abbreviations	7
Abstract	8
Chapter 1. Introduction	9
1.1 Overview	9
1.2 Bleach activators	11
1.3 Bleach catalysts	12
1.4 Mechanism of bleaching using a dinuclear manganese complex of the ligand 1,4,7-trimethyl-1,4,7-triazacyclononane	14
1.5 Alkene epoxidation using manganese complexes of 1,4,7-triazacyclononane in aqueous solution	16
1.6 Alkene epoxidation using manganese complexes of 1,4,7-triazacyclononane in organic media	17
1.7 Additives in catalytic epoxidation using manganese complexes of 1,4,7- triazacyclononane	22
1.8 Oxidation of alcohols using manganese complexes of 1,4,7-trimethyl-1,4,7- triazacyclononane	33
1.9 Summary of the proposed mechanistic details involving manganese complexes of 1,4,7-triazacyclononane in alkene epoxidation	36
1.10 Other manganese bleaching and epoxidation catalysts	41
1.11 Manganese Schiff-base complexes in bleaching	41
1.12 Manganese Schiff-base complexes in alkene epoxidation	42
1.13 Manganese cross-bridged macrocyclic complexes in bleaching	45
1.14 Manganese complexes of 2,2':6,2' terpyridine in bleaching	46
1.15 Manganese complexes of polypyridineamine ligands in bleaching	46
1.16 Manganese salts as bleaching catalysts	47
1.17 Manganese salts in alkene epoxidation	47
1.18 Ligand design	50
1.19 Conclusions	54

1.20	References	54
Chapter 2. Ligand Synthesis		58
2.1	General remarks	58
2.2	Synthesis of ligand 62	60
2.3	Synthesis of 67 , 68 and 69	65
2.4	Synthesis of compound 60	68
2.5	Synthesis of compound 63	70
2.6	Synthesis of compound 61	75
2.7	Synthesis of compound 65	79
2.8	Conclusions	81
2.9	References	82
Chapter 3. Results and Discussion		84
3.1	General remarks	84
3.2	The primary screening test	84
3.3	Initial stain removal test (Wash-test)	88
3.4	Investigation into the catalytic activity of cobalt complexes of ligands 62 and 67	89
3.5	A complex of ligand 67	91
3.6	Summary for a cobalt of complex ligand 67	93
3.7	A UV-Vis study of complex 114 and the 1:1 complex of ligand 62 with CoCl ₂ .6H ₂ O	94
3.8	Cobalt complexes of ligand 62	97
3.9	Magnetic moment measurements 114 and 115	100
3.10	Summary of the catalytic bleaching results	101
3.11	Epoxidation catalysis	102
3.12	Epoxidation using complex 114 and 115	103
3.13	Epoxidation involving manganese systems of ligands incorporating the piperazine backbone	104
3.14	The nature of the piperazine ligands involved in alkene epoxidation	108
3.15	Conclusions	110

3.16	References	110
	Chapter 4. Experimental	112
	Appendix 1	145
	Appendix 2	151
	Appendix 3	152

Declaration

I certify that this thesis, and the research to which it refers, are the product of my own work, and that any ideas or quotations from the work of other people, published or otherwise, are fully acknowledged in accordance with the standard referencing practices of the discipline. I acknowledge the helpful guidance and support of my supervisor, Prof. Michael Watkinson.

Acknowledgements

I must take this opportunity to extend my gratitude to those who have contributed to making this course of study possible and a success. First of all, I would like to thank Prof. Michael Watkinson for taking the brave step of accepting me as his student, for his unwavering support and careful guidance.

I extend my gratitude to all the occupants of the JP building (past and present). I am sure that without the friendship shown and support given by many individuals (you know who you are!) in my four years there, my experience at QMUL would not have been so enjoyable.

I would like to thank Majid Motevalli for carrying out X-ray crystallography measurements, solving the structures on my behalf and for taking the time to discuss the results. My thanks also go to Rory Wilson and those at Southampton (EPSRC Crystallographic Service) for their contribution. I must also thank Greg Coumbarides for his advice on carrying out NMR experiments. I also wish to thank the analysts at Swansea (EPSRC National Mass Spectrometry Service) for providing all my mass spectrometry data and those at the UCL department of chemistry who carried out elemental analysis on my behalf.

My thanks also go to Alan, Ian, Jalal, Janet, John and Trevor for their invaluable help. I also wish to thank all those at Warwick International Ltd. who I have worked with during my research.

I would like to thank all my family for their patience and continued support over the years.

Finally, I acknowledge the financial support from the EPSRC and my industrial sponsor, Warwick International Ltd.

Abbreviations

ATR = Attenuated Total Reflection

BOC = *tert*-Butyloxycarbonyl

CI = Chemical Ionisation

DIPEA = di-Isopropylethylamine

DMF = *N,N*-Dimethylformamide

DMSO = Dimethylsulfoxide

EI = Electron Ionisation

EPR = Electron Paramagnetic Resonance

eq. = Equivalents

e.s.ds. = Estimated Standard Deviations

ESI = Electrospray Ionisation

GC = Gas Chromatography

HATU = *O*-(7-Azabenzotriazol-1-yl)-*N,N,N',N'*-tetramethyluronium
hexafluorophosphate

HHPP = 2-Hydroxy-2-hydroperoxypropane

HOMO = Highest Occupied Molecular Orbital

HPLC = High Pressure Liquid Chromatography

LUMO = Lowest Unoccupied Molecular Orbital

MO = Molecular Orbital

MS = Mass Spectroscopy

NMR = Nuclear Magnetic Resonance

OTs = Toluenesulfonate

PBS = Sodium Perborate

TACN = 1,4,7-Triazacyclononane

TAED = Tetraacetylenediamine

TBHP = *t*-butyl hydroperoxide

TFA = Trifluoroacetic acid

TMTACN = 1,4,7-trimethyl-1,4,7-triazacyclononane

TON(s) = Turnover Number(s)

UV-Vis = Ultraviolet-Visible

wrt = With Respect To

Abstract

Following reports that the dinuclear manganese complex of the ligand 1, 4, 7-trimethyl-1, 4, 7-triazacyclononane (TMTACN) was a potent bleaching catalyst, its catalytic oxidative activity was thoroughly studied. Apart from its catalytic bleaching activity, it has shown to be a versatile catalyst in terms of its substrate scope. In bleaching, it still remains the benchmark with regards to its catalytic bleaching activity against which systems in development are compared.

Chapter one discusses the need for a bleaching catalyst in detergent formulations and the advantages it offers over existing technologies. Studies into the bleaching mechanism involving the manganese TMTACN system are then explored, followed by a description of its application in the oxidation of alkenes amongst other substrates. Other manganese based bleaching and epoxidation catalysts are considered briefly. This is followed by a discussion on ligand design for use in manganese and other first row transition metal based oxidation catalysts and the initially proposed ligand synthesis for this research.

Chapter two details the synthetic strategies employed in the synthesis of the planned ligands along with an evaluation of the effectiveness of these strategies. The structural features of a number of novel ligands and their precursors are then explored in terms of their single crystal X-ray structures which were obtained during this research.

Chapter three presents the most relevant results obtained during the course of this research with regards to the testing of the synthesised ligands and their efficacy in bleaching and epoxidation catalysis. A number of ligands demonstrated some activity in epoxidation catalysis using different manganese salts. These results are discussed in detail with an attempt to rationalise the observed catalytic activity with reference to the ligand structure and identity of the manganese salt utilised being made.

The final chapter provides the necessary details of the experimental work carried out along with supporting characterisation data for the materials prepared.

Chapter 1. Introduction

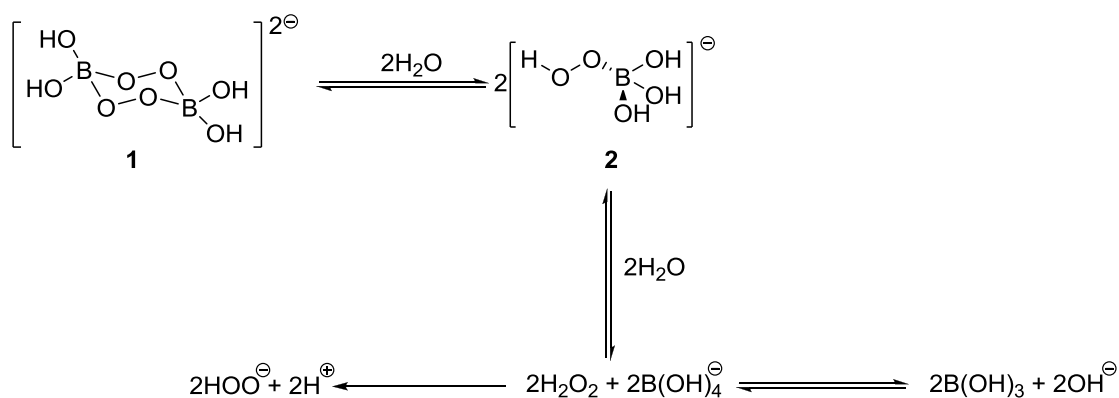
1.1 Overview

The colour of persistent stains which cannot be removed by the mechanical work done in any laundry process originates predominantly from conjugated π -bonding systems. Destructive oxidative processes can be used to remove such stains by partial or complete saturation of conjugated bonding systems, thus making the stain invisible. Another complementary effect of the oxidation process in stain removal is to increase the hydrophilic nature of stain molecules allowing them to be easily washed away in the effluent.

Solid forms of hydrogen peroxide, such as sodium perborate (PBS, $\text{NaBO}_3 \cdot n\text{H}_2\text{O}$, where $n = 1$ or 4) and sodium percarbonate, have been the oxidants of choice in many detergent formulations, due to their reduced environmental impact compared, for example, to sodium hypochlorite. Another obvious advantage of this solid form of hydrogen peroxide is that it can be included in solid detergent formulations. Also from a health and safety viewpoint, PBS offers relative stability compared to potentially explosive, aqueous solutions of hydrogen peroxide.

Crystalline PBS exists as a dimeric cyclic peroxodiborate salt **1**,¹ which under aqueous conditions, rapidly hydrolyses to form an equilibrium solution of peroxoborate species such as **2**, which then converts into hydrogen peroxide and tetrahydroxy borate anions (Scheme 1). Under the basic conditions of the laundry washing process, the hydrogen peroxide ($\text{p}K_{\text{a}} = 11.6$) thus formed is converted to the nucleophilic oxidant, the perhydroxyl anion.

However, the crucial drawback for PBS is in its requirement of temperatures above $60\text{ }^\circ\text{C}$ to be an effective oxidant. Such high temperature requirements make the laundry washing process a source of pollutants for the environment. This is partly to do with the high heat capacity of water (water has a relatively high specific heat capacity (c_p) of $4.180\text{ J g}^{-1}\text{ K}^{-1}$ ($25\text{ }^\circ\text{C}$)² compared to other liquids), resulting in energy intensive wash cycles in order to gain an acceptable level of cleanliness for domestic laundry.



Scheme 1. Formation of the perhydroxyl anion from PBS

Hydrogen peroxide, once released from PBS would be expected to be a potent oxidant based on its oxidation potential ($E^0 = 1.78 \text{ V (SHE)}$). However, for the majority of its applications, it requires activation owing to its kinetic inertness and methods for achieving this, such as Fenton's reagent,³ have been known for over a century. In terms of the bleaching process the physical parameters which become available for adjustment in order to activate hydrogen peroxide, become clear from equations **1** and **2**. By assuming both the oxidant and substrate (stain) are in solution, second order kinetics can be proposed⁴ where the rate of bleaching is given by equation **1**.

$$\text{Rate} = k[\text{oxidant}][\text{stain}] \qquad \qquad \qquad \text{Equation 1}$$

It can be seen from equation **1**, that the rate of the reaction can be increased with higher concentrations of both oxidant and substrate. However, increasing the concentration of the oxidant in the detergent formulation means higher costs; also cost would be further increased by factors linked to the resulting reduction in volume efficiency (*vide infra*). The Arrhenius equation (Equation **2**) shows the dependence of the rate constant (k) on temperature (T) and the activation energy (E_a) (also, A is a constant and R is the gas constant).

$$k = Ae^{-E_a/RT} \qquad \qquad \qquad \text{Equation 2}$$

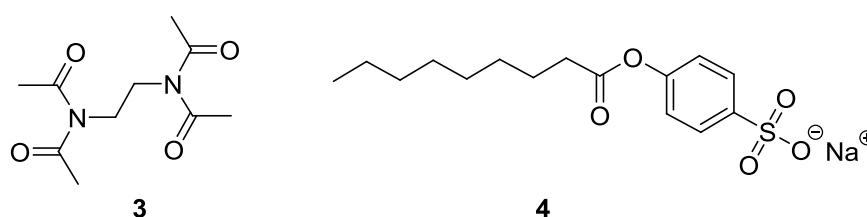
From equation **2**, it can be seen that increasing the wash temperature would result in a greater rate constant and a higher reaction rate, however, this is not an option due to the negative cost and environmental implications (*vide supra*). The only remaining option

in order to increase the reaction rate is to decrease the activation energy (E_a); this has been achieved by the use of bleach activators and catalysts.

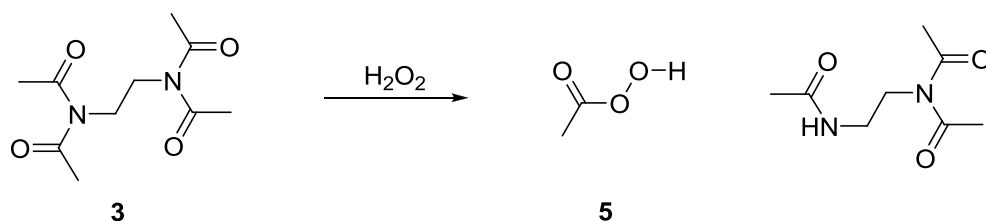
1.2 Bleach activators

The first breakthrough for hydrogen peroxide activation in the context of laundry bleaching came in the form of bleach activators such as tetraacetythylenediamine (TAED, **3**). Such activators have enjoyed commercial success as they are able to reduce the operating temperature for hydrogen peroxide and as a consequence reduce the detrimental environmental impact of heating water over 60 °C.

Bleach activators such as TAED and sodium nonanoyloxybenzenesulfonate (SNOBS, **4**) are able to reduce the operating temperature for hydrogen peroxide from >60 °C to between 40-60 °C. TAED is commonly used in Europe and SNOBS is largely utilised in the USA. SNOBS with its long alkyl chain is better able to interact with more hydrophobic stains which results in superior stain bleaching to TAED for such stains.



TAED is produced by the reaction of ethylenediamine with two equivalents of acetic acid forming the bis-amide, which is subsequently reacted with a further two equivalents of acetic anhydride to yield **3**.⁵ TAED reacts with hydrogen peroxide (Scheme 2) to form a peracid (**5**) which is able to react with stain substrates at lower temperatures.



Scheme 2. The formation of peracetic acid from TAED and hydrogen peroxide

The rate at which TAED is able to convert hydrogen peroxide (in the form of PBS) to its corresponding peracid is increased with the ratio of PBS:TAED. The rate of peracid formation is further increased with higher temperatures and pH. However, as peracid bleaching is optimal at a lower pH a compromise pH at which both processes are able to occur at a reasonable rate needs to be reached.⁵

The main drawback in the use of bleach activators is that it is required in at least stoichiometric amounts to the oxidant, adding to the volume and weight⁶ of the detergent formulation. This has negative cost implications stemming from transport and storage considerations. Despite this, by the early 1980s most European detergent formulations incorporated TAED.

1.3 Bleach catalysts

Further development in textile bleaching technology came in the form of the manganese complex (**6**) of the ligand 1,4,7-trimethyl-1,4,7-triazacyclononane (TMTACN, **7**), introduced by Unilever in one of its detergent formulations in 1994.⁷ The original claims included high bleaching activity of tea stains when **6** was used at 40 °C in combination with hydrogen peroxide. The tea stain bleaching activity was found to be pH dependent with the optimal being pH 9-11. Wine, fruit and curry stains were also bleached efficiently using hydrogen peroxide as the oxidant. This catalyst **6**, was later withdrawn due to massive fabric and dye damage it caused (Figure 1). Work towards effective bleach catalysts persists as this would have significant advantages over bleach activators *viz.* volume efficiency, reduced wash temperatures (20-40 °C) and increased atom economy; reducing costs in both a monetary and environmental sense.

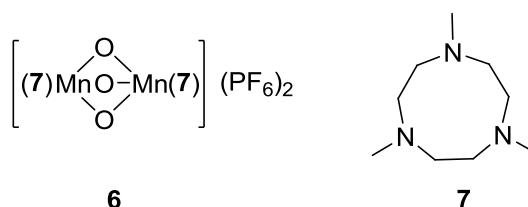




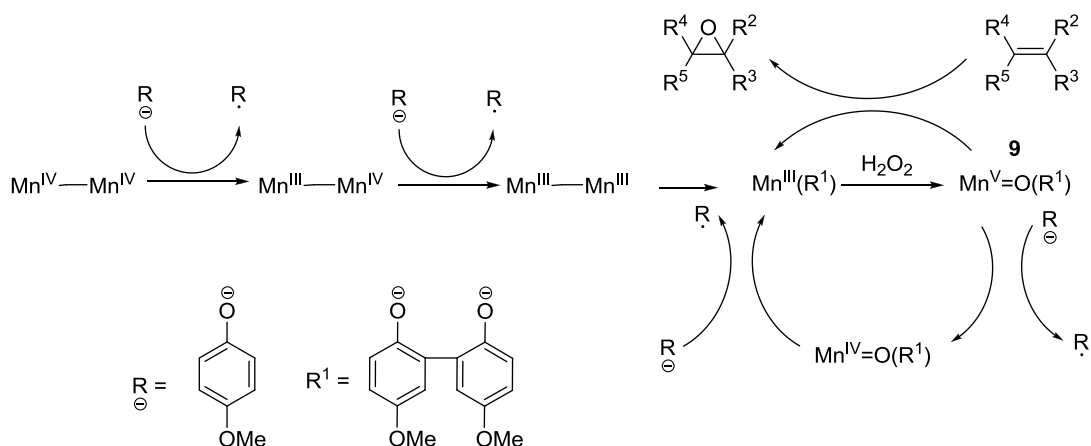
Figure 1. Marks & Spencer's Boxer Shorts (after and before 20 repeat washes at 50 °C)

Interest has focused on iron and manganese complexes as viable bleach catalysts due to their acceptability from an environmental and toxicological point of view. A major issue in catalyst development has been the specific requirements of the laundry process under which a catalyst must operate. The catalysts must be active at low temperatures, in aqueous media under alkaline conditions.⁸ In alkaline media, manganese and iron complexes have a propensity to form insoluble oxide and hydroxides. Furthermore, the complexes need to exhibit oxidative robustness throughout the wash cycle, as this is an inherently oxidising environment. The catalytic activity needs to be applicable to chemically varied stain substrates, yet selective enough to avoid unwanted dye and fabric damage.

The undesirable dye and fabric damage caused by catalyst **6** under the conditions of laundry washing has been speculated to result from the decomposition of the catalyst and subsequent deposition of manganese salts onto the fabric.⁹ Presumably such manganese species were able to cause dye and fabric damage over a number of wash cycles through non-selective oxidation processes.

1.4 Mechanism of bleaching using a dinuclear manganese complex of the ligand 1,4,7-trimethyl-1,4,7-triazacyclononane

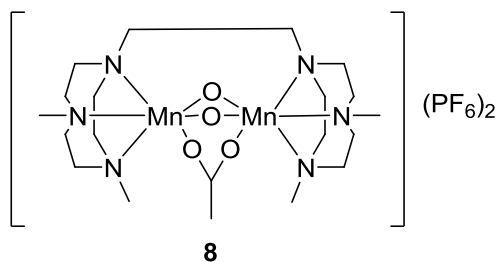
Stains derived from wine and fruit are complex mixtures of polyphenolic compounds. A consequence of studying the bleaching process with such substrates is extremely complicated.¹⁰ As a result, simpler compounds based on phenols and alkenes have been employed in order to study the reactivity of catalysts such as **6**. Extensive spectroscopic studies have been carried out in attempts to characterise the nature of the active catalytic species in solution. Catalyst **6** is stable in alkaline solution, however, in the presence of certain polyphenols such as catechol (a polyphenol used as a model for tea stains) the EPR silent $[\text{Mn}^{\text{IV}}_2(\mu\text{-O})_3(\mathbf{7})_2]^{2+}$ complex was suggested to take part in a 1 electron reduction from the phenolate ion producing a 16-line EPR signal consistent with a $\text{Mn}^{\text{III}}\text{Mn}^{\text{IV}}$ dinuclear core (Scheme 3).^{7, 11} The aforementioned single electron reduction was observed in both the presence and absence of hydrogen peroxide. The single electron reduction appeared to be necessary to labilise the stable $\text{Mn}^{\text{IV}}\text{Mn}^{\text{IV}}$ dinuclear core and was suggested to involve a single electron or a proton coupled electron transfer.



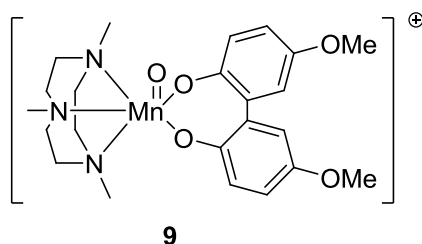
Scheme 3. Abridged version of the mechanism proposed by Lindsay Smith *et al.*^{11c}

Following this reduction of the dinuclear complex **6**, oxidation of manganese to a high valent species such as manganese(IV) or manganese(V) is generally supported, although the nuclearity of the active catalyst is in doubt. Both mononuclear and dinuclear species have been suggested. Hage⁷ suggested that mononuclear species are responsible for

catalytic bleaching involving **6** and other manganese complexes (*vide infra*) at pH < 9.5 and dinuclear species above this pH. This was partially based on the observation of superior stain bleaching using **6** at pH < 9.5 compared to the dinuclear complex **8**, and the ability of **6** to form mononuclear manganese(IV) species under such pH conditions. In addition, this was supported by the optimal bleaching ability of **8**, observed to occur above pH 9.5 and its apparent dinuclear structure persisting throughout the bleaching process.



Further support for a mononuclear manganese based oxidant was presented during studies relating to the oxidation of various phenolic substrates using catalyst **6** and hydrogen peroxide at pH 10. In the oxidation of 4-methoxyphenol, a mononuclear species consistent with [(2,2-bisphenolato)-(7)Mn^V=O]⁺ (**9**) was detected using ESI-MS along with its manganese(III) precursor which was thought to form **9** by oxidation using hydrogen peroxide (Scheme 3).^{11b, c} The same group have proposed another mononuclear Mn^V=O species when using catalyst **6** in the oxidation of azo-containing dyes.¹² The involvement of hydroxyl radicals in the oxidation mechanism was discounted as they were not detected using EPR spectroscopy.

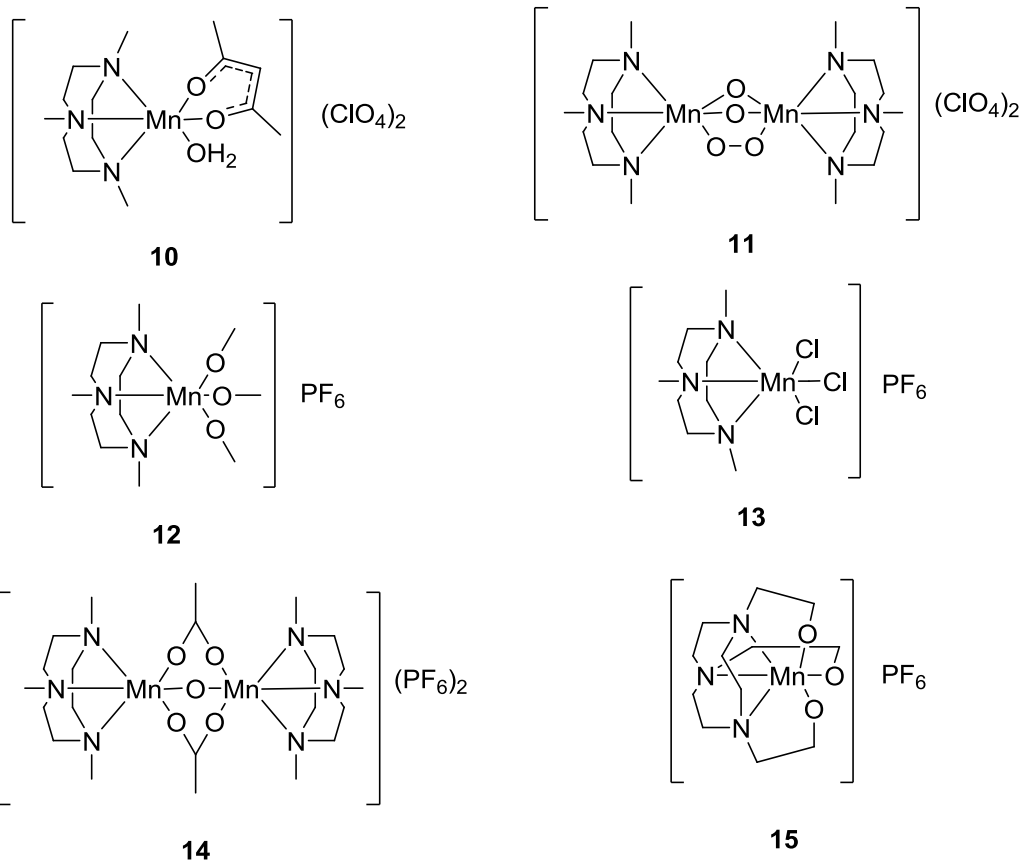


Contrary to this, other workers proposed that the hydroxyl radical was responsible for oxidation. They studied the oxidation of catechol using catalyst **6** and hydrogen peroxide in the presence and absence of mannitol and found that the degradation of the oxidised, quinone form of catechol to occur faster in the absence of mannitol than in its

presence.¹³ This was interpreted as the hydroxyl radical being trapped by mannitol, thus causing the proposed hydroxyl radical promoted degradation of the quinone form to become retarded compared to the degradation observed in its absence.

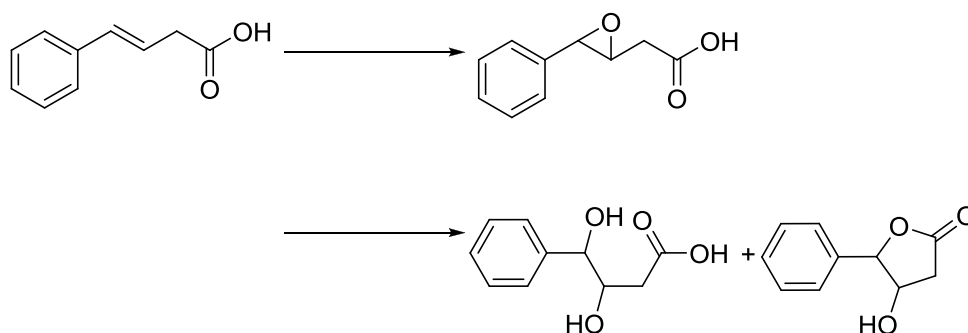
1.5 Alkene epoxidation using manganese complexes of 1,4,7-triazacyclononane in aqueous solution

Epoxidation of alkenes using catalyst **6** was reported along with its catalytic bleaching activity using hydrogen peroxide as the oxidant.⁷ In addition, other manganese complexes based on ligand **7** and derivatives (**8**, **10-15**) were discussed in relation to the catalytic oxidation of stains and alkenes. Epoxidation of 4-vinylbenzoic acid (in carbonate buffer, pH 8) and styrene (in methanol/ carbonate buffer, pH 9) was found to be catalysed by **6**, **8**, **12** (4-vinylbenzoic acid was not tested using catalyst **12**) and **15** using hydrogen peroxide as the oxidant. Almost quantitative conversions were observed for all of the systems. The rate of epoxidation was found to be optimal at pH 8 and that of bleaching was found to be optimal at pH 10, suggesting that the two processes follow different mechanisms. Also **15**, which was shown to be an effective epoxidation catalyst, was inactive in catalytic bleaching.



Furthermore, using mononuclear complex **15**, the same constant catalytic activity was found to be persistent for four consecutive additions of 4-vinylbenzoic acid. This showed the catalytic system was stable under the conditions used. Using catalyst **15**, all of the oxygen in the epoxide product was found to be ^{18}O labelled when $\text{H}_2^{18}\text{O}_2$ was used; this suggested the oxygen in the product was derived exclusively from hydrogen peroxide and not H_2O .

In another study, complex **12** was found to be catalytically active in the epoxidation of water soluble alkenes in aqueous media under mild conditions.¹⁴ The catalyst based on ligand **7** cleanly converted 4-vinylbenzoic acid to the epoxide using hydrogen peroxide (pH 9 at 25 °C). However, styrylacetic acid was oxidised to a mixture of products using the same conditions (Scheme 4).



Scheme 4. The conversion of styrylacetic acid to a mixture of oxidation products using hydrogen peroxide at pH 9

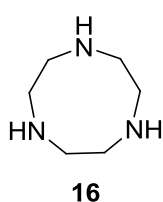
A 98% conversion was achieved for both substrates requiring 1.5 hours and 3 hours for 4-vinylbenzoic acid and styrylacetic acid respectively. The catalytic species was found to give a 12-fold enhancement in rate compared to hydrogen peroxide, with a catalyst loading of 1 mol%. Further, the catalyst stability was demonstrated by the addition of a second aliquot of substrate and oxidant, exhibiting TONs of up to 400.

1.6 Alkene epoxidation using manganese complexes of 1,4,7-triazacyclononane in organic media

The epoxidation systems described thus far required large amounts of hydrogen peroxide through its wasteful decomposition via catalase-like pathways and often

required oxidant to substrate ratios of 100:1. Apart from being undesirable from both an environmental and economic viewpoint, the resulting dilute conditions may potentially be hampering the conversion of less reactive alkenes. De Vos and Bein¹⁵ reported the use of an *in situ* preparation of a manganese catalyst of ligand **7**, which under specific reaction conditions, limited the hydrogen peroxide disproportionation and permitted the epoxidation of less reactive alkenes. The *in situ* preparation of a catalytic species was assumed on mixing together ligand **7** and a manganese(II) salt. The procedure entailed the gradual addition of a hydrogen peroxide solution to a mixture of alkene and the catalytic species which were dissolved in an organic solvent.

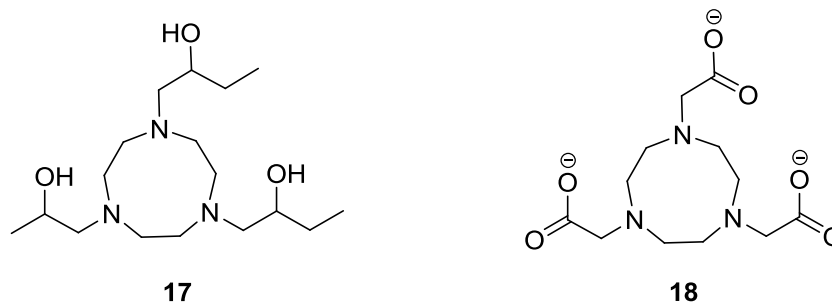
Temperature and solvent were found to have a large influence on the epoxidation reaction. Alcoholic solvents and acetonitrile were found to produce very little of the epoxide product. However, where cold acetone was used as the solvent very little hydrogen peroxide decomposition occurred. Further, large increases in catalyst TONs were observed under these conditions. For styrene at 273 K, using acetone as the solvent, complete conversion was observed within three hours with 98% epoxide selectivity, using only 1.5 eq. of hydrogen peroxide with a catalyst TON of 1000. No epoxidation was observed in the absence of either ligand **7** or a manganese salt. Interestingly, the use of the non-methylated 1,4,7-triazacyclononane (TACN, **16**) as a ligand resulted in strong peroxide disproportionation with no conversion of the substrate.



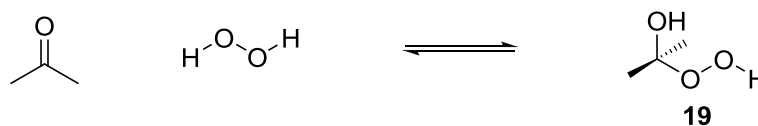
A dependence of the manganese(II) salt counterion on the epoxidation activity was observed, with acetate and sulfate ions giving 4 times higher epoxide yields compared to chloride or perchlorate salts. These differences were suggested to originate from the known bridging ability of acetate and sulfate anions which were proposed to promote the formation of oxidised manganese dimers. Analysis by EPR spectroscopy confirmed the presence of a manganese dimer in both cases with a strong 16-line signal attributed to a Mn^{III}Mn^{IV} dimer being observed. In the case of the chloride and perchlorate salts, a 6-line signal consistent with a manganese(II) monomeric species was observed.

Epoxide selectivity was high for the system and selectivity increased in the order *trans*-hept-3-ene (81%) < *trans*-hex-2-ene < cyclohexene < *cis*-hex-3-ene (98%) which suggested a system with a preference for *cis*-alkenes. Also, retention of alkene configuration in the epoxide product was high, with *cis*-hept-3-ene producing a product ratio of *cis:trans* epoxide of 77:23.

De Vos and Bein later reported the catalytic activity of manganese complexes of ligand **7** and related ligands **17** and **18**.¹⁶ The catalytic manganese systems based on these ligands exhibited differences in their epoxidation activity under different solvent and temperature conditions using hydrogen peroxide as the oxidant. Ligands **17** and **18** are potentially hexadentate, with three nitrogen donors from the macrocycle and three oxygen donors from either alcohol or carboxylate pendant arms. The difference in epoxidation activity was suggested to originate from the differences in the interactions between the respective ligands and the metal salt, resulting in different catalytic species in solution.



The *in situ* method of catalyst generation was again used by De Vos and Bein in this work, with the gradual addition of hydrogen peroxide (2 eq.), dissolved in an organic solvent, to the catalyst and alkene. Under these conditions significant epoxidation using a manganese(II) salt in combination with ligand **7** was only observed for the reaction in acetone. For cyclohexene, a 79% and 25% yield of epoxide was obtained at 273 K and 295 K respectively after a three hour reaction time. A similar trend was seen for styrene, with 98% and 33% epoxide product being observed at 273 K and 295 K respectively within the same time period. With other reaction solvents, significant hydrogen peroxide decomposition occurred, accompanied by little epoxide formation. Investigation into this phenomenon resulted in it being rationalised in terms of the formation of 2-hydroxy-2-hydroperoxypropane (HHPP, **19**) from the reaction of hydrogen peroxide and acetone (Scheme 5).



Scheme 5. The equilibrium between acetone and hydrogen peroxide with HHPP

The presence of **19** was confirmed by ^1H NMR spectroscopy and at 300 K, the equilibrium constant for the hemiketalisation was found to be $K = 0.078 \text{ M}^{-1}$, and 0.23 M^{-1} at 273 K, which corresponds to 66% and 85% **19** present in solution for the respective temperatures. It was then suggested that the high epoxidation activity using acetone as the solvent resulted from the reduced concentration of hydrogen peroxide and increased concentration of **19** especially at lower temperatures. HHPP was proposed to act as a hydrogen peroxide reservoir reducing oxidant decomposition by increasing the alkene to oxidant ratio, favouring epoxidation over peroxide decomposition.

With ligands **17** and **18**, the epoxidation reactions were markedly slower than with ligand **7** and as a consequence a higher catalyst loading was required for appreciable yields after a three hour reaction time. For ligand **17** and **18** a 0.5 mol% catalyst loading was required compared to the 0.1 mol% loading for ligand **7**. However, and more interestingly, peroxide decomposition for ligands **17** and **18** was markedly reduced and significant epoxidation activity was observed in solvents other than acetone. Epoxidation was also observed in methanol for ligand **18**, however very little epoxidation was observed for both ligands in acetonitrile and tetrahydrofuran. The solvent effects were far less pronounced for ligand **17**.

For both ligands **17** and **18**, the mode of coordination around manganese could be hexadentate under the conditions of the reaction. However, the catalytic activity observed for both ligands suggested that at least one of the pendant arms dissociated during the catalytic process allowing access to the manganese centre for the oxidant and substrate. It was also suggested that the stronger solvent influence on the reactivity of **18** compared to **17** originates from the more polar nature of the carboxylate group. Pendant arm dissociation requires stabilisation of the polar carboxylate functionality by interaction with a polar solvent or through hydrogen bonding, in the case of methanol. Owing to the reduced polarity of the pendant arms in **17** compared to **18**, the solvent influences were not as prominent on the catalytic activity of **17** as that observed in the

case of **18**. This model of a dissociating/associating pendant arm/s in a six-coordinate manganese centre also accounts, to some extent, for the reduced hydrogen peroxide decomposition when using **17** and **18** compared to ligand **7**. Peroxide decomposition requires the interaction of a second molecule of hydrogen peroxide which must gain access to the already oxidised manganese centre; this was restricted in manganese systems using **17** and **18** where most of the coordination sites were blocked. Coordination sites become available less frequently compared to manganese complexes of ligand **7** (*vide supra*), which would be expected to have three labile coordination sites.

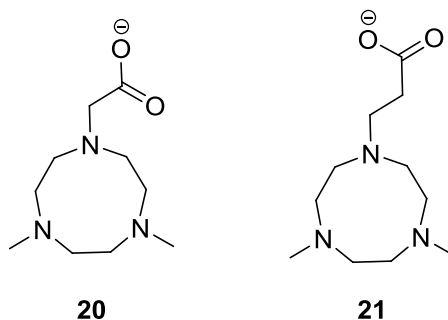
There was relative temperature independence for ligands **17** and **18** on the epoxide yield using methanol as the reaction solvent compared to the situation when acetone was used. When acetone was used, cooling of the reaction mixture resulted in increased epoxidation which suggested the importance of the formation of **19** on the epoxide yield. Similar temperature dependence was observed for the ligand **7** system when using acetone.

The epoxide selectivity was high for the manganese systems of all three ligands, but more so for **17** and **18** compared to **7**. This was exemplified in the epoxidation of cyclooctene where the ligand **7** system only yielded 71% epoxide (in acetone) compared to the 90% and 95% epoxide observed for **17** and **18** respectively (both in methanol). Reactions carried out at 298 K in methanol exhibited solvolysis, especially in the case of reactive epoxide products such as styrene oxide and isoprene oxide. However, this was suppressed at 273 K even for styrene where a 90% epoxide yield was obtained.

The stereoselectivity of the manganese systems of ligands **7**, **17** and **18** were probed using *cis*- and *trans*- 2-hexenes and 3-heptenes. As expected the stereoretention was higher for the thermodynamically favoured *trans*-alkenes. Significant scrambling of configuration was only observed for the manganese system using ligand **7** in acetone with 33% *trans*-2,3-epoxyhexane being obtained from *cis*-2-hexene. Stereoretention was higher in methanol than in acetone for all three ligands and generally the retention of configuration increased in the order ligand **7** < **17** < **18**.

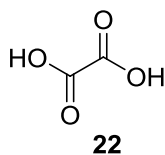
More recently, Shul'pin and co-workers synthesised and investigated the catalytic potential of manganese complexes of **20** and **21**.¹⁷ These systems were conceived on the

basis of the previously observed beneficial influence of carboxylates in catalytic epoxidation systems.¹⁸ The *in situ* method of catalyst generation was used in this work, with a 0.1 mol% catalyst loading (generated from the respective ligands and manganese(II) sulfate), a water/acetonitrile solvent system (50% v/v) with hydrogen peroxide (2 eq.) as the oxidant and a two hour reaction time. In the epoxidation of indene, significant epoxidation activity was observed, with a TON of 326 (33% conversion) and 450 (45% conversion) for **20** and **21** respectively. High epoxide selectivity was observed in both cases (93%), with only small amounts of the ketone by-product (2-indanone) being formed. The system employing ligand **21** represents the most active epoxidation catalyst in terms of system TON in the absence of a co-catalyst or the formation of HHPP.



1.7 Additives in catalytic epoxidation using manganese complexes of 1,4,7-triazacyclononane

The use of additives in order to improve catalytic activity and/or selectivity for manganese catalysts based on ligand **7** has been an area of much interest. De Vos and co-workers^{18b} investigated the use of 1,3-diones and dicarboxylic acids as additives in order to improve the epoxidation reactions of electron deficient and terminal alkenes and reduce the problematic hydrogen peroxide decomposition. Again the *in situ* method of catalyst generation was utilised in this work. Oxalic acid (**22**) was found to be a very efficient additive in the conversion of 1-hexene to the epoxide product. Sodium oxalate was found to give higher reaction rates whereas oxalic acid resulted in better yields in the conversion of this substrate. Thus a compromise using a 1:1 solution mixture of the aforementioned compounds, producing a buffer, was found to be optimal in terms of rate and efficiency.



Use of this buffer (0.3 mol%) at 298 K, in combination with the catalyst (0.15 mol%) and hydrogen peroxide (1.5 eq.) in water and acetonitrile converted both 1-hexene and allyl acetate in >99% yield with >99% epoxide selectivity within twenty minutes. This corresponds to a catalyst TON of 660. Exclusion of either the manganese salt, ligand **7** or the oxalate buffer resulted in a dramatic decrease in epoxidation activity, showing that all three components were required for the formation of the active species.

The use of TFA or acetic acid as the additive resulted in a similar retardation of the catalytic activity indicating that epoxidation was not occurring through a mechanism involving a peracid species. Also, the stereoselectivity for the conversion of both *cis*- and *trans*-2-hexene was high, in both cases >98% stereoretention was observed in the respective epoxides. This represented an improvement in comparison to a previously reported epoxidation using a manganese-ligand **7** system in acetone using hydrogen peroxide, where 33% of the *trans*-epoxide was formed from *cis*-2-hexene.¹⁶

Contrary to the reports by De Vos^{18b} that acetic acid does not promote catalytic oxidation using the manganese-ligand **7** system, Shul'pin and co-workers¹⁹ found acetic acid to enhance the oxidation of alkenes under specific reaction conditions, although the preformed catalyst **6** was employed during this work. Using 1-hexene as the substrate, hydrogen peroxide (2.2 eq.), acetic acid (1.1 eq.) and catalyst **6** in acetonitrile, quantitative yields of the epoxide were obtained with catalyst TON >4000 after 30 minutes at 295 K. Excluding the acetic acid additive, resulted in only small amounts of the epoxide product being observed even after one hour under the same conditions. Using similar conditions, epoxidation of styrene and cyclohexene proceeded with hydrogen peroxide decomposition, prolonged reaction times and reduced yields. Interestingly, it was found that the acetic acid catalytic enhancement of the epoxidation reaction was somewhat retarded when acetone was used as the reaction solvent. The rate of epoxidation (1-hexene) was markedly reduced and the reaction did not go to completion even after 24 hours.

Following this report, Shul'pin and co-workers²⁰ reported a kinetic and mechanistic study on the epoxidation of 1-decene using various carboxylic acids as additives in combination with catalyst **6**. The conditions were similar to those already described for the epoxidation of 1-hexene.¹⁹ High TONs were observed for electron withdrawing *para*-substituted benzoic acids such as *p*-trifluoromethylbenzoic acid (1940), *p*-cyanobenzoic acid (2440) and *p*-nitrobenzoic acid (2560) (Table 1, entries 4-6). The major product in all cases was the epoxide, however, a significant amount of the decane-1,2-diol was also obtained. The reactions were carried out at 298 K, using hydrogen peroxide (2.6 eq.), carboxylic acid (0.2 eq.) and acetonitrile as solvent with a reaction time of two hours. Use of ascorbic acid in combination with catalyst **6** under the same conditions gave no catalytic activity.

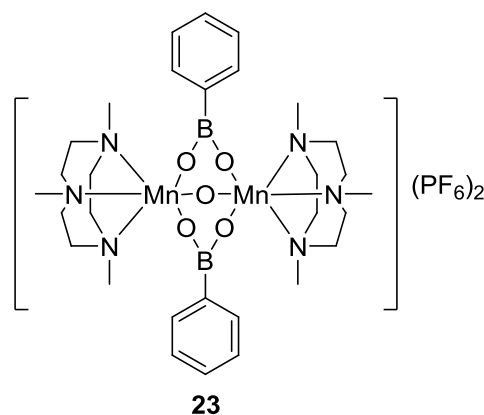
Table 1. Epoxidation of 1-decene

Entry	Additive	Yield ^a %		TON
		Epoxide	<i>cis</i> -diol	
1	Oxalic acid	68	0	3420
2	Oxalic acid ^b	80	2.4	4120
3	Oxalic acid ^c	79	0	3960
4	<i>p</i> -Trifluoromethylbenzoic acid	30	9	1940
5	<i>p</i> -Cyanobenzoic acid	36	13	2440
6	<i>p</i> -Nitrobenzoic acid	38	13	2560
7	Ascorbic acid	0	0	0
8	Citric acid	0	0	0

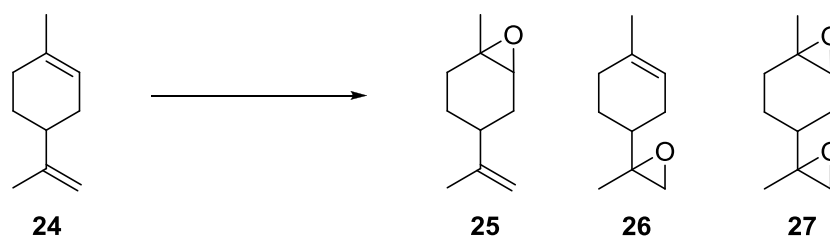
Conditions: Temperature, 298 K; 1-decene, 0.25 mol dm⁻³; additive, 0.05 mol dm⁻³ (oxalic acid 0.025 mol dm⁻³); catalyst **6**, 5 x 10⁻⁵ mol dm⁻³; H₂O₂ (30% aq.), 0.65 mol dm⁻³; reaction time, 2 hours. ^aAfter 2 hours. ^bAfter 3 hours. ^cH₂O₂ (70% aq.), 0.65 mol dm⁻³; 3 hours

Oxalic acid (Entries 1-3) was found to promote the epoxidation reaction with the highest TON (3420 under the conditions used for the benzoic acid additives), and after three hours this increased to >4000. Also the epoxide selectivity for the reaction was very high compared to that observed for the benzoic acid additives. After two hours, only the epoxide product was observed, this decreased only slightly after three hours, to 97% epoxide selectivity, with the decane-1,2-diol making up the balance. This is in agreement with the work already described by De Vos^{18b} where an oxalate buffer was found to promote the catalytic epoxidation of 1-hexene.

The epoxidation of 1-decene was also probed using complexes **6**, **12** and **23** using both hydrogen peroxide and *t*-butylhydroperoxide with the other conditions remaining the same. Acetic acid was used as the additive but no significant epoxidation was observed except in the case of catalyst **6** using hydrogen peroxide (4000 TON). Also, only moderate levels of epoxidation was observed using catalyst **23** and *t*-butylhydroperoxide (40 TON).



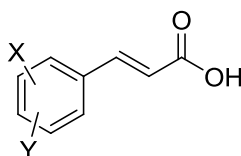
The epoxidation involving limonene (**24**) was probed using catalyst **6** and carboxylic acid additives. The internal epoxide (**25**) and external epoxide (**26**) were obtained using both acetic acid and oxalic acid as additives and using hydrogen peroxide as the oxidant. An excess of the oxidant produced significant amounts of the diepoxide product (**27**). Interestingly, the selectivity for either internal or external double bond epoxidation was reversed on changing from acetic to oxalic acid as the co-catalyst. The acetic acid co-catalyst favours epoxide **25** whereas the use of oxalic acid favours the formation of epoxide **26**.



Berkessel and Sklorz^{18a} reported the use of catalyst **6** (generated *in situ* from ligand **7** and manganese(II) acetate) in combination with the sodium salt of ascorbic acid as additive to enhance the catalytic activity in epoxidation and alcohol oxidation. Both 1-octene and methyl acrylate were converted to the epoxide with high TONs using either a

sodium ascorbate buffer or sodium ascorbate as co-catalyst respectively. Methyl acrylate was converted efficiently using a catalyst loading of 0.03 mol%, and 0.24 mol% of the additive with a 97% yield (>3200 TON) after two hours. The conversion of 1-octene was less favourable, with a substrate:catalyst ratio of 1333:1, 0.2 mol% of the ascorbate buffer giving an epoxide yield of 83% (>1000 TON). For both substrates 2-2.6 eq. of the oxidant was used. The effectiveness of the use of sodium ascorbate as additive is exemplified by its activity compared to the oxalate system. The efficacy in epoxidation of the sodium ascorbate system was demonstrated to be twice as high compared to the use of the oxalate buffer used by De Vos^{18b} in the conversion of 1-octene. Using the sodium ascorbate system an alkene:manganese(II) ratio of 1333:1 was used compared to the oxalate buffered system where a 666:1 ratio was required. Furthermore the conversion of *E* and *Z*-1-deuterio-1-octene to the epoxide product was found to proceed with high stereospecificity. In both cases 94±2% of the epoxide products was found to retain the alkene configuration.

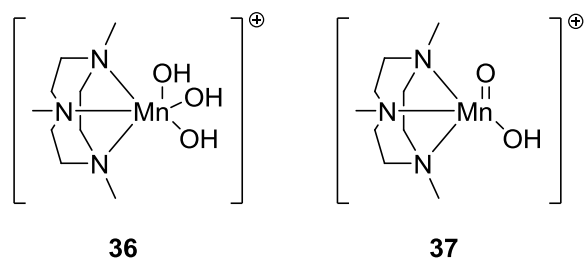
Gilbert *et al.*²¹ report a mechanistic study involving the epoxidation of various cinnamic acids (**28-35**) using the *in situ* catalyst generation method described by De Vos.¹⁵ The reactions were carried out in an aqueous acetonitrile environment using MnSO₄:7:substrate:hydrogen peroxide ratio of 1:3:6:100 under basic conditions. The influence of a large class of additives was also investigated.



Compound	X	Y
28	H	H
29	H	4-OMe
30	H	4-Me
31	H	4-Cl
32	H	4-CF ₃
33	H	3-NO ₂
34	H	4-NO ₂
35	3-CF ₃	5-CF ₃

Oxalic and ascorbic acid along with naphthalene-2,3-diol-sulfonate were found to enhance the rate 3-5 fold compared to the system excluding the use of additives. The electronic influence of substituents on the aryl ring of various cinnamic acids (**28-35**) and its manifestation in the potential modulation of the rate of epoxidation was also investigated. The reaction rates were determined using UV-Vis spectroscopy and ESI-MS was employed to identify species in solution.

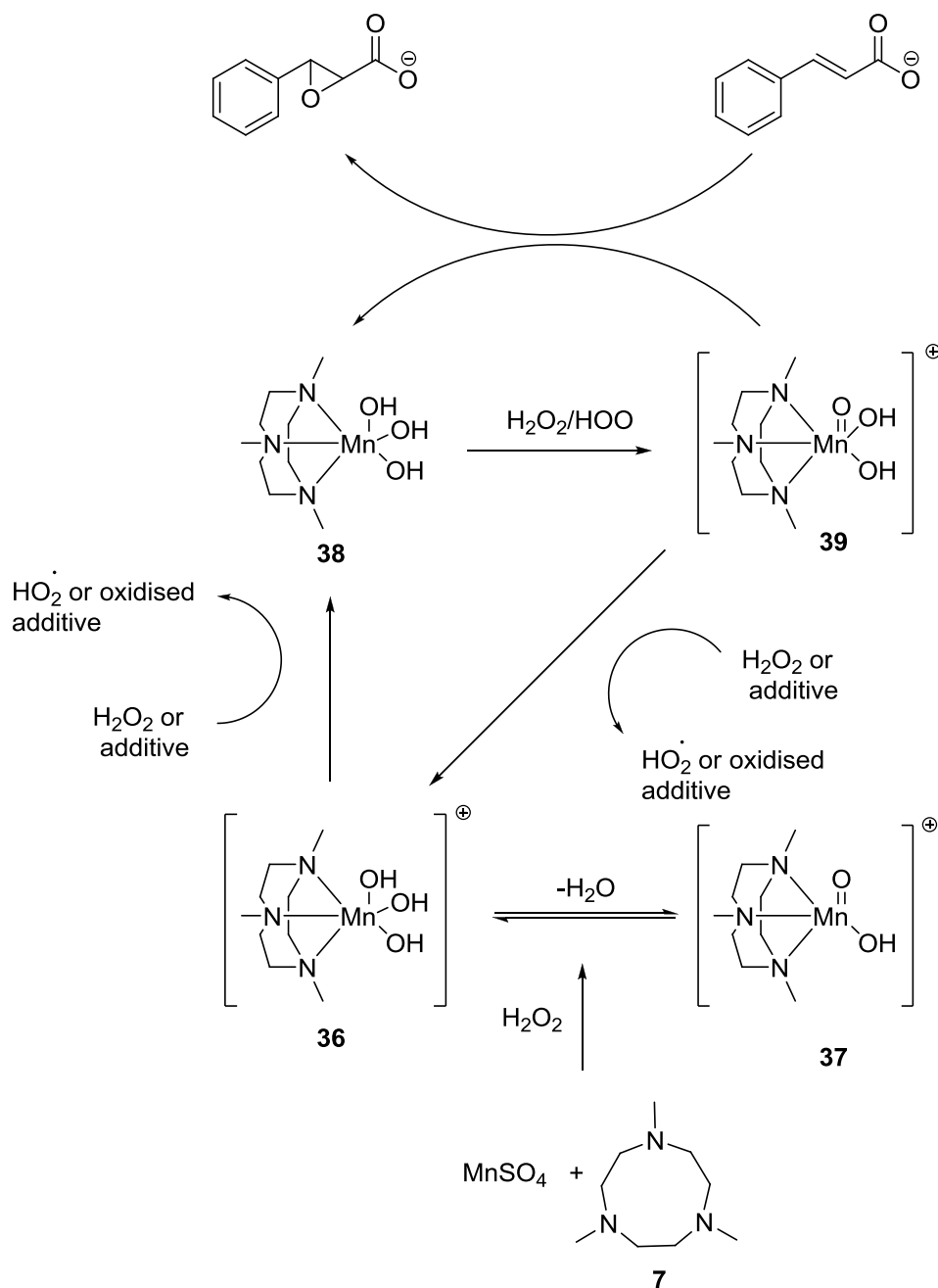
The catalytic systems, both in the absence and presence of additives, all exhibited pseudo-first-order kinetics in the epoxidation of cinnamic acid. In some cases a lag-phase was observed followed by the first-order decay of cinnamic acid. In the absence of any additives and using ESI-MS, the build up of manganese species **36** and **37** was suggested, based on the observation of ions in the ESI-MS at m/z 277 and 259. These and other ions previously¹² associated with the oxidative decay of ligand **7** were also reported in the epoxidation of cinnamic acid.



In the presence of the three additives found to be rate enhancing in the epoxidation of cinnamic acid, similar fragmentation patterns were observed. However mixed ligand species which would indicate the participation of the additive in the formation of a manganese/additive complex were not observed. This was suggested to be a consequence of such a species either forming and then decaying during MS analysis or that the species was uncharged. Finally the lack of formation of such species is also a possibility. Gilbert *et al.* also suggested an alternative in that the additives used are able to have a rate influencing effect by acting as a redox co-catalyst (Scheme 6). However, it should be noted that mixed ligand species such as **9** have been shown to form in the presence of hydrogen peroxide, from catalyst **6** and have been detected using ESI-MS spectroscopy.^{11b, c}

Oxalic acid, found to have the greatest rate enhancing influence in the epoxidation of cinnamic acid, was used to investigate the initial reaction rates in the epoxidation of

various substituted cinnamic acids (**28-35**). A plot of these initial rates versus the Hammett substituent constants σ for the respective substituents gave a ρ values of -0.63 ± 0.05 (correlation coefficient of 0.979); the negative ρ value indicates an electrophilic oxidant which is consistent with a $\text{Mn}^{\text{V}}=\text{O}$ species, rather than a manganese(III) (hydroperoxo) species. Such a species as the active oxidant would be expected to be nucleophilic²² and give positive ρ value from the Hammett plot. Thus, Gilbert *et al.* propose a $\text{Mn}^{\text{V}}=\text{O}$ species as the active oxidant in the epoxidation of cinnamic acids using the *in situ* prepared catalytic system with oxalic acid as the additive. Based on this evidence and the ESI-MS studies the following oxidation cycle (Scheme 6) was proposed.

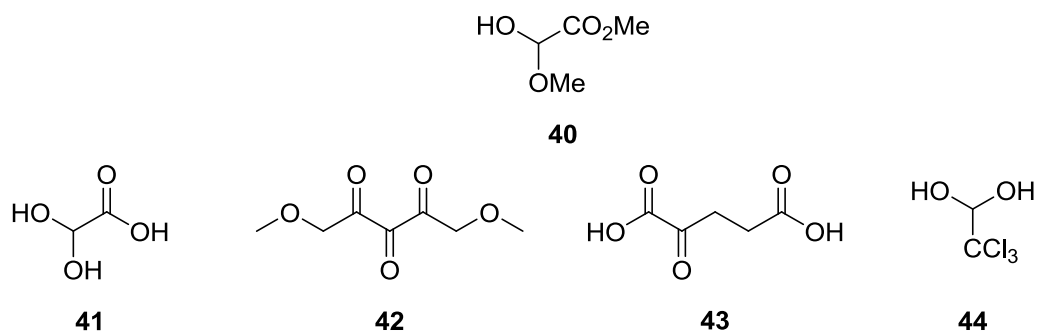


Scheme 6. Suggested mechanistic pathway for the epoxidation of cinnamic acids²¹

Complexation of the manganese(II) salt with ligand **7** and oxidation by hydrogen peroxide leads to the species **36** and **37**, which have been detected by ESI-MS studies. These were then suggested to undergo a one electron reduction to the charge neutral manganese(III) species (**38**), facilitated either by hydrogen peroxide or the additive. Subsequent oxidation by hydrogen peroxide generated species **39** which was proposed to be the active oxidant rather than the manganese(IV) species **36** and **37**. This conclusion was drawn from the observation that epoxidation using the system manganese(II)/**7**/H₂O₂ in the presence of oxalic acid has been shown to be efficient and stereospecific compared to the oxidation without the additive.¹⁵⁻¹⁶ Parallels for this type of behaviour can be found in the epoxidation of alkenes using manganese porphyrin systems where a Mn^V=O species was reported to be an efficient and stereospecific epoxidising agent. This was in contrast to the Mn^{IV}=O species which was found to be less efficient leading to the loss of stereochemistry in the epoxidation of alkenes.²³ Gilbert *et al.* therefore suggested that in the presence of oxalic acid, the formation of species **39** was favoured either by ligation to the manganese centre or by reductively removing the manganese(IV) species, **36** or **37**.

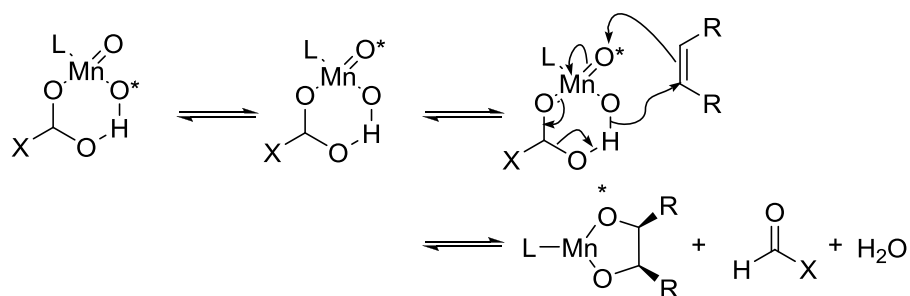
Feringa and co-workers²⁴ reported the use of various co-catalysts (**40-44**) in order to reduce hydrogen peroxide decomposition in the catalytic oxidation of alkenes using catalyst **6**. Epoxidation with high TONs were observed using GMHA (**40**) (25 mol%), a catalyst loading of 0.1 mol%, and hydrogen peroxide (1.3 eq.), which was added over six hours at 0 °C. Also, in comparison to the use of the oxalate additive, conversions were in most cases higher. In the case of styrene (97% conversion, 970 TON), the epoxide was the major product (860 TON) with a small amount of the *cis*-diol product (60 TON) and some higher oxidation products. However, under the same conditions, cyclooctene yielded the *cis*-diol as the major product (420 TON) with the epoxide being formed with 360 TON (90% total conversion). The *cis*-diol was demonstrated not to originate from hydrolysis of the epoxide product (*vide infra*). Using a mixture of **40** (25 mol%) and oxalate (0.3%) as the additive resulted in quantitative conversion of sterically unhindered substrates with an even higher selectivity for the epoxide. In the case of cyclooctene (100% conversion), the high epoxide selectivity was exemplified with a TON of 840 versus the low *cis*-diol formation (TON = 60). *cis/trans* Isomerism in manganese-catalysed alkene epoxidations has been suggested to indicate a manganese-oxo species; with the formation of epoxide occurring after bond rotation about a C-C bond of a carbon centred radical which is sufficiently long-lived to allow

bond rotation.²⁵ In line with this, it was found that alkenes which are able to form stable radical intermediates, such as *cis*-stilbene, undergo substantial scrambling of configuration in the epoxide product.



Co-catalysts other than **40** were tested using cyclooctene as the substrate, at 25 mol% loading using hydrogen peroxide (1.3 eq.) as the oxidant. Compounds **41-44** were found to have some influence on catalyst selectivity. Use of glyoxylic acid hydrate (**41**) as additive resulted in 840 TON for the epoxide with *cis*-diol formation almost completely suppressed. Using **42** and **43** epoxidation predominated, with modest *cis*-diol formation (250 TON). However, using **44** resulted in inversion of product selectivity compared with **41-43** with *cis*-diol formation predominating (370 TON) over epoxide production (310 TON). Thus additives **41-44** have shown the ability to reduce catalase activity of catalyst **6** and tune its selectivity for either epoxide, or more notably, for *cis*-diol.

Addition of an epoxide as the substrate using the catalytic systems under discussion did not lead to *cis*-diol formation, excluding epoxide hydrolysis as the mechanism for *cis*-dihydroxylation. Feringa suggested a mononuclear manganese-oxohydroxo species (Scheme 7) was responsible for *cis*-diol formation. The dinuclear manganese catalyst **6** was suggested to dissociate to a mononuclear species on coordination of the hydrated carbonyl compound which acted as a coordinating ligand. *cis*-Diol formation was thought to be favoured through a cyclic six-membered transition state in a concerted pathway.

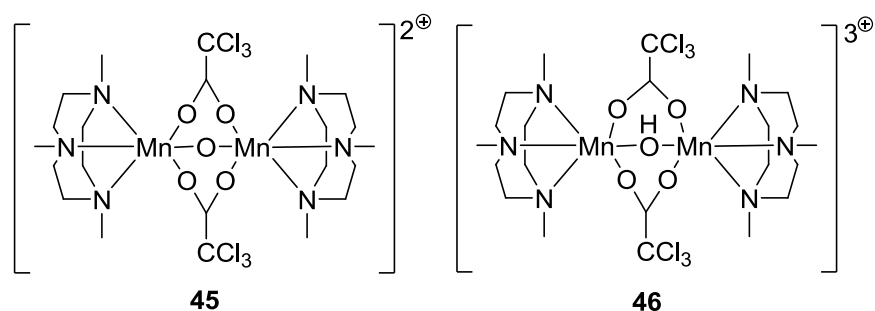


Scheme 7. Proposed *cis*-dihydroxylation mechanism using catalyst **6** (L = ligand **7**, X = CO₂Me, CCl₃)²⁴

Reoxidation of the metal centre, release of the *cis*-diol product and hydration of the carbonyl compound then closes the catalytic cycle.

In summary, the catalytic system developed by Feringa using catalyst **6** and a variety of activated carbonyl compounds has been shown to suppress catalase activity, give high epoxidation activity (860 TON) as well as *cis*-diol selectivity (420 TON).

Feringa *et al.*²⁶ later reported the use of carboxylic acids at co-catalytic levels to catalyst **6** to reduce catalase activity and allow the tuning of catalyst selectivity towards the conversion of alkenes to either epoxide or the *cis*-diol product. Also catalysts **45** and **46** which were proposed to be the type of complexes formed from the reaction of catalyst **6** and carboxylic acids, were prepared and their respective activity screened.



Use of trichloroacetic acid at 1 mol% loading of catalyst **6** shows *cis*-diol selectivity (440 TON) over epoxide production (245 TON) with good conversion (91%, Table 2, entry 1). Interestingly, lowering the additive loading increased the *cis*-diol selectivity, but lowered the catalyst activity (Entries 1-3). The suggestion that catalyst **6** forms

species such as **45** in the presence of carboxylic acids was supported by a similar product distribution being observed for complex **45** in the absence of trichloroacetic acid (compare entries 1 and 6).

Table 2. Oxidation of cyclooctene

Entry	Catalyst/ co-catalyst (mol%)	Conversion ^a (%)	TON	
			<i>cis</i> -Diol	Epoxide
1	6/CCl ₃ CO ₂ H (1.0)	91	440	245
2	6/ CCl ₃ CO ₂ H (0.2)	59	340	145
3	6/ CCl ₃ CO ₂ H (0.1)	9	65	25
4	6/-	3	10	5
5	6/HPF ₆ (1.0)	3	10	20
6	45/-	44	270	110
7	45/ CCl ₃ CO ₂ H (1.0)	93	380	260
8	46/ CCl ₃ CO ₂ H (1.0)	90	380	280
9	6/2,6-Cl ₂ PhCO ₂ H (3.0)	67	525	75
10	6/Salicylic acid (1.0)	82	60	695
11	6/ CCl ₃ CO ₂ H (25)	96	325	405

Conditions: **6**/cyclooctene/H₂O₂, 1/1000/1300, H₂O₂ added over 6 hours, reported data after 7 hours. ^awrt substrate consumed

A lag-phase in the catalytic activity (~1 hour) for catalyst **6** in combination with trichloroacetic acid (Entry 1) was observed by UV-Vis spectroscopy and was attributed to the formation of catalyst **45** *in situ*. Complex **45** was suggested to be the active catalytic species or the precursor to the active catalyst. Indeed, the catalytic and spectroscopic properties observed for **45** and **46** (Entries 7 and 8) in the oxidation of cyclooctene were remarkably similar to that of the system catalyst **6** and trichloroacetic acid (Entry 1).

The screening of other carboxylic acids led to the identification of acids able to impart greater selectivity towards either epoxidation or *cis*-diol production in the oxidation of cyclooctene (Entries 9 and 10). 2,6-Dichlorobenzoic acid was found to result in *cis*-diol selective oxidation of cyclooctene with a TON of 525 (*c.f.* TON of 75 for epoxide) using hydrogen peroxide as the oxidant. Use of salicylic acid, again added at co-

catalytic levels resulted in the selectivity being inverted, with the epoxide being produced as the major product with only small amounts of the *cis*-diol being produced. Use of other substrates such as *cis*-2-heptene in combination with the three carboxylic acids identified to tune selectivity resulted in the same selectivity being observed for cyclooctene in terms of the major oxidation product. Also, the stereoretention in both the *cis*-diol and epoxide product is high, with *cis*-2-heptene producing either the *cis*-diol or the *cis*-epoxide with >96% and >95% retention of configuration respectively (depending on the additive used). This suggested a concerted pathway in the reaction between alkene and the catalyst. The electrophilic nature of the catalyst was also suggested based on the low reactivity of electron deficient alkenes such as dimethyl fumarate with higher reactivity being observed for electron rich alkenes. The high activity of the catalytic systems resulted in further oxidation of products, as the alkene substrate concentration becomes low. In the case of cyclooctene, maintaining a pseudo-steady-state level of this substrate suppressed the overoxidation process and TONs of up to 2000 for the *cis*-diol product were observed.

Feringa *et al.*²⁷ later report on a detailed mechanistic study on the oxidation catalyst **6** in combination with carboxylic acid co-catalysts using hydrogen peroxide as the oxidant and cyclooctene as the substrate. Species **45** was found to be the major species in solution (>85%) once the catalytic oxidation had commenced.

1.8 Oxidation of alcohols using manganese complexes of 1,4,7-trimethyl-1,4,7-triazacyclononane

Many procedures for the conversion of alcohols to aldehydes are known using stoichiometric amounts of reagent including metal-based oxidants.²⁸ Metal-based catalytic systems are also known, using 1-10 mol% catalyst loading and using iodosylbenzene or *t*-butyl hydroperoxide (TBHP) as oxidant.²⁹ Feringa *et al.*³⁰ reported the use of catalyst **6** in the efficient and selective oxidation of alcohols using hydrogen peroxide and TBHP as the oxidant soon after Hage's reports on the utility of **6** in bleaching and epoxidation catalysis.

Initial results in the conversion of benzyl alcohol to the aldehyde using 0.1 mol% catalyst using hydrogen peroxide in acetone under air yielded the desired product with highly selective but modest catalytic activity (280 TON). Attempts to increase the

conversion by using a very large excess of hydrogen peroxide (80k eq.) yielded benzoic acid as the only product. This was overcome by the addition of hydrogen peroxide (2k eq.), dissolved in acetone, over a ten hour period, giving the product aldehyde with a 380 TON. Addition of benzoic acid to catalyst **6** (2:1 eq. respectively) under a nitrogen atmosphere resulted in the alcohol remaining unchanged, suggesting inactivation of the catalyst. However, under similar conditions, under air, conversion to benzoic acid occurs over time.

Curiously, pre-treating catalyst **6** with hydrogen peroxide (3k eq.) for 30 minutes prior to the addition of the substrate and a further aliquot of oxidant (8k eq.), dramatically improved the catalytic process (Method A). This was carried out under nitrogen, resulting in the quantitative formation of the product benzaldehyde from the alcohol with a TON of 360 (Table 3 entry 1). For other substituted benzyl alcohols, using the same method, TONs of 400-700 are observed for the conversion to the corresponding benzaldehyde with over 99% selectivity (Table 3, entries 2-11).

Table 3. Oxidation of alcohols using catalyst **6**

Entry	Substrate	Method A		Method B	
		TON	Time /mins	TON	Time /mins
1	Benzyl alcohol	360	60	480	150
2	4-Methoxybenzyl alcohol	710	45	1000	45
3	3,4-Dimethoxybenzyl alcohol	300	60	1000	20
4	4-(Dimethylamino)benzyl alcohol	-	-	1000	20
5	4-Chlorobenzyl alcohol	700	45	1000	25
6	2-Chlorobenzyl alcohol	490	45	1000	40
7	2,6-Dichlorobenzyl alcohol	80	90	-	-
8	4-Nitrobenzyl alcohol	530	15	1000	45
9	3-Nitrobenzyl alcohol	580	20	1000	25
10	2-Nitrobenzyl alcohol	240	15	1000	35
11	4-Trifluoromethylbenzyl alcohol	340	210	600	50
12	Octan-2-ol ^a	360	100	360	90

Conditions: In all cases a ratio of 1000:1 of alcohol to **6**. Alcohols were dissolved in acetone under an inert atmosphere; the reactions were followed by GC and terminated when the conversion ceased to give benzaldehyde as product (the selectivity for aldehyde in all cases was above 99%). ^aA secondary alcohol, producing the ketone product

Using TBHP and catalyst **6** under the conditions initially employed (*vide supra*), no conversion of the benzyl alcohol was observed. However pre-treatment of catalyst **6** with hydrogen peroxide (as in Method A), followed by the use of TBHP instead of hydrogen peroxide resulted in the full conversion of all the benzylic alcohols with excellent selectivities at room temperature within one hour using 0.1 mol% catalyst **6**. The use of TBHP instead of hydrogen peroxide (as substitute oxidant not for the pre-treatment of catalyst **6**) for the conversion of alcohols was referred to as Method B.

The electronic properties of the substituted benzyl alcohols appeared to influence the reaction rate. Electron-donating substituents such as dimethoxy and dimethylamine on the benzene ring of the alcohol appeared to enhance the reaction rate (Entries 3 and 4, Method B) compared to electron withdrawing substituents (Entry 11, Method B). Also, using method A, a small steric influence on reaction rate was observed. *ortho*-Substituted substrates reacted sluggishly compared to *meta*- and *para*-substituted benzyl alcohols, whilst 2,6-dichlorobenzyl alcohol was almost completely unreactive (Entry 7). Finally, secondary alcohols were converted to the ketone, however the reaction was insensitive to the method used (Entry 12).

The manganese(II) salt, ligand **7** system described for the epoxidation of alkenes (*vide supra*) was used by Berkessel and Sklorz^{18a} for the oxidation of alcohols. The oxidation of pentan-2-ol using this catalytic system catalyst (0.03 mol%), sodium ascorbate (0.30 mol%) and hydrogen peroxide (2 eq.) in acetonitrile gave the corresponding ketone with high selectivity (97%) and a TON >3200. The conversion of butan-1-ol was less efficient, but still required less than 0.5 mol% catalyst and gave a TON of 240.

Shul'pin and co-workers¹⁹ found catalyst **6** in combination with acetic acid as an additive to enhance the catalytic activity compared to the activity observed in its absence in the oxidation of alcohols. Conversion of various secondary alcohols using catalyst **6**, hydrogen peroxide and acetic acid in acetonitrile at 293 K after three hours occurred with almost quantitative conversion and selectivity to the corresponding ketone. Further investigation into isopropanol oxidation revealed, in the absence of acetic acid that only hydrogen peroxide decomposition occurred. Also the catalyst was found to be more efficient in acetonitrile than in acetone for the oxidation of alcohols. It was found that the oxidation of primary alcohols with the aforementioned conditions

was more difficult giving less than 60% conversion and a mixture of aldehyde and carboxylic acid as products.

1.9 Summary of the proposed mechanistic details involving manganese complexes of 1,4,7-triazacyclononane in alkene epoxidation

The elusive nature of catalyst **6** in terms of its bleaching mechanism and the active catalytic species in alkaline solution continues to be a subject of some conjecture. This despite over a decade of study in order to shed light on the intricate workings of this highly active oxidation catalyst. This lack of understanding is mirrored in the field of epoxidation catalysis involving **6**, in organic media. The same is also true in the case of systems generated *in situ* from manganese salts and ligand **7** or derivatives of **7** which maintain the TACN backbone.

Using a catalytic system generated *in situ*, De Vos¹⁵ found the acetate and sulfate salts of manganese gave significantly increased catalytic activity over the chloride and perchlorate salts when combined with ligand **7** in epoxidation. This may or may not have been linked to the suggested bridging capabilities of the acetate and sulfate anions compared to the chloride and perchlorate anions. Nevertheless, a 16-line EPR signal consistent with a Mn^{III}Mn^{IV} dimeric species was observed for the acetate and sulfate anions compared to the 6-line EPR signal observed for the chloride and perchlorate containing species. The aforementioned mixed valent, dimeric manganese species was implicated in both the bleaching mechanism^{11c} involving **6** and in epoxidation catalysis²⁷, however in both the epoxidation and bleaching processes, such a species is usually regarded as a precursor to the active catalyst. No further mechanistic investigations were carried out during this study.

In a later study, De Vos¹⁶ used the *in situ* method to generate catalytic species from ligands **7**, **17** and **18**. EPR investigations into the species formed after the addition of hydrogen peroxide indicated the presence of both manganese(IV) and manganese(II) in the case of ligand **17**. Using UV-Vis, the presence of a manganese(III) species was detected in relation to ligand **18**. However, De Vos suggested the same active catalytic species in all cases based on their similar catalytic activity profiles. Interestingly, significant scrambling of alkene configuration in the epoxide product for the manganese

system utilising ligand **7** (*vide supra*) may be pointing towards an oxygen transfer process involving the formation of radical intermediates.

Various additives in combination with catalyst **6** and systems generated *in situ* from ligand **7** and manganese salts have been demonstrated to increase catalyst activity, selectivity, decrease hydrogen peroxide decomposition and even tune the catalyst selectivity to produce either epoxide or *cis*-diol product. De Vos^{18b} used an oxalate buffer in order to oxidise terminal alkenes quantitatively to the epoxide product, in a stereoselective manner using almost a stoichiometric amount of hydrogen peroxide. The reaction efficiency was suggested to be increased by the coordination of the additive, influencing the catalyst nuclearity and or by changing its redox potential.

Gilbert and co-workers²¹ studied the conversion of a series of cinnamic acids to their corresponding epoxide products using hydrogen peroxide and an *in situ* generated manganese system in combination with ligand **7**. A Hammett plot based on reactions carried out in the presence of oxalic acid suggested an electrophilic manganese based oxidant. In the absence of any additives, the build up of two mononuclear manganese(IV) species, **36** and **37** were detected using ESI-MS. Despite this ESI-MS data, Gilbert suggested a $\text{Mn}^{\text{V}}=\text{O}$ species as the active oxidant rather than the observed $\text{Mn}^{\text{IV}}=\text{O}$ species. This was justified by drawing parallels between this work and the work of De Vos where scrambling of alkene configuration in the epoxide product was reported in the absence of additives¹⁶ and stereospecific conversions were observed when using oxalic acid.^{18b} This was explained by comparisons with alkene epoxidations using manganese porphyrins, where $\text{Mn}^{\text{V}}=\text{O}$ porphyrins were reported to give stereospecific conversions compared to a $\text{Mn}^{\text{IV}}=\text{O}$ species. Presumably, Gilbert was suggesting a $\text{Mn}^{\text{IV}}=\text{O}$ species as the possible active species involved in the non-stereospecific epoxidations described by De Vos in the absence of oxalic acid, also explaining the detection of a $\text{Mn}^{\text{IV}}=\text{O}$ (using ESI-MS) in his own work.

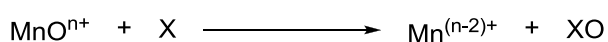
Feringa²⁴ suggested a manganese-oxo species with radical character in the epoxidation of aryl-substituted alkenes using catalyst **6**, hydrogen peroxide and GMHA as the additive. This was based on the observed *cis/trans* isomerisation during epoxidation for substrates such as *trans*-stilbene which are thought to be able to stabilise a carbon-centred radical long enough for C-C bond rotation to occur. This was similar to an

active catalyst with radical character, suggested by the epoxidation results obtained by De Vos¹⁶.

Shul'pin²⁰ demonstrated the use of catalyst **6** in combination with carboxylic acids to increase catalytic turnover, acetic acid was found to be particularly effective. In addition, using a variety of *para*-substituted benzoic acids as an additive indicated a clear trend where an electron-withdrawing substituent was found to be beneficial to catalytic activity. Such a trend may be indicating an electrophilic manganese catalyst.

Feringa and co-workers²⁶ later reported the use of catalyst **6** and carboxylic acid additives and found electron deficient alkenes to be less reactive. Again, this suggested an electrophilic oxidant, in line with the observation by Shul'pin²⁰. Further, using particular carboxylic acids as an additive (*vide supra*), the catalyst was shown to be highly selective for either epoxidation or *cis*-dihydroxylation. Also in this work, carboxylato-bridged dinuclear manganese species such as **45** were suggested to be the active species or a precursor to such an entity on the basis of the similar reactivity profiles of both the authentic complex **45** and catalyst **6** in combination with carboxylic acid additives. The high stereoretention observed for these systems during epoxidation, suggested a concerted mechanistic pathway. A later study²⁷ confirmed **45** (> 85%) as the dominant species in solution once the conversion of substrates had commenced. However, in order to account for all the observations, another dinuclear Mn^{III}-Mn^{III} species, was suggested as the active catalytic species.

Manganese-oxo species have been frequently suggested as the active oxygen transfer agent in the bleaching process and in the epoxidation of alkenes involving manganese based catalytic systems of ligand **7** (*vide supra*). High-valent manganese-oxo species have also been the basis of many mechanistic pathways postulated for alkene epoxidation in the field of manganese Schiff-base mediated oxidations (*vide infra*). Oxidation of substrates involving such species can be summarised by the following process (Scheme 8);



Scheme 8. The oxygen transfer process from a metal-oxo species to a substrate (X)

A high-valent manganese-oxo species, transfers oxygen to the substrate with the concomitant two electron reduction of the metal-oxo species. In particular, high-valent $\text{Mn}^{\text{V}}=\text{O}$ species have been frequently suggested. The formation and reactivity of this species and other manganese-oxo species can to some extent be understood by considering the bonding in these transient species from a molecular orbital (MO) perspective.

A MO description of the bonding between an oxygen and a metal centre was described nearly fifty years ago,³¹ detailing the interaction between the metal d -orbitals and oxygen p -orbitals and the resulting molecular orbitals and their ordering in terms of energy. By replacing an axial ligand in an octahedral complex (metal-oxo species can occur in other geometries) with an oxygen, the symmetry of the d -orbitals is changed to C_{4v} . The t_{2g} symmetry is lowered to $b_2(d_{xy})$ and $e(d_{xz}, d_{yz})$ and the e_g symmetry to $b_1(d_x^2 - y^2)$ and $a_1(d_z^2)$. Owing to the short axial metal-oxygen bond, the d_z^2 orbital is raised in energy and due to π -donor ability of the O^{2-} ligand, the d_{xz} and d_{yz} orbital energies are raised in energy compared to its octahedral parentage (Figure 2).

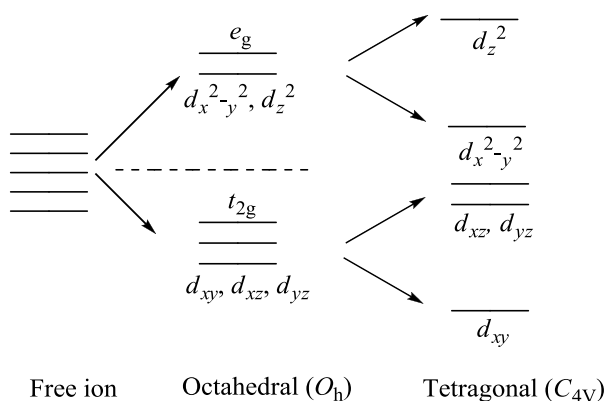


Figure 2. A representation of the d -orbital splitting in an octahedral field and a tetragonal field, relative to the degenerate d -orbitals in the free ion

Furthermore, due to the strong σ and π interactions between the metal centre and the oxo-ligand, the ligand *trans* to the metal-oxo bond is typically weak or missing.³² Using this atomic d -orbital splitting and the resulting relative energies of the metal orbitals, a MO description of the bonding in metal-oxo complexes can be obtained (Figure 3).

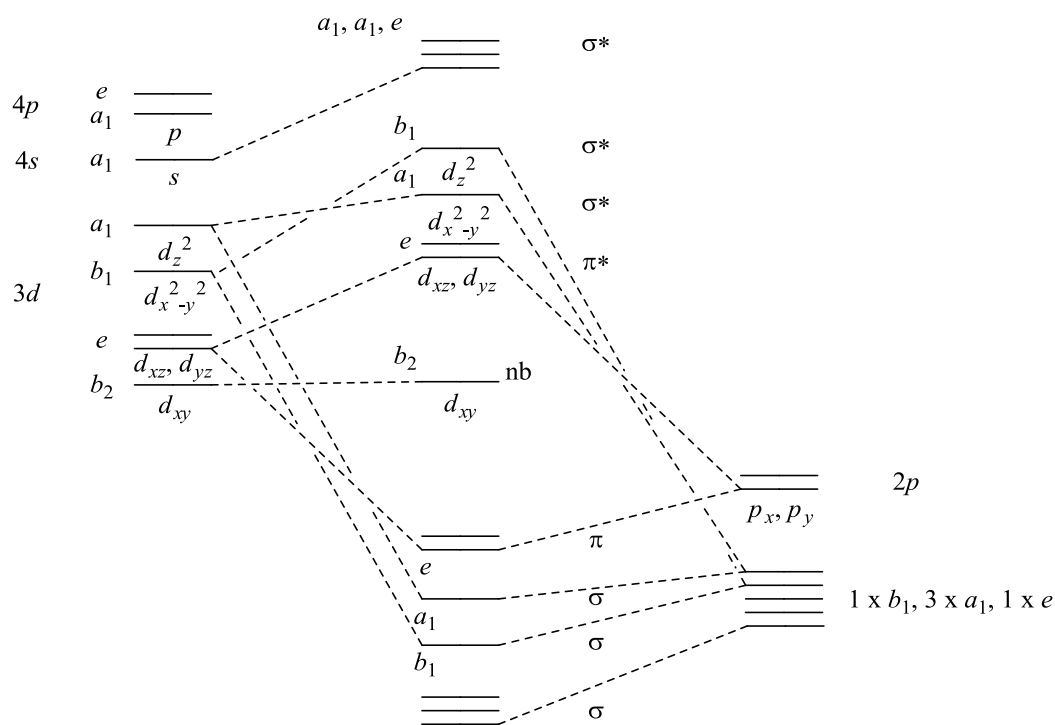
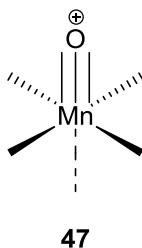


Figure 3. A molecular orbital diagram showing the bonding in a complex of tetragonal symmetry containing a metal-oxo bond

Filling this MO diagram with 16 electrons (14 electron from the ligands (assuming the *trans* ligand is absent) and with 2 *d*-electrons from manganese in the penta-valent state), we can calculate the total bond order (B.O) for a complex. We obtain a total B.O. of 7 and as there are only 5 sigma-bonds, we must have 2 π -bonds between the manganese and the oxo ligand and therefore a B.O. of 3 between the metal-oxo as shown in **47**.



With three bonds to oxygen, the penta-valent manganese-oxo species is frequently incorrectly represented in the literature. However, in keeping with the literature, it has been and will be represented as $\text{Mn}^{\text{V}}=\text{O}$ in this thesis. More importantly, Nocera³² assigns the LUMO (lowest unoccupied molecular orbital) as being the π^* orbitals of the M-O bond. With a d^2 $\text{Mn}^{\text{V}}=\text{O}$ species these π^* orbitals are completely empty and this

was suggested as the origins of the electrophilic nature of the $\text{Mn}^{\text{V}}=\text{O}$. Where a $\text{Mn}^{\text{V}}=\text{O}$ has been suggested as the active metal oxidant, its electrophilic nature was usually inferred from the behaviour of the catalyst with different substrates (*vide supra*). An electrophilic $\text{Mn}^{\text{V}}=\text{O}$ is also largely accepted as the oxygen transfer agent in manganese Schiff-base catalysed epoxidation (*vide infra*).

Also, in the case of a $\text{Mn}^{\text{IV}}=\text{O}$, with a *d*-electron count of three, we obtain a B.O. of 2.5 for the metal-oxo bond. An unpaired electron, suggests some radical character for such an oxidant. Indeed, Gilbert *et al.* have suggested the $\text{Mn}^{\text{IV}}=\text{O}$ active species to be involved in non-stereospecific alkene epoxidations (*vide supra*).²¹ Scrambling of alkene geometry in epoxide product has been suggested to involve radical intermediates.

It is clear from the mechanistic studies involving manganese catalysts of ligand **7** and derivatives, in both bleaching (*vide supra*) and epoxidation, that a complex set of parameters govern its activity and selectivity. This complex mechanistic landscape means that these systems remain poorly understood. In view of this and in order to cover a fuller range of manganese based oxidation catalysts, systems based on different classes of ligands are also described (*vide infra*).

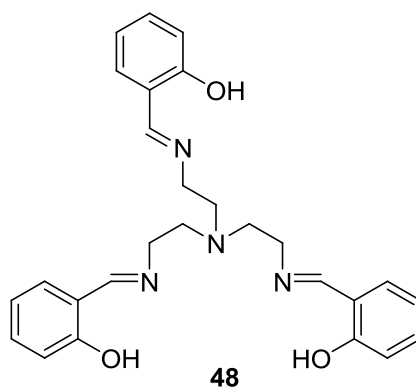
1.10 Other Manganese bleaching and epoxidation catalysts

Catalyst **6**, despite its demonstrated efficacy in the bleaching of commonly encountered stains, was not viable in commercial detergent products due to its detrimental dye and fabric damage. However, its catalytic bleaching activity remains the benchmark against which other bleaching catalysts are evaluated, certainly amongst some industrial researchers (Chapter 4, 4.35). In the search for a commercially feasible bleaching catalyst, work towards different classes of catalysts has persisted. A summary of these catalysts follows, with a focus on manganese based systems. Like **6** and its derivatives, other manganese based catalysts have shown potential for application in epoxidation. This aspect of reactivity of these oxidation catalysts is also explored.

1.11 Manganese Schiff-base complexes in bleaching

A variety of manganese complexes with Schiff-base ligands (**48**), have been

patented for stain bleaching and dye-transfer inhibition.³³ Dye transfer inhibition prevents deposition of dyes onto acceptor fabrics which have leached out of other fabrics in the laundry by oxidation of the rogue dye whilst still in solution. The complexes are generally in the +3 oxidation state and catalytic enhancement in tea stain bleaching has in some cases been observed compared to TAED/percarbonate bleaching systems using hydrogen peroxide as the oxidant. However, these manganese Schiff-base complexes are less efficient bleaching catalysts in relation to manganese complexes based on **7**. Mechanistic details in relation to these Schiff-base complexes in bleaching have not been published neither has any information regarding their incorporation into commercial laundry products. However the reactivity of such systems have been extensively studied in the epoxidation of alkenes.



1.12 Manganese Schiff-base complexes in alkene epoxidation

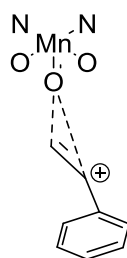
Following reports by Kochi that cationic chromium³⁴ and manganese(III)³⁵ salen complexes were able to effect epoxidation of alkenes using PhIO as the oxidant, Jacobsen³⁶ and Katsuki³⁷ reported several asymmetric versions of this class of catalyst able to catalyse the enantioselective conversion of alkenes. Despite its success in terms of its widespread utility and observed high enantioselectivities, the origins of this enantioselectivity remain unclear along with the mode of oxygen transfer to the alkene, and is the subject of much debate.³⁸

Different mechanisms for oxygen transfer, including multi-step and concerted processes have been suggested.³⁹ Radical, metallaoxetane and cationic intermediates have been suggested for multi-step pathways. Various approaches of the alkene towards the

catalyst have also been suggested, including a number of side-on and even an end-on approach. Depending on reaction conditions, a number of different active species have been proposed; manganese-oxygen species in different oxidation states of varying nuclearities have been postulated. However, for the majority of the Jacobsen-Katsuki epoxidation systems, an electrophilic $\text{Mn}^{\text{V}}=\text{O}$ species is accepted as being the active metal based oxidant. In the manganese-ligand **7** catalytic system, a $\text{Mn}^{\text{V}}=\text{O}$ active species has also been either suggested or detected in the oxidation of various substrates. In the oxidation of phenolic substrates, a $\text{Mn}^{\text{V}}=\text{O}$ has been detected by ESI-MS.^{11b, c} The same species has been postulated in the epoxidation of cinnamic acid²¹ and in the bleaching of azo-dyes.¹² Despite this, a $\text{Mn}^{\text{IV}}=\text{O}$ species has recently been detected after the oxidation of a manganese salen complex using *m*-chloroperoxybenzoic acid.⁴⁰

Conjugated (*Z*)-1,2-disubstituted alkenes are observed to undergo highly enantioselective epoxidations along with conjugated trisubstituted olefins. Also, substitution of an electron donating group *para*- to the phenolic hydroxyl of the Schiff-base ligand, enhances enantioselectivity and conversely a nitro-group has the opposite influence. Corey has recently proposed a model which goes some way to explaining these observations and the observed facial selectivity in the epoxidation of achiral alkenes.³⁸

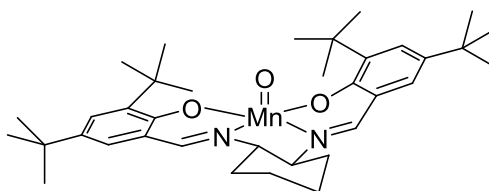
The model is based on two assumptions, firstly, electrophilic attack by $\text{Mn}^{\text{V}}=\text{O}$ on a conjugated alkene double bond is assumed to occur in an asynchronous manner generating an unsymmetrical three membered transition state, **49**. A consequence of this is that a positive charge develops on one of the two alkene carbons which interacts more weakly with the oxygen of the $\text{Mn}^{\text{V}}=\text{O}$. In the example given in **49** the O-CH₂ bond formation is likely to precede the O-CH-Ph bond formation as this order of bond formation would allow the positive charge to be placed where it can be best stabilised.



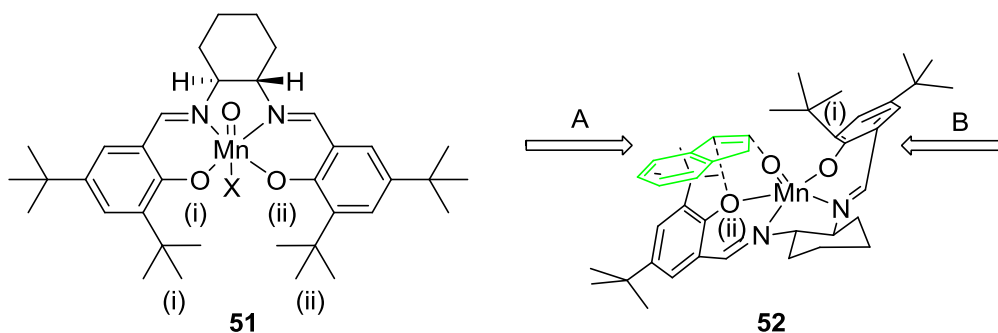
49

Secondly, it is assumed the six-membered chelate rings of the salen ligand are canted relative to each other (**50**). This is a consequence of chirality of the 1,2-diaminocyclohexane backbone and as a result the *t*-butyl groups *ortho*- to the coordinated phenolic oxygen take positions above and below the N-Mn-N plane. More specifically, from the representation in **51**, of (*S,S*)-1,2-diaminocyclohexane, (i) represents the group above the plane of the paper and (ii) represents a group below the plane of the paper. Making these assumptions and using indene as the substrate it can be seen (from **52**, which depicts the arrangement for the manganese complex of (*S,S*)-1,2-diaminocyclohexane) that the possibility of an electrostatic interaction between the benzylic carbon (δ^+) of the double bond and that of the phenolic oxygen (ii) (δ^-) is present on approach A for only one face of the alkene. Further, it is apparent from **52** that unfavourable steric interactions between the *t*-butyl groups (i) and (ii) are dissipated in this arrangement. It can also be seen from **52** that the aromatic ring of indene and that of the salen ligand are in parallel planes, allowing for favourable π -stacking interactions. This unique three dimensional arrangement is suggested to imply a pathway for the preferential epoxidation of a single face of the alkene. Approach B for the alkene is disfavoured due to steric repulsion between the aromatic ring of the alkene and the bulky *t*-butyl group.

Indeed the epoxide product observed for the catalyst (*S,S*)-1,2-diaminocyclohexane is the one predicted by the model and is the (*S,R*)-enantiomer. Also the low enantioselectivities obtained for *trans*-1,2-disubstituted alkenes using catalyst **51** can be explained using the same model. The basis for face selection is lacking as steric repulsion will occur for both approach A and B. The increase in enantioselectivity with more electron donating substituents on the aromatic ring of the salen ligand can be explained by an increase in electron density on the phenoxy oxygen allowing for a stronger electrostatic interaction between a specific face of the alkene and catalyst.



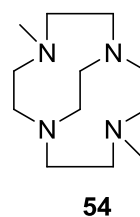
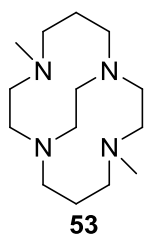
50



1.13 Manganese cross-bridged macrocyclic complexes in bleaching

Manganese complexes of cross-bridged macrocyclic ligands such as **53** and **54** have been patented by Procter and Gamble for stain bleaching.⁴¹ No stain bleaching data was included in the patents and there is a lack of mechanistic details on their mode of action. However, ligand **53** is preferred as the manganese(II) complex shows high kinetic stability and no MnO_2 was observed to form even after several weeks in 2M NaOH solution.

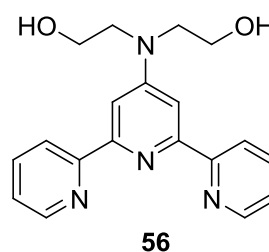
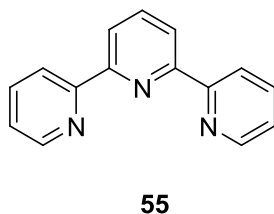
Busch and co-workers⁴² reported a manganese complex of ligand **53**, $[\text{Mn}^{\text{II}}(\mathbf{53})\text{Cl}_2]$, with the ability to catalyse the oxidation of alkenes to the epoxide product. Alkenes such as norbornylene, styrene and *cis*-stilbene were selectively converted to their respective epoxide products using hydrogen peroxide as the oxidant. Furthermore, in the case of *cis*-stilbene, the observed stereoretention was high. Evidence for the involvement of a Lewis acid mechanism in these manganese catalysed epoxidation reactions was presented as opposed to the familiar redox pathway suggested for high-valent manganese-oxo species (*vide supra*, 1.9). In support of the suggested Lewis acid mechanism, a hydrogen peroxide adduct of a high-valent manganese(IV) complex of ligand **53**, $[\text{Mn}^{\text{IV}}(\mathbf{53})(\text{O})(\text{OOH})]^+$ was detected by mass spectrometry (m/z 358) in the reaction mixture involving the epoxidation of alkenes using the complex $[\text{Mn}^{\text{II}}(\mathbf{53})\text{Cl}_2]$ and hydrogen peroxide. This hydrogen peroxide adduct was suggested to be the active oxidant in these epoxidation reactions and as such, this was the first reported manganese catalysed epoxidation by a Lewis acid pathway.



1.14 Manganese complexes of 2,2':6,2' terpyridine in bleaching

Ciba have published a number of patents⁴³ describing manganese complexes of ligands such as **55** and **56** as bleaching catalysts which are able to activate hydrogen peroxide and outperform the TAED/percarbonate system in tea stain bleaching on cotton fabrics. No significant dye damage was observed for coloured cotton fabrics with dyes such as Levafix Scarlett E-2GA and Cibanone Blue RS when ligand **56** was used in the catalytic system. Also described are related compounds which are able to activate dioxygen as exemplified by their utility in tea stain bleaching in detergent formulations in which the hydrogen peroxide oxidant had been excluded.

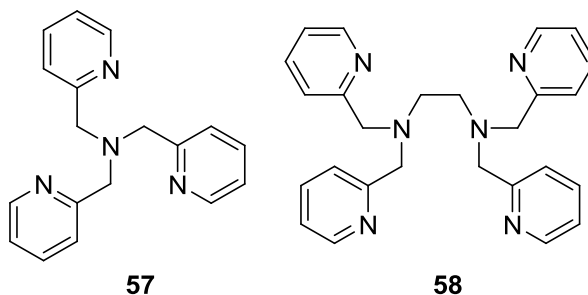
Also, a manganese-ligand **56** system was used to exemplify the utility of these ligands in the epoxidation of alkenes. Using the *in situ* method of catalyst generation, ethyl acrylate was converted to the corresponding epoxide using hydrogen peroxide (2 eq.) as the oxidant, in acetonitrile with a small TON (36). Sodium ascorbate was added as an additive (3 eq. to alkene).



1.15 Manganese complexes of polypyridineamine ligands in bleaching

Manganese complexes of **57** have been patented by Henkel for stain bleaching but no examples are given.⁴⁴ The data provided, however, shows enhanced bleaching of Morin using $[\text{Mn}^{\text{II}}(\mathbf{57})_2(\mu\text{-CH}_3\text{COO})_2]^{2+}$. Morin (see **112**, 3.2) is a polyphenolic pigment which is found in tea and fruit and often used as a model substrate in catalytic bleaching

studies. Clariant have claimed manganese complexes of **58** in combination with hydrogen peroxide and peracids catalyse the stain bleaching process using tea, red beetroot and curry stains.⁴⁵



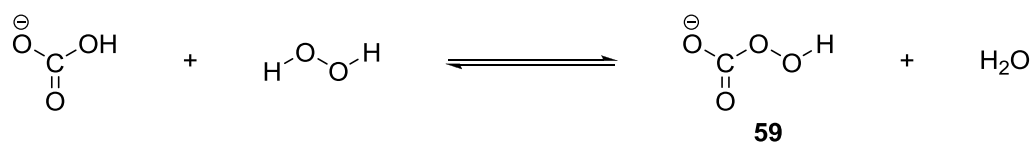
1.16 Manganese salts as bleaching catalysts

Manganese salts have been claimed to be hydrogen peroxide activators in detergent formulations containing sodium carbonate.⁴⁶ Some bleaching activity has been observed when using tea-model stain BC-1 at 40 °C. However, application of such systems has been limited due to the potential for manganese dioxide deposition onto fabrics causing undesirable staining.

1.17 Manganese salts in alkene epoxidation

Use of transition metal salts in the epoxidation of alkenes have distinct advantages over other systems. It negates the use of elaborate ligands and this makes the use of metal salts atom economic, cheap and where metal salts such as those based on manganese are used, it makes the process environmentally benign. Burgess and co-workers⁴⁷ reported the use of manganese sulfate (0.1-1.0 mol%) in the epoxidation of a variety of alkenes using hydrogen peroxide in the presence of bicarbonate with either *t*-BuOH or DMF as the reaction solvent. The catalyst was shown to have a wide substrate scope, transforming aromatic, cyclic, and tri-substituted alkenes to their respective epoxides. However, terminal alkenes could not be oxidised using this system.

The presence of bicarbonate was found to be essential for catalytic activity and was shown to form peroxydicarbonate (Scheme 9, **59**) in the presence of hydrogen peroxide.

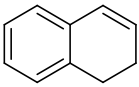
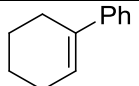
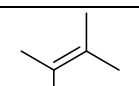


Scheme 9. The formation of peroxymonocarbonate from hydrogen peroxide and bicarbonate

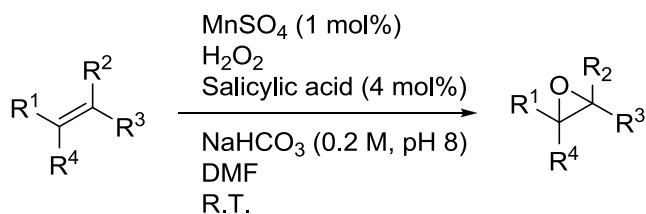
Peroxymonocarbonate (**59**) was found to epoxidise alkenes, but at an extremely slow rate (1-2 days). It was therefore suggested that **59** reacts with the manganese salt to form the catalytically active species. Using EPR spectroscopy to monitor the reaction, it was found that the manganese(II) species was consumed in the initial stages of the reaction and regenerated once the hydrogen peroxide was spent. It was inferred from this that manganese(II) is oxidised to a high-valent manganese(IV) species and then reduced back to the manganese(II) state at the end of the catalytic cycle.

In order to increase catalytic activity, reduce hydrogen peroxide decomposition and increase substrate scope, 68 different additives were screened. The additives, sodium acetate (6 mol%) in *t*-BuOH and salicylic acid (4 mol%) in DMF were found to reduce the amount of hydrogen peroxide required, decrease reaction times and increase the yields of less reactive alkenes (Table 4, Scheme 10).

Table 4. Alkene epoxidation using a manganese salt

Substrate	No additive		4 mol% salicylic acid	
	H ₂ O ₂ equivalents	% Yield	H ₂ O ₂ equivalents	% Yield
	10	78	5	97
	10	93	5	95
	10	51	5	81

Conditions: As shown in Scheme 10



Scheme 10. The conditions employed for the conversion of alkenes using manganese sulfate and salicylic acid as additive

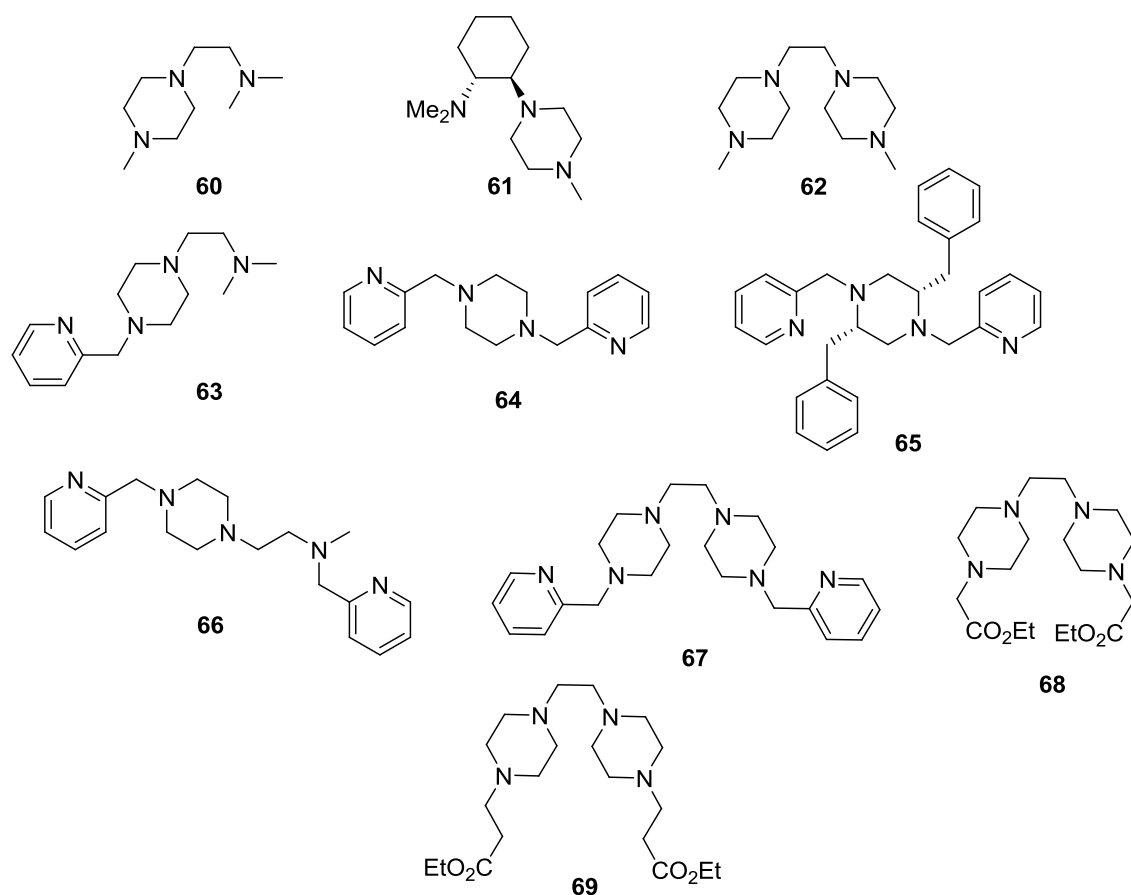
A later report on the use of manganese salts in the efficient epoxidation of terminal alkenes was particularly interesting.⁴⁸ A survey of the first row transition metals in various oxidation states in the epoxidation of 1-decene revealed di- and trivalent manganese salts as the only catalytically active species. Manganese perchlorate (0.4 mol%) was found to give the highest catalytic activity using peracetic acid (2 eq.) in acetonitrile using an ammonium bicarbonate buffer at room temperature. Greater than 99% conversion of 1-decene and 93% epoxide selectivity was observed using GC analysis after thirty minutes.

Competition experiments between 1-nonene and *cis*-3-nonene, showed the catalyst to be selective for the internal alkene in the first twenty minutes, however once the majority of this substrate (85%) had been depleted, the substrate 1-nonene was converted to the epoxide at an even faster rate to that observed for the epoxidation of *cis*-3-nonene. This intriguing behaviour of the catalytic system was interpreted as being controlled by two factors, both of which were based on the assumption that a high-valent electrophilic manganese species was operating as the active species. Firstly, by the binding affinity of the substrate for an electrophilic metal centre and secondly by the process of oxygen atom transfer from the manganese-oxo species to the alkene substrate. The latter of the two processes was suggested to be rate determining. This was used to explain the initial selectivity of the catalyst for the internal olefin. With its higher electron density, compared to the terminal olefin, it was able to react faster with the catalyst, albeit at a slower rate compared to the later conversion of the terminal alkene. Once the majority of the *cis*-3-nonene had been consumed, sites on the metal catalysts become free for coordination by 1-nonene, which was then converted to the epoxide. Further support for this explanation came from independent epoxidation experiments, where 1-nonene was converted to the epoxide product at a significantly faster rate to the *cis*-3-nonene, under the same

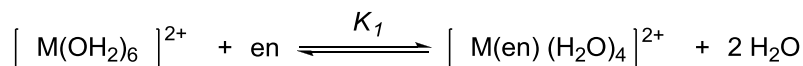
conditions.

1.18 Ligand design

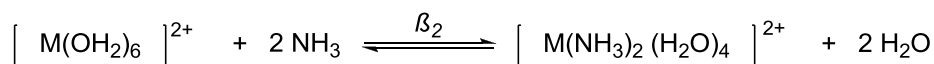
The stability of a catalyst should facilitate its survival under the conditions of the reaction to be catalysed, yet not be so stable that its activity is reduced. For bleaching and epoxidation catalysts, they must survive the inherent oxidising environment that both these classes of reactions necessitate and in the case of a bleaching catalyst, it must also be hydrolytically stable under basic conditions. Ligands **60-69** all contain a number of key common features, they are polydentate, contain tertiary nitrogen donors and they all contain the piperazine backbone. Ligands **60-66** have 3-5 potential donor atoms, this is the same or similar to the number of potential donors observed for the ligands discussed in relation to established catalytic oxidation systems (or systems claimed as bleaching catalysts) using manganese (*vide supra*). These ligands would leave one or more sites free or coordinated by solvent/s, effectively making them labile site/s for interaction with the reactants.



The polydentate nature of the ligands which were planned for synthesis has important consequences as far as complexation to a metal is concerned. It effectively imparts stability to a metal complex through the chelate effect and this is reflected in the larger formation constant (K) involving such ligands compared to their analogous monodentate ligands. The chelate effect can be exemplified by a polydentate ligand such as ethylenediamine (en) and its analogous monodentate ligand, ammonia and their complexation to a particular metal centre (Scheme 11).



M = Cu, $\log K_1 = 10.6$



M = Cu, $\log \beta_2 = 7.7$

Scheme 11. The formation of complexes from ethylenediamine (K_1) and ammonia (β_2)

When K_1 for the polydentate ligand ethylenediamine is compared against the overall formation constant (β_2) for the corresponding bisamine complex, it is found that the former is larger and this is generally true,⁴⁹ and exemplified for copper in Scheme 11. The equilibrium constant and Gibbs free energy (ΔG) of complexation are related by equation 3.

$$\Delta G = \Delta H - T\Delta S = -RT \ln K \quad \text{Equation 3}$$

It can be seen that a larger value for the formation constant (K) will arise from a more negative value for ΔG which could result from a smaller value for ΔH . However, as both complexes contain the same number of bonds of roughly equal strength, the ΔH term is approximately the same for both complexes containing either ethylenediamine or ammonia. The difference arises in the entropic term (ΔS), where an increase in entropy results from the complexation of the polydentate ligand and this can be seen in Scheme 11, where one molecule of the polydentate ligand enters the coordination sphere of the complex and two molecules of water leave, causing an increase in disorder of the system. For the analogous reaction involving the monodentate ligands, two molecules of ammonia replace two molecules of water (Scheme 11), as a result, there is

no net change in the entropic term. The increase in the entropic term involving polydentate ligands compared to their monodentate analogue means a more negative Gibbs free energy value, leading to a larger formation constant, reflected in the greater stability in complexes of polydentate ligands which contain chelate rings.

More specifically, in relation to chelate ring size, coordination of the piperazine moiety to a metal centre would result in two five-membered chelate rings. Five-membered chelate rings formed from saturated organic ligands are able to impart the greatest stability to a complex relative to other chelate ring sizes. This stability in octahedral complexes has its origins in the lack of steric effects owing to the ability of the saturated ligand to fold in order to accommodate the tetrahedral bond angles in the ligand and accommodate the ligand-metal-ligand bite angle of 90° , typical for octahedral complexes.⁴⁹ Furthermore, in terms of equation 3, this reduced steric effect within the coordination sphere compared to other ring sizes serves to reduce the enthalpic term (ΔH) resulting in a more negative Gibbs free energy term (ΔG). Another pertinent reason for the incorporation of the piperazine backbone in ligand systems **60-69**, involves the limited reports of this moiety in ligand systems for use in oxidation catalysts. As such, the piperazine backbone remains a potentially untapped source of ligands for application in oxidation catalysis.

Another common feature in ligands **60-69** are the tertiary nitrogen donor atoms, which are also ubiquitous in the manganese based oxidation catalysts discussed in relation to bleaching and epoxidation catalysis. Interestingly, use of secondary nitrogen donors in place of tertiary ones has been shown to result in non-productive hydrogen peroxide decomposition only, during the attempted alkene epoxidation in the work of De Vos.¹⁵ Tertiary amines are relatively strong field ligands (e.g. compared to iodide), allowing a greater ligand field stabilisation in its transition metal complexes (however, it should be noted that the degree of ligand field stabilisation energy for a particular complex is also dependant on the identity of the metal and its position in the periodic table, its *d*-electron count and its geometry). This is evident from its position in the spectrochemical series for ligands, where members are arranged in order of increasing energy of transitions that occur when they are present in a complex of a particular transition metal.

Furthermore, nitrogen donors are hard donors and they are best able to interact with hard metal centres. The qualitative concept of hard and soft comes from the observation that metals such as those of the first row transition metal series form more stable interactions with elements early in the periodic table and larger metals showing a preference for coordination to larger elements. This definition can be further elaborated to hard metals being classed as having a high positive charge, small size with a high energy LUMO and hard ligands as those with low polarisability, high electronegativity and a low energy HOMO. Soft metals and ligand donors have the opposite characteristic. As such, the bonding interaction between hard metal centres and ligands tend to be more ionic in character compared to interactions involving soft metals and ligands. In the context of a complex in bleaching and epoxidation catalysis, the hard nature of the nitrogen ligand means that it can better stabilise high valent metal-oxo species, which would be expected to have the characteristic of a hard metal species. Such high valent metal species, $\text{Mn}^{\text{IV}}\text{-oxo}$ and $\text{Mn}^{\text{V}}\text{-oxo}$, have been frequently suggested in mechanistic studies concerning the bleaching and epoxidation catalysts discussed (*vide supra*).

Pyridine as a ligand, has the potential to become involved in back-bonding interactions with a metal species. Such an interaction is known to facilitate the increased reactivity of a ligand in a position *trans* to the back-bonding ligand and can be observed in terms of the increased rate of displacement of the *trans*-ligand. This kinetic phenomenon is known as the *trans*-effect and has its origins in the ability of the back-bonding ligand to stabilise higher coordinate transition states. The increased kinetic lability of a ligand *trans* to ligands such as pyridine allows a metal complex a certain amount of reactivity required of a catalytic species. Pyridine is also close to amines in the spectrochemical series for ligands which means that it can potentially impart stability to a metal complex as a whole through ligand field stabilisation. The potential balance between complex stability and reactivity which ligands such as pyridine can impart on a catalytic species may explain the success of the pyridine moiety in oxidation catalysts discussed for manganese (*vide supra*). More specifically, ligands with tertiary nitrogen atoms substituted with the methyl pyridine moiety are particularly common in the aforementioned manganese oxidation catalysts. Such a pyridine moiety was therefore included in the ligand systems (**63-67**), intended for synthesis.

Both ligands **68** and **69** incorporate the ester functionality; these are expected to undergo saponification to the corresponding carboxylate function *in situ*, under the basic conditions of the bleach screening test. This has the advantage of reducing the number of synthetic steps. The pendant carboxylate arm has been incorporated into a number of ligand systems such as **18**, **20** and **21**. These ligands, as part of a manganese based system, have been found to promote the catalytic epoxidation reaction.¹⁶⁻¹⁷

1.19 Conclusions

Bleaching catalysts are certainly the way forward for making the laundry washing process efficient and their environmental and financial advantages have been discussed. The successful inclusion of a bleaching catalyst in a commercial detergent formulation is yet to be reported. However, systems which have been reported for stain bleaching activity have given some insight into the features of ligands which appear to be beneficial in catalytic bleaching systems. This has aided the design of ligands in this work and will allow us to evaluate the efficacy of these features once testing of the proposed ligands has been completed.

However, it must be noted that many of the oxidation systems discussed, in particular catalyst **6** and its derivatives, are poorly understood in terms of their oxidation mechanism in both bleaching and epoxidation. The current work may contribute to this in some way.

1.20 References

1. K. Shastri, Ph.D. Thesis, University of London, 2004.
2. *CRC Handbook of Chemistry and Physics*, ed. D. R. Lide, Taylor and Francis, Boca Raton, FL, 87th edn., 2007.
3. H. J. H. Fenton, *J. Chem. Soc.*, 1894, **65**, 899-910.
4. N. Milne, *Journal of Surfactants and Detergents*, 1998, **1**, 253-261.
5. E. W. C. Cheng. Ph.D. Thesis, University of London, 2010.
6. L. Jae-Duk and L. Man-Ho, *J. Ind. Eng. Chem.*, 2001, **7**, 137-142.
7. R. Hage, J. E. Iburg, J. Kerschner, J. H. Koek, E. L. M. Lempers, R. J. Martens, U. S. Racherla, S. W. Russell, T. Swarthoff, M. R. P. van Vliet, J. B. Warnaar, L. van der Wolf and B. Krijnen, *Nature*, 1994, **369**, 637-639.

8. T. Wieprecht, M. Hazenkamp, H. Rohwer, G. Schlingloff and J. Xia, *C. R. Chimie*, 2007, **10**, 326-340.
9. K. Shastri, E. W. C. Cheng, M. Motevalli, J. Schofield, J. S. Wilkinson and M. Watkinson, *Green Chem.*, 2007, **9**, 996-1007.
10. R. Hage and A. Lienke, *J. Mol. Catal. A: Chem.*, 2006, **251**, 150-158.
11. (a) B. C. Gilbert, N. W. J. Kamp, J. R. Lindsay Smith and J. Oakes, *J. Chem. Soc., Perkin Trans. 2*, 1997, 2161-2165; (b) B. C. Gilbert, N. W. J. Kamp, J. R. Lindsay Smith and J. Oakes, *J. Chem. Soc., Perkin Trans. 2*, 1998, 1841-1843; (c) B. C. Gilbert, J. R. Lindsay Smith, A. M. i Payeras and J. Oakes, *Org. Biomol. Chem.*, 2004, **2**, 1176-1180.
12. B. C. Gilbert, J. R. Lindsay Smith, M. S. Newton, J. Oakes and R. Pons i Prats, *Org. Biomol. Chem.*, 2003, **1**, 1568-1577.
13. A. Sorokin, L. Fraisse, A. Rabion and B. Meunier, *J. Mol. Catal. A: Chem.*, 1997, **117**, 103-114.
14. V. C. Quee-Smith, L. DelPizzo, S. H. Jureller, J. L. Kerschner and R. Hage, *Inorg. Chem.*, 1996, **35**, 6461-6465.
15. D. De Vos and T. Bein, *Chem. Commun.*, 1996, 917-918.
16. D. E. De Vos and T. Bein, *J. Organomet. Chem.*, 1996, **520**, 195-200.
17. V. B. Romakh, B. Therrien, G. Süß-Fink and G. B. Shul'pin, *Inorg. Chem.*, 2007, **46**, 1315-1331.
18. (a) A. Berkessel and C. A. Sklorz, *Tetrahedron Lett.*, 1999, **40**, 7965-7968; (b) D. E. De Vos, B. F. Sels, M. Reynaers, Y. V. Subba Rao and P. A. Jacobs, *Tetrahedron Lett.*, 1998, **39**, 3221-3224.
19. G. B. Shul'pin, G. Süß-Fink and L. S. Shul'pina, *J. Mol. Catal. A: Chem.*, 2001, **170**, 17-34.
20. C. B. Woitiski, Y. N. Kozlov, D. Mandelli, G. V. Nizova, U. Schuchardt and G. B. Shul'pin, *J. Mol. Catal. A: Chem.*, 2004, **222**, 103-119.
21. B. C. Gilbert, J. R. Lindsay Smith, A. Mairata i Payeras, J. Oakes and R. Pons i Prats, *J. Mol. Catal. A: Chem.*, 2004, **219**, 265-272.
22. *Biomimetic Oxidations Catalysed by Transition Metal Complexes*, ed. B. Meunier, Imperial College Press, London, 2000.
23. (a) J. T. Groves, J. Lee and S. S. Marla, *J. Am. Chem. Soc.*, 1997, **119**, 6269-6273; (b) J. T. Groves and M. K. Stern, *J. Am. Chem. Soc.*, 1988, **110**, 8628-8638.

24. J. Brinksmas, L. Schmieder, G. van Vliet, R. Boaron, R. Hage, D. E. De Vos, P. L. Alsters and B. L. Feringa, *Tetrahedron Lett.*, 2002, **43**, 2619-2622.
25. E. N. Jacobsen, L. Deng, Y. Furukawa and L. E. Martínez, *Tetrahedron*, 1994, **50**, 4323-4334.
26. J. W. de Boer, J. Brinksmas, W. R. Browne, A. Meetsma, P. L. Alsters, R. Hage and B. L. Feringa, *J. Am. Chem. Soc.*, 2005, **127**, 7990-7991.
27. J. W. de Boer, W. R. Browne, J. Brinksmas, P. L. Alsters, R. Hage and B. L. Feringa, *Inorg. Chem.*, 2007, **46**, 6353-6372.
28. (a) E. J. Corey and J. W. Suggs, *Tetrahedron Lett.*, 1975, **16**, 2647-2650; (b) J. March, in *Advanced Organic Chemistry*, Wiley, New York, 1992.
29. (a) P. Müller and J. Godoy, *Tetrahedron Lett.*, 1981, **22**, 2361-2364; (b) S. Kanemoto, K. Oshima, S. Matsubara, K. Takai and H. Nozaki, *Tetrahedron Lett.*, 1983, **24**, 2185-2188; (c) W. P. Griffith, S. V. Ley, G. P. Whitcombe and A. D. White, *J. Chem. Soc., Chem. Commun.*, 1987, 1625-1627.
30. C. Zondervan, R. Hage. and B. L. Feringa, *Chem. Commun.*, 1997, 419-420.
31. C. J. Ballhausen and H. B. Gray, *Inorg. Chem.*, 1962, **1**, 111-122.
32. T. A. Betley, Q. Wu, T. Van Voorhis and D. G. Nocera, *Inorg. Chem.*, 2008, **47**, 1849-1861.
33. R. Hage and A. Lienke, *Angew. Chem., Int. Ed.*, 2006, **45**, 206-222.
34. (a) E. G. Samsel, K. Srinivasan and J. K. Kochi, *J. Am. Chem. Soc.*, 1985, **107**, 7606-7617; (b) T. L. Siddall, N. Miyaura, J. C. Huffman and J. K. Kochi, *J. Chem. Soc., Chem. Commun.*, 1983, 1185-1186.
35. K. Srinivasan, P. Michaud and J. K. Kochi, *J. Am. Chem. Soc.*, 1986, **108**, 2309-2320.
36. (a) W. Zhang, J. L. Loebach, S. R. Wilson, and E. N. Jacobsen, *J. Am. Chem. Soc.*, 1990, **112**, 2801-2803; (b) W. Zhang and E. N. Jacobsen, *J. Org. Chem.*, 1991, **56**, 2296-2298.
37. R. Irie, K. Noda, Y. Ito, N. Matsumoto and T. Katsuki, *Tetrahedron Lett.*, 1990, **31**, 7345-7348.
38. L. Kürti, M. M. Blewett and E. J. Corey, *Org. Lett.*, 2009, **11**, 4592-4595.
39. E. M. McGarrigle and D. G. Gilheany, *Chem. Rev.*, 2005, **105**, 1563-1602.
40. T. Kurahashi, A. Kikuchi, Y. Shiro, M. Hada and H. Fujii, *Inorg. Chem.*, 2010, **49**, 6664-6672.

41. (a) D. H. Busch, S. R. Collinson and T. Hubin, WO-A-9839098, 1998; (b) C. M. Perkins, R. Labeque, B. K. Williams, J. P. Johnston, D. J. Kitko, J. C. Burckett-St. Laurent and E. M. Burns, WO-A-9839405, 1997.
42. (a) G. Yin, M. Buchalova, A. M. Danby, C. M. Perkins, D. Kitko, J. D. Carter, W. M. Scheper and D. H. Busch, *Inorg. Chem.*, 2006, **45**, 3467-3474; (b) G. Yin, M. Buchalova, A. M. Danby, C. M. Perkins, D. Kitko, J. D. Carter, W. M. Scheper and D. H. Busch, *J. Am. Chem. Soc.*, 2005, **127**, 17170-17171.
43. (a) G. Schlingloff, T. Wieprecht, F. Bachmann, J. Dannacher, M. J. Dubs, M. Hazenkamp and G. Richter, WO-A-2002088289, 2001; (b) G. Schlingloff, T. Wieprecht, F. Bachmann, J. Dannacher, M. J. Dubs, M. Hazenkamp, U. Heinz, M. Frey and A. Schneider, WO-A-2004007657, 2004; (c) T. Wieprecht, G. Schlingloff, J. Xia, U. Heinz, A. Schneider, M. J. Dubs and F. Bachman, WO 2004039933, 2004.
44. H. Blum, B. Mayer, U. Pegelow, H. D. Speckmann, B. Krebs, M. Duda, C. Nazikkol and J. Reim, WO-A-9730144, 1996.
45. A. Tafesh, M. Beller, V. Friderichs and G. Reinhardt, EP-B-0783035, 1996.
46. J. Oakes, EP-A-0082563, 1981.
47. (a) S. Lane, M. Vogt, V. J. DeRose and K Burgess, *J. Am. Chem. Soc.*, 2002, **124**, 11946-11954; (b) B. S. Lane and K. Burgess, *J. Am. Chem. Soc.*, 2001, **123**, 2933-2934.
48. K. P. Ho, W. L. Wong, K. M. Lam, C. P. Lai, T. H. Chan and K. Y. Wong, *Chem. Eur. J.*, 2008, **14**, 7988-7996.
49. D. F. Shriver and P. W. Atkins, in *Inorganic Chemistry*, Oxford University Press, Oxford, UK, 3rd edn., 1999.

Chapter 2. Ligand Synthesis

2.1 General remarks

Multi-step synthesis involving amines presents a challenge, especially during purification which is a particular problem with solids, where distillation is no longer an option. Flash column chromatography using silica gel as the stationary phase results in the amines being retained on the solid-phase owing to the relative acidity of the Si-OH functionality ($pK_a \sim 7.0$).¹ Pre-treatment of silica using strong bases (e.g. triethylamine) in order to temper the strong interaction between the solid phase and the amines were tried in the course of this work, but this was found to result in poor separation and/or low yields.

Use of neutral alumina in chromatography resulted in better separation and yields, as would be expected, but it was found to be extremely impractical. Very small changes in gradient needed to be performed over large volumes of solvent elution. This was the result of the chromatographic separations displaying extreme sensitivity to small increases in polarity. Using dichloromethane and methanol as the solvent system, a final composition ratio of less than 99:1 (dichloromethane:methanol *v/v*) did not allow separation of the fractions and caused them to elute together and in some cases required much higher ratios (99.999:0.001). A consequence of this was considerable volumes of solvents were required over long periods of time in order to achieve purification of these amines by flash column chromatography.

Use of the *p*-toluenesulfonyl protecting groups in intermediates during the course of this work addressed some of these purification issues as the sulfonamide basicity is significantly reduced and consequently, with such intermediates, purification on silica gel was possible. Furthermore, the presence of the *p*-toluenesulfonyl group was found to facilitate crystallisation and this of course is the most convenient way of purifying a compound.

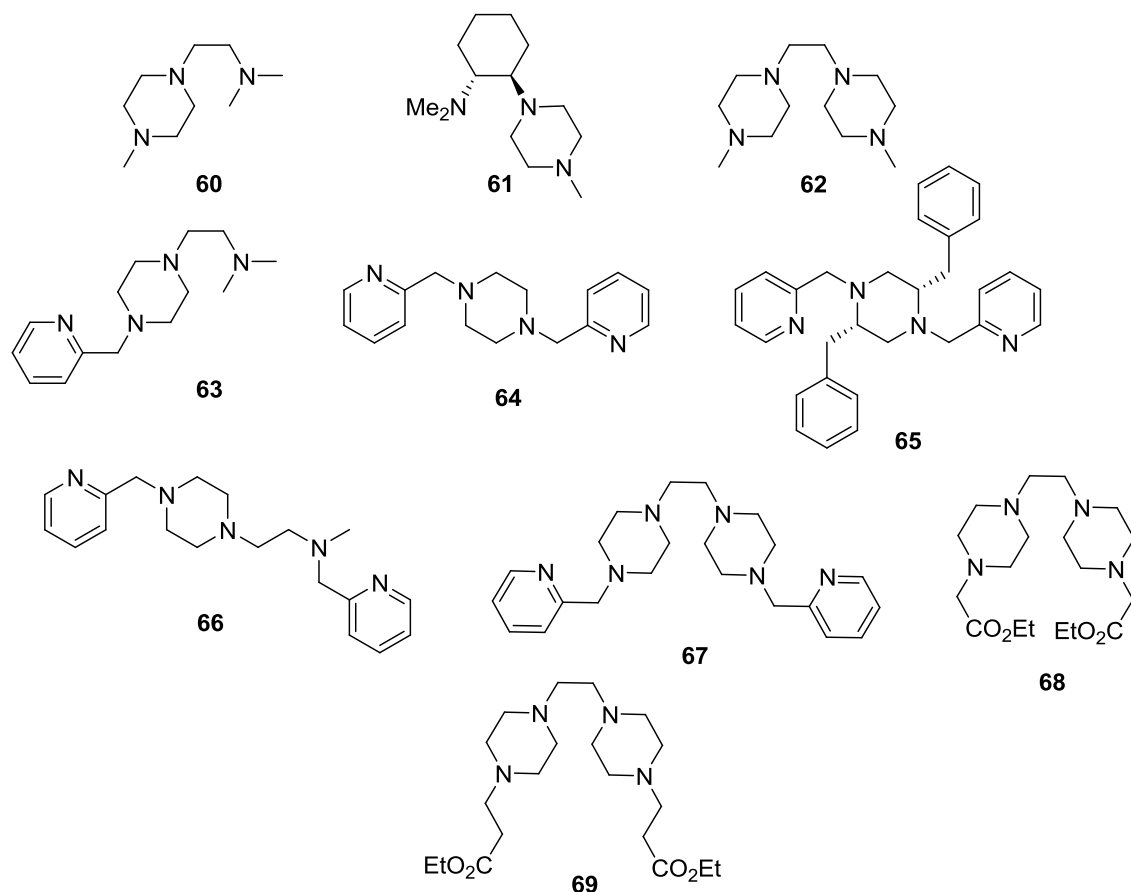
Use of the *p*-toluenesulfonyl protecting group in synthesis has a disadvantage in terms of atom economy with significant loss of mass in the deprotected product owing to the high molecular weight of the protecting group. Furthermore, the removal of the *p*-

toluenesulfonyl protecting group often requires lengthy reaction times and/or harsh reaction conditions.² The deprotection method employed in this work was the reliable yet harsh, concentrated sulfuric acid protocol which requires the sulfonamide to be heated at high temperatures, yielding the sulfate salt. Although the deprotection steps invariably worked well, isolation of the resulting hygroscopic sulfate salts presented many difficulties and in all cases, they proved impossible to isolate and the reagents for the next synthetic step were thus added to the sulfate salt immediately after its formation (a strategy often found to be successful in the Eschweiler-Clarke³ *N*-methylation reactions). The hydrobromide salts of many of the amines were found to be much more stable and the sulfate salts were sometimes easily converted by addition of concentrated HBr. The HBr salts, where isolable, were found to be a suitable means of storing intermediates one or two synthetic steps from the final ligand. This strategy was necessary as amines are reactive species which display facile reactivity with atmospheric components such as CO₂ and O₂. A consequence of this reactivity in this work was that the final amine containing ligands were rarely stable for more than two months, even when refrigerated under an atmosphere of dry N₂. This meant a great deal of repeat synthetic work had to be carried out during this work, often from step one of the synthesis where a stable HBr salt intermediate could not be obtained.

All of the target ligands are polydentate, contain tertiary nitrogen donors and the piperazine backbone in order to impart stability in their metal complexes (see section 1.18). Some of these ligands also contain the pyridine moiety and others a precursor to the carboxylate functionality. Both of these features have been found to be beneficial in catalytic oxidation systems.

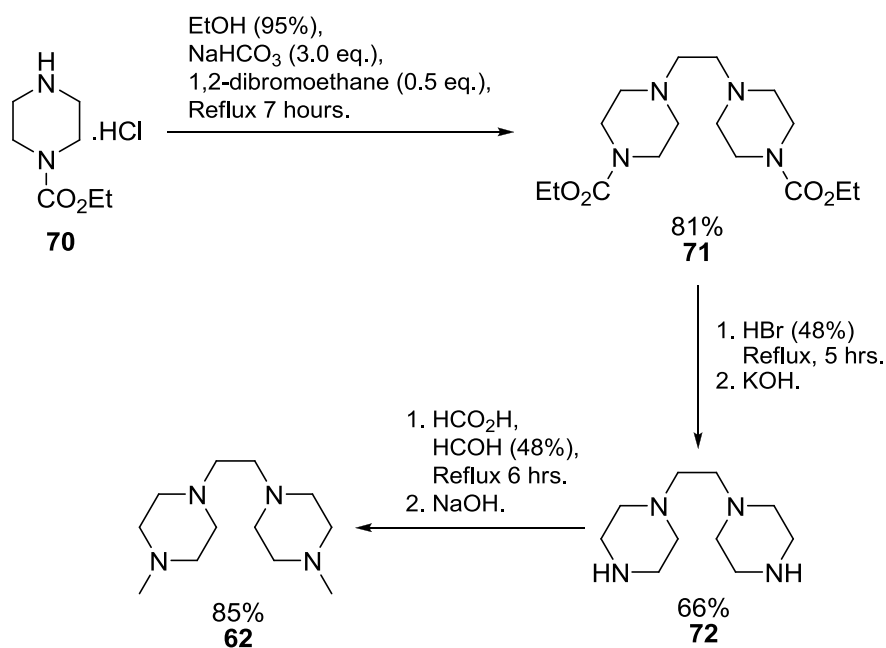
Compounds **61**, **63**, **65**, and **67-69** are all new compounds. Methodologies for the synthesis of **60** (see section 2.4), **62** (see section 2.2) and **64** (see section 4.17) have been reported, however, **60** and **62** along with their respective precursors were synthesised by methods developed during the course of this research. Modifications to the synthetic protocol used in the synthesis of **62** were used in the preparation of new compounds **67-69** (see section 2.3). Similarly, novel compound **63** was accessed using an analogous synthetic strategy (see section 2.5) developed for the synthesis of compound **60**. Also, in order to facilitate the synthesis of **63** a novel precursor, **96**, was prepared. Furthermore, all the known precursors to compound **63** were synthesised by methods developed during the current work. During the synthesis of novel compound

61 (an asymmetric variant of **60**), it was necessary to prepare a new precursor, compound **102** (see section 2.6). All the known precursors to compound **61** were prepared using existing methodologies (see chapter 4). Likewise, all precursors to novel chiral compound **65** were synthesised using methodologies previously described (see section 2.7). However, compound **65** was synthesised from a known precursor by a method developed during the course of this research.



2.2 Synthesis of ligand **62**

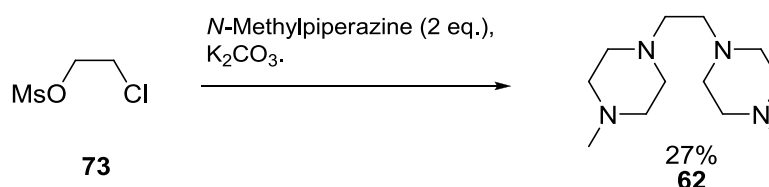
The synthesis of ligand **62** has been reported previously,⁴ the different methods are described in more detail in Schemes 12-14. Mann and Baker^{4b} (Scheme 12) start with carbamate **70**, which on reaction with 1,2-dibromoethane furnished intermediate **71** in 81% yield.



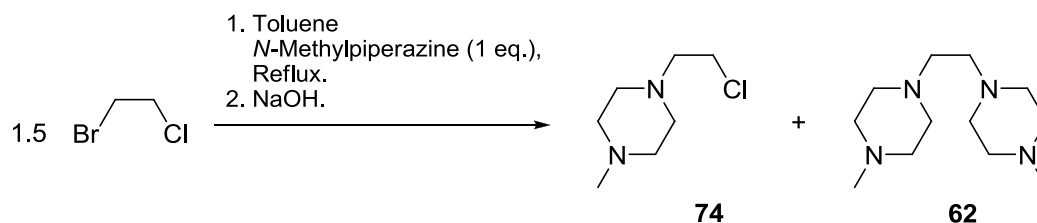
Scheme 12. Synthesis of ligand **62** carried out by Mann and Baker^{4b}

Hydrolysis of **71** using hydrobromic acid followed by a basic work-up, yielded the hygroscopic free amine **72** (66%), which was *N*-methylated using the Eschweiler-Clarke methodology (*vide infra*) to give compound **62** in 85% yield (45% overall yield in three steps). Distillation was required to obtain intermediate **72** and compound **62** in their pure forms.

A later synthesis (Scheme 13) described^{4c} the formation of **62**, in a very inefficient manner, using **73** as the electrophile and *N*-methylpiperazine, giving compound **62** in only 27% yield after purification by distillation. Synthesis of compound **62** has also been described more recently^{4a} as a by-product in an attempted synthesis of another species (**74**), although the yield for **62** was not reported (Scheme 14).

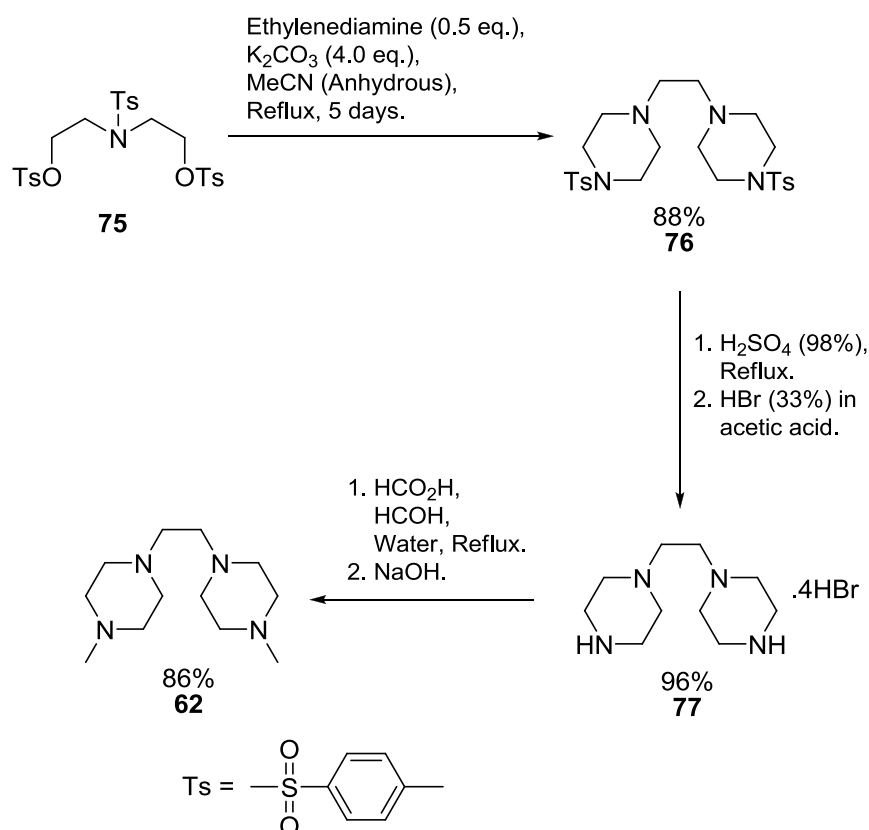


Scheme 13. Synthesis of ligand **62** carried out by Cohen *et al.*^{4c}



Scheme 14. Synthesis of ligand **62** carried out by Caliendo *et al.*^{4a}

The routes to compound **62** discussed so far all require one (or more) distillation step in order to obtain the pure product and the yield in at least one case was very poor. The method used to synthesise **62** in the current work is outlined in Scheme 15. It involved the formation of the piperazine rings *in situ* from electrophile (**75**) and ethylenediamine producing intermediate **76** in good yield (88%).

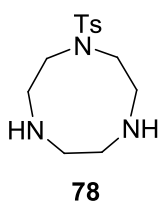


Scheme 15. Synthesis of ligand **62** undertaken in this work

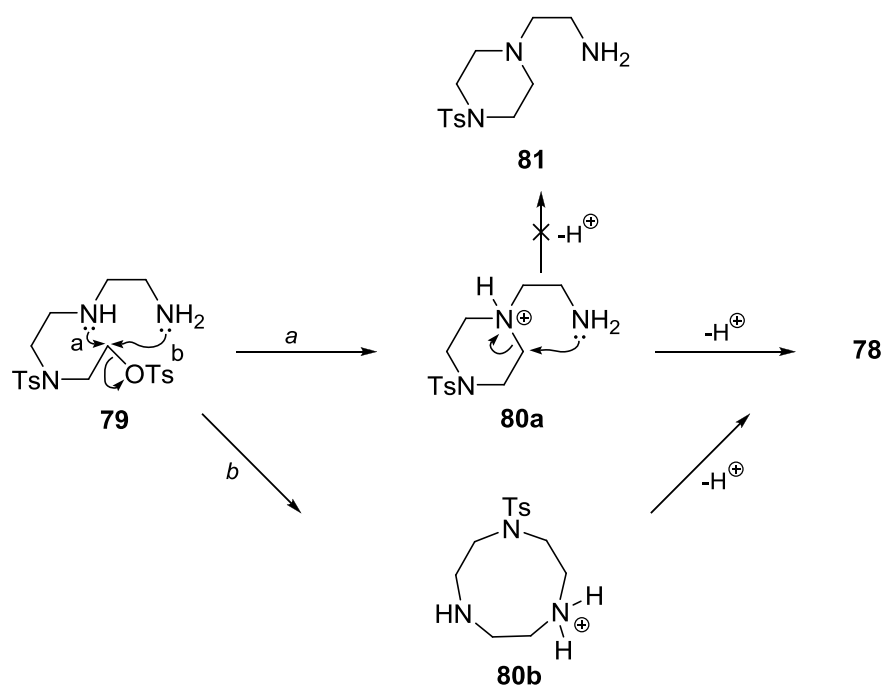
Detosylation of **76** using concentrated sulfuric acid yielded the sulfate salt which along with the free amine was found to be extremely hygroscopic (*vide supra*). Addition of concentrated HBr (48%) to the crude sulfate salt resulted in the formation of the

tetrahydrobromide salt **77**, in excellent yield (96%) which was found to be stable. This salt could be conveniently recrystallised from water allowing a pure form of the free amine to be obtained. Any impurities carried forward from either the earlier cyclisation or detosylation steps were easily removed giving **77** as a storable source of the free amine. *N*-Methylation of this salt using the Eschweiler-Clarke protocol furnished compound **62** (86%) with an overall yield of 73% in three steps. This represents a much improved synthesis of **62** in terms of the ease of preparation (requiring no involved purification) and the yield obtained, compared to the synthesis already described where a 45% overall yield was reported in three steps.

Interestingly using the same reaction conditions as in the synthesis of **76** and changing the ratio of ethylenediamine:**75** from 1:2 to 1:1, the formation of compound **78** has very recently⁵ been reported as the major product (78%). This type of reactivity has not been observed in the present work (*vide infra*).

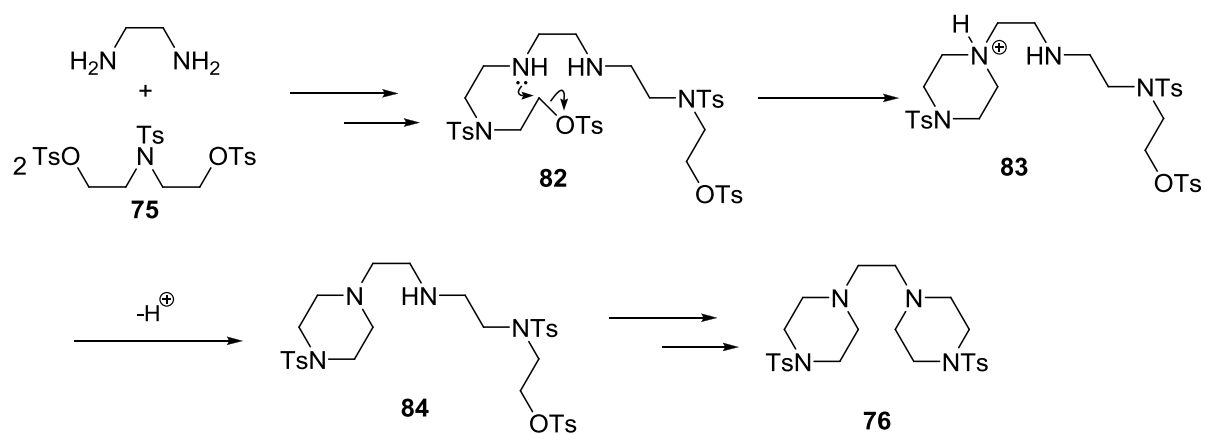


The reasons behind the formation of a nine-membered ring (**78**) are unclear. Using a 1:1 ratio of the aforementioned reagents, two pathways, *a* and *b*, to cyclisation become available to an intermediate **79** (Scheme 16). With pathways *a* or *b* leading to either a six-membered or nine-membered ring respectively. A direct route to **78** *via* pathway *b* was the favoured mechanism in the reported synthesis of **78**.⁵ However, on the basis of ring strain in the respective products, and the well established thermodynamics of cyclisation, pathway *a* should predominate⁶, leading to a relatively strain free six-membered ring in cationic intermediate **80a**. Deprotonation of **80a** would then lead to **81**, which is not the major product reported. Instead what must be occurring is a fast intra-molecular nucleophilic attack by the primary amine leading to the observed kinetic product **78**. However, attempts to repeat the synthesis of **78** as reported were unsuccessful.

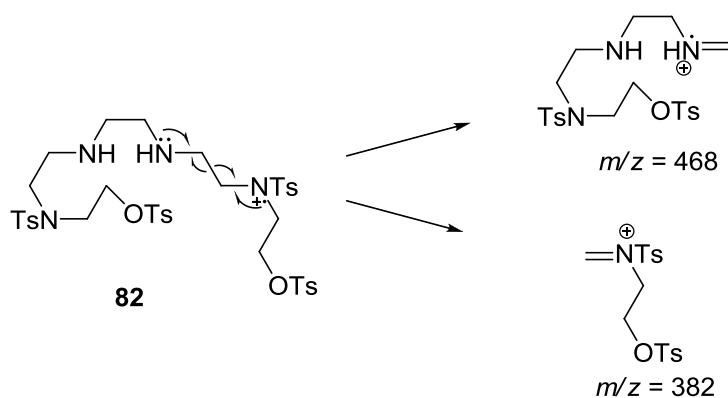


Scheme 16. Suggested mechanisms for the formation of compound **78** (Pathway *a*) as opposed to that postulated by Chan *et al.* (Pathway *b*).⁵

Using a 1:2 ratio of ethylenediamine:**75**, an analogous substitution reaction in intermediate **82** (as in intermediate **79**, pathway *a*) leading to a six-membered cationic intermediate, **83**, is again, tentatively suggested (Scheme 17). In this case, deprotonation in **83** becomes faster than attack by the sterically hindered secondary amine, which in this case has already undergone the first substitution reaction with a second equivalent of the electrophile **75**. This leads to the formation of intermediate **84**, which under the basic conditions of the reaction is unlikely to be reversibly protonated, eventually producing **76**. Using GCMS, intermediates relating to **82** have been observed in the reaction mixture. Under the harsh conditions of electron ionisation, fragments corresponding to **82** at $m/z = 468$ and 382 have been observed (Scheme 18), providing support for the suggested mechanisms. Subsequent analysis by high resolution ESI-MS of the reaction mixture sampled at different times showed the molecular ion corresponding to **82** at m/z 851.2479 ($M + H^+$), with the relative abundance of this signal (for **82**) found to be decreasing with time, as would be expected based on the mechanism proposed in Scheme 17.



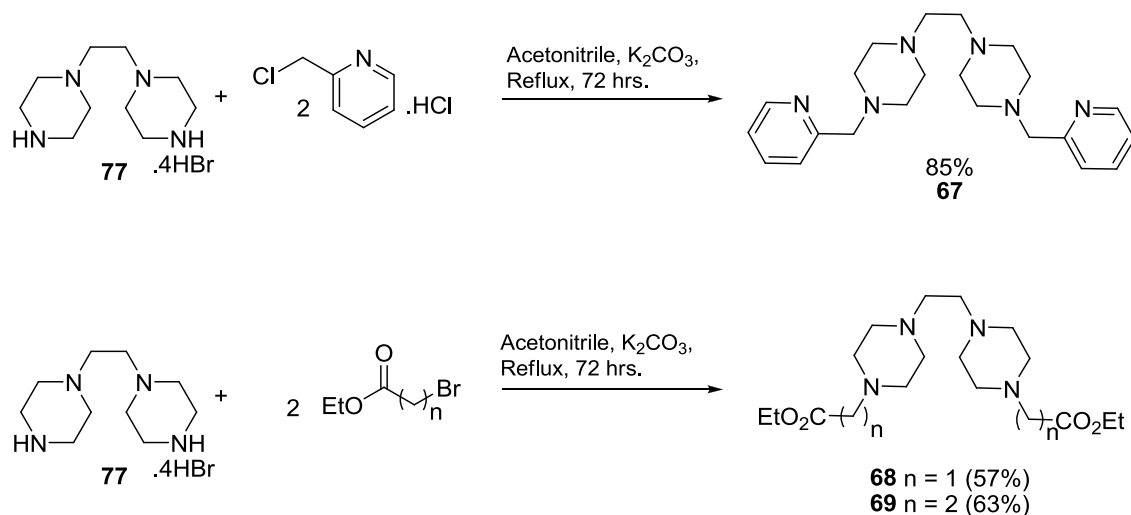
Scheme 17. Suggested mechanism leading to compound **76**



Scheme 18. Proposed fragmentation of **82** under EI during GCMS analysis

2.3 Synthesis of **67**, **68** and **69**

Compounds **67**, **68** and **69** are all novel and were synthesised in good yield from the tetrahydrobromide salt **77** (Scheme 19). Crystals of compound **67**, suitable for X-ray analysis were produced from a solution of diethyl ether and a crystal structure obtained. The structure confirms the formation of the six-membered rings in compound **76** (*vide supra*), a precursor to compound **67** and the structure is consistent with all other spectroscopic data for compound **67**.



Scheme 19. Synthesis of **67**, **68** and **69**

The crystal structure shows (Figure 4) the piperazine ring in the expected thermodynamically favoured chair-like conformation. The bulkier substituents on the piperazine nitrogens are in the equatorial positions leaving the lone pairs to assume axial positions. The packing arrangement of the molecules of **67** within the unit cell is shown in Figure 5. Selected bond lengths and angles are shown below (Table 5) and they are not dissimilar to other 2-pyridylmethyl derivatives.⁷

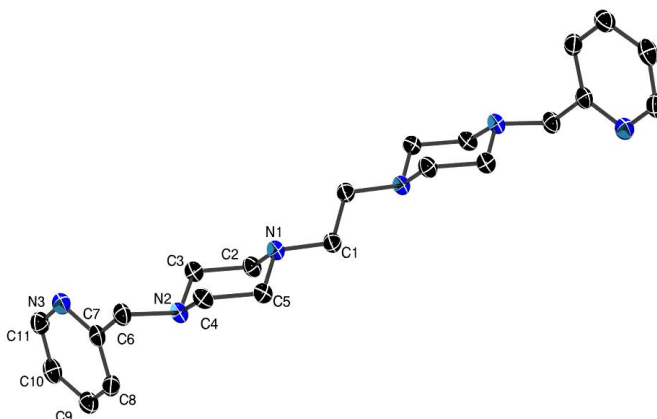


Figure 4. ORTEP⁸ plot of the single crystal X-ray structure of **67** with 50% probability displacement ellipsoids

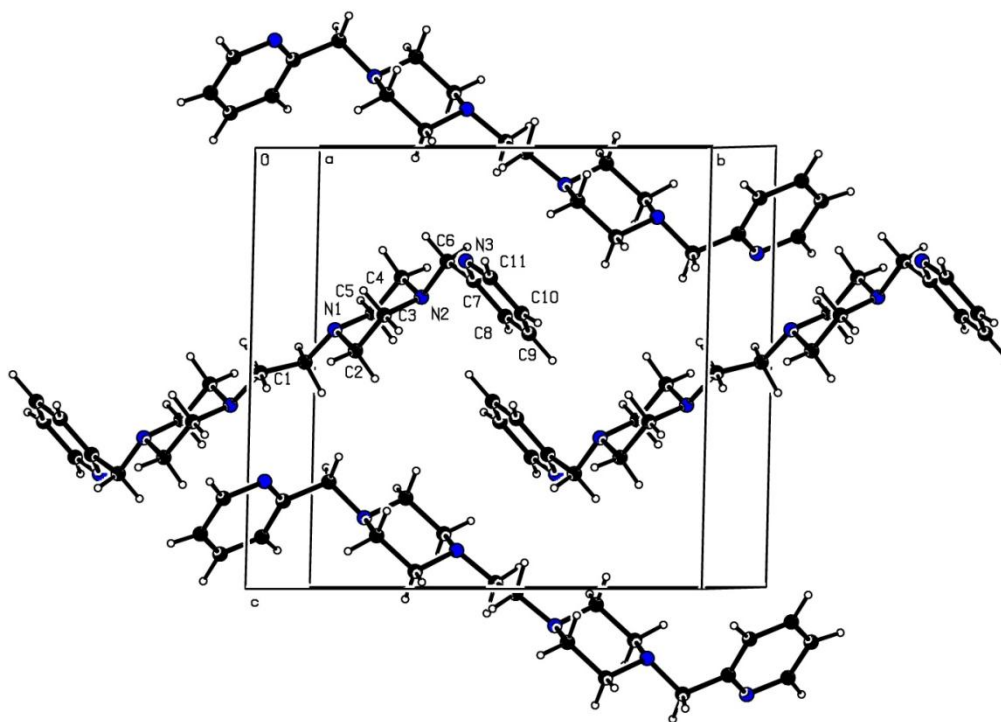


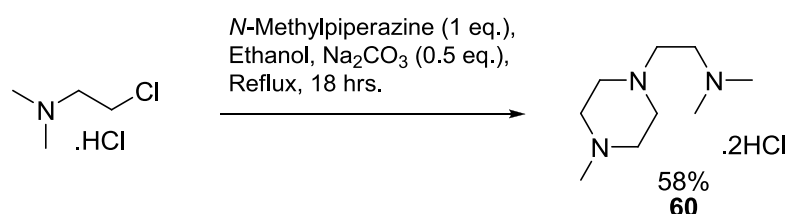
Figure 5. A Platon⁹ representation of a fragment of the crystal lattice for compound **67**, showing the packing arrangement of the molecules

Table 5. Selected bond lengths (Å) and angles (°) for compound **67** with e.s.ds

Bond	Length (Å)	Bond	Angle (°)
C(1)-N(1)	1.466(3)	N(1)-C(2)-C(3)	110.22(16)
C(2)-N(1)	1.467(2)	C(5)-N(1)-C(2)	108.01(15)
C(2)-C(3)	1.517(3)	C(6)-N(2)-C(3)	109.88(15)
C(3)-N(2)	1.464(2)	N(2)-C(4)-C(5)	110.87(15)
C(6)-N(2)	1.462(3)	N(2)-C(6)-C(7)	112.62(15)
C(6)-C(7)	1.507(3)	N(3)-C(7)-C(8)	122.81(18)
C(7)-N(3)	1.345(3)	N(3)-C(7)-C(6)	117.17(19)
C(7)-C(8)	1.387(3)	C(8)-C(7)-C(6)	120.02(18)
C(8)-C(9)	1.381(3)	C(9)-C(8)-C(7)	119.11(19)
C(9)-C(10)	1.382(3)	C(8)-C(9)-C(10)	118.8(2)
C(10)-C(11)	1.372(3)	C(7)-N(3)-C(11)	116.81(19)
C(11)-N(3)	1.352(3)	N(3)-C(11)-C(10)	123.77(19)

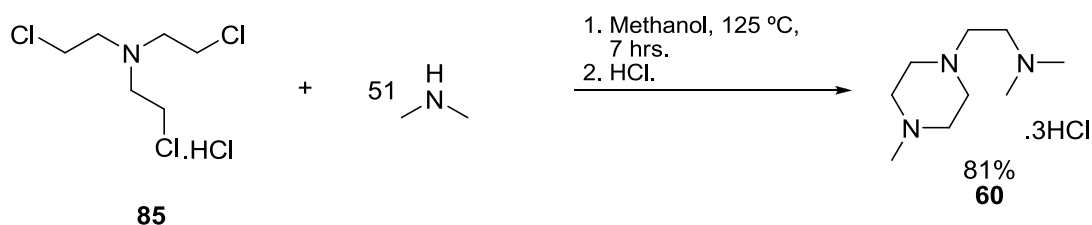
2.4 Synthesis of compound 60

The synthesis of ligand **60** has been reported in detail previously with reasonable yields.^{4b, 10} The method used by Stewart and Turner *et al.*¹⁰ is outlined in Scheme 20 and produced the dihydrochloride salt of **60** in moderate yield.



Scheme 20. Synthesis of the hydrochloride salt of **60** carried out by Stewart and Turner *et al.*¹⁰

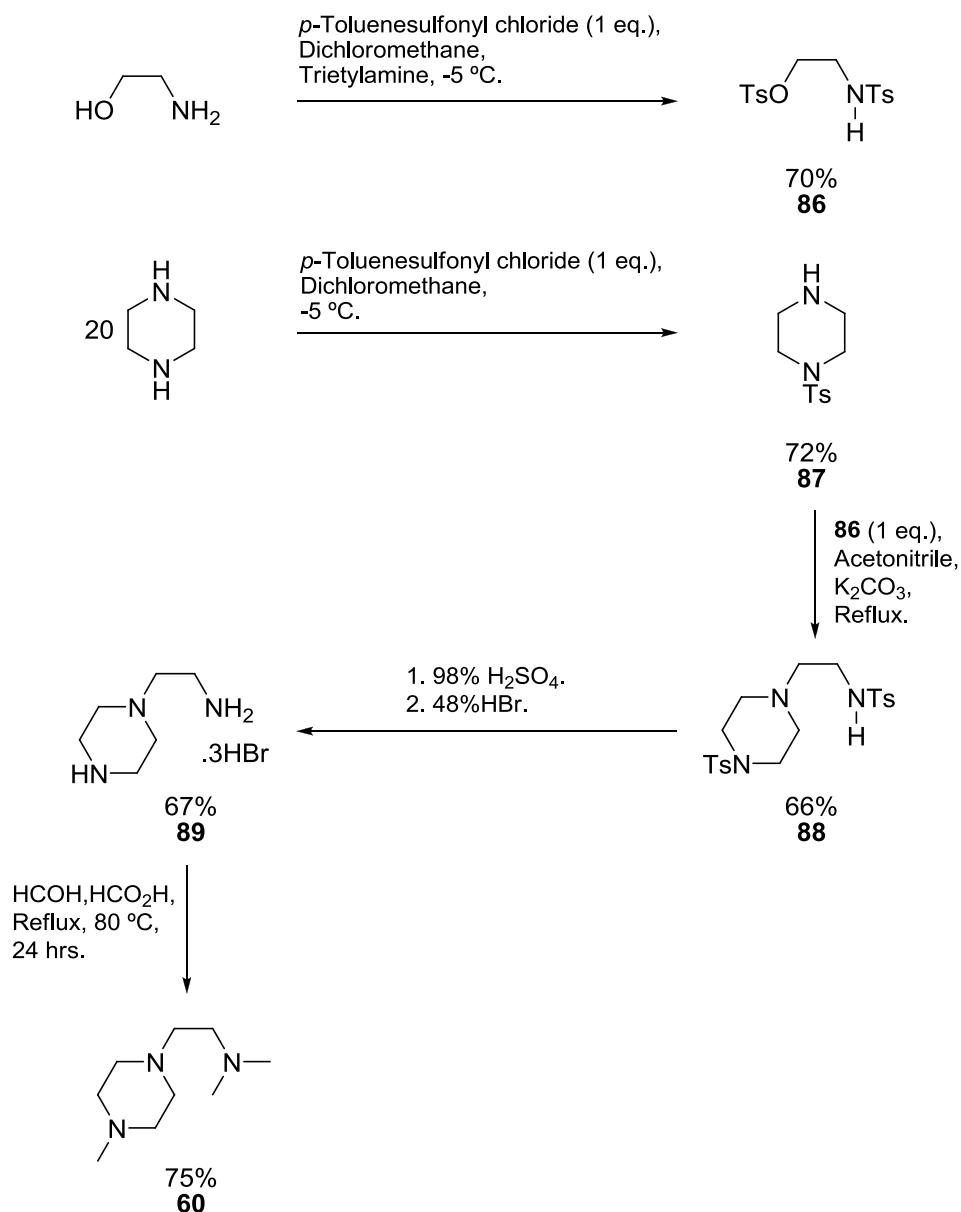
A later synthesis by Mann and Baker^{4b} reports an improved yield to that already discussed. It is outlined in Scheme 21 for the formation of the trihydrochloride salt of **60**. However reagent **85** is an unpleasant compound and a suspected carcinogen, making this route to compound **60** undesirable.



Scheme 21. Synthesis of the HCl salt derivative of **60** carried out by Mann and Baker^{4b}

The favoured route to **60** is outlined in Scheme 22 and has the advantage over those depicted above of opening up routes to the synthesis of derivatives of compound **60**. Precursor **86** was synthesised in good yield as was compound **87**. In the synthesis of **87**, anhydrous piperazine was added in a twenty-fold excess to *p*-toluenesulfonyl chloride to statistically favour the synthesis of the mono-tosylated derivative **87**. Indeed the strategy worked very well, with the formation of the doubly-tosylated piperazine derivative not being detected by ¹H NMR spectroscopy or high resolution mass spectrometry (ESI). The excess piperazine (some) also functioned as the required base

in order to remove the stoichiometrically produced hydrochloric acid. This strategy of mono-functionalisation of the piperazine ring later found utility in the synthesis of another derivative of compound **60** (*vide infra*).



Scheme 22. Synthetic strategy undertaken in this work in obtaining compound **60**

With both **86** and **87** in-hand, the substitution reaction producing **88** proceeded in moderately good yield. Using a concentrated sulfuric acid detosylation protocol for **88** yielded the extremely hygroscopic sulfate salt, which was converted to the relatively stable trihydrobromide salt (**89**) by addition of concentrated HBr (48%). However, the analyst carrying out elemental analysis on a sample of **89** noted that it was gaining

weight during weighing, probably demonstrating its hygroscopic nature, albeit to a lesser degree than the sulfate salt. Despite this, **89** appeared to be stable, when stored under anhydrous conditions, for a number of months. Isolation and storage of **89** as a relatively stable precursor to **60** was necessary as compound **60** itself was found to be unstable over long periods of time, even when refrigerated under an atmosphere of dry nitrogen. As compound **60** was required for testing over a number of years throughout this research, **89** served as a useful precursor to **60**, and was one step away using a reliable transformation (*vide infra*).

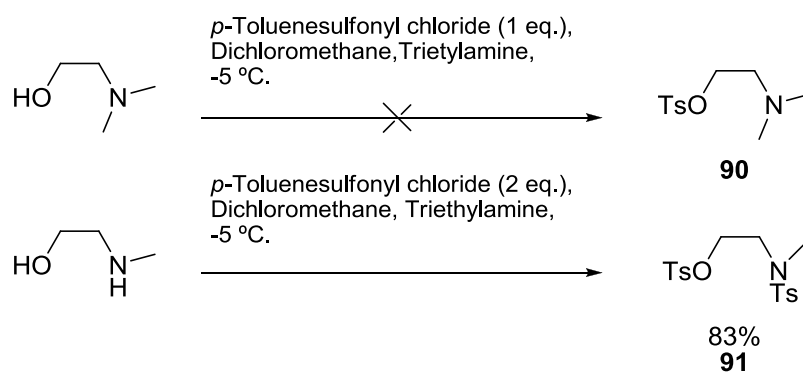
The Eschweiler-Clarke methodology was used to *N*-methylate the free base of **89**, with both the primary and secondary amines of the piperazine ring being alkylated. This methodology was selected as it had been demonstrated to form less of the quaternary ammonium salt by-product which can be problematic, particularly when using alkyl halides such as methyl iodide as the electrophile.¹¹ The methodology used, gave the desired amine **60** in good yield directly from the salt, **89**.

2.5 Synthesis of compound **63**

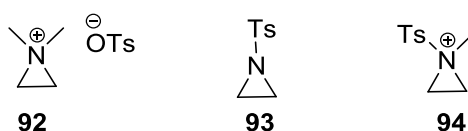
The first step in a possible synthesis of the novel compound **63**, analogous to the strategy used for **60**, was expected to be unsuccessful (Scheme 23). Attempts to synthesise the tosyl-protected amino alcohol **90** using *N,N*-dimethyl ethanolamine under the conditions used for both **86** and **91** would almost certainly result in the formation of aziridinium species **92**. Compound **90** has been reported to have been prepared using an *in situ* methodology but was not isolated.¹² A reasonable explanation for the instability of compound **90** compared to **86** and **91** is the increasing nucleophilicity of the respective nitrogen atoms in this series of compounds, where it is increasing in the order **86** < **91** < **90**. For **90**, tosylation of the precursor alcohol in *N,N*-dimethyl ethanolamine should be followed by a fast intra-molecular nucleophilic attack by the tertiary nitrogen, leading to compound **92**. Similar formation of aziridinium species by mesylation of β -amino alcohols has been previously reported.¹³

Further support for the formation of aziridinium species such as **92** comes from the observation that species **86** and **91** also exhibited the formation of related three-membered rings, albeit in a greatly reduced manner (as expected on the basis of their reduced nucleophilicity), giving the three-membered aziridine (**93**) and aziridinium (**94**)

species respectively, which were detected as impurities by mass spectrometry. For compound **86**, using EI-MS, a molecular ion consistent with **93** was detected at $m/z = 197.0$ (M^+). Similarly for **91**, using ESI-MS a molecular ion consistent with **94** was detected at $m/z = 212.1$ (M^+).



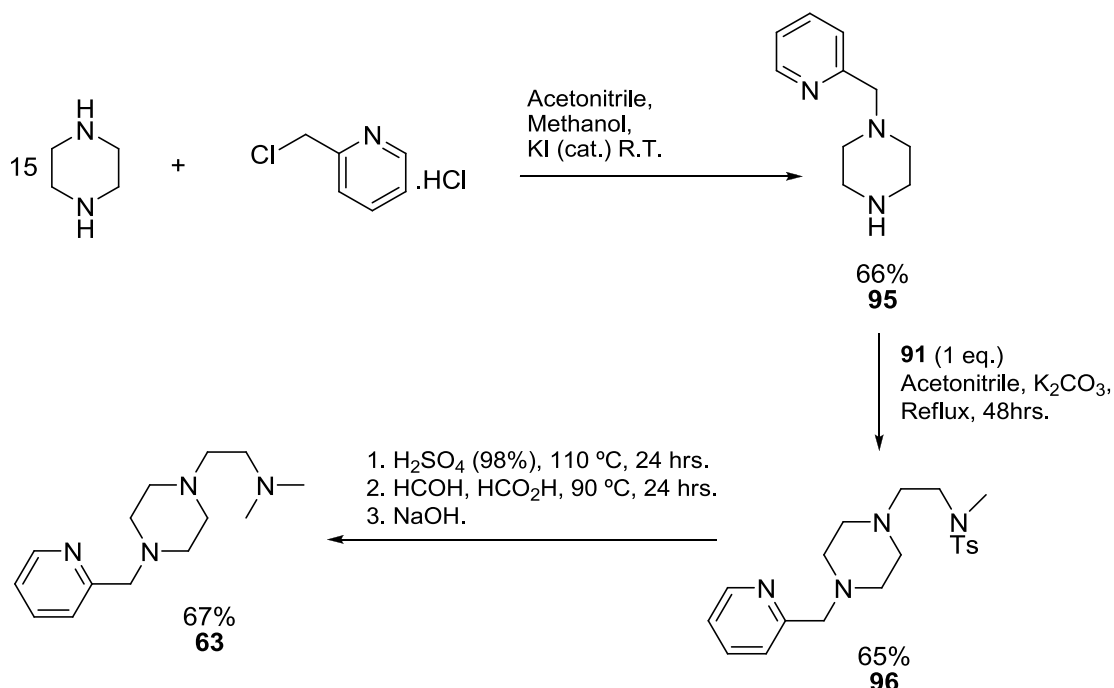
Scheme 23. Synthesis of Compound **91**



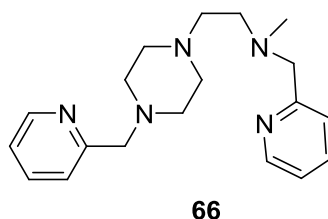
Attempts at synthesising compound **95** (Scheme 24) using an analogous strategy as that used to generate **87** proved successful. The principle of using a large excess of piperazine, in order to favour the mono-functionalisation of one piperazine nitrogen over complete *N*-functionalisation was again employed to achieve this. However, as this is a statistically favoured reaction, small amounts of the 1,4-bis substituted piperazine were formed but in larger quantities than that observed in the synthesis of **87**. Purification by column chromatography was required using neutral alumina and as a consequence a lower yield (66%) of **95** was obtained in comparison to that obtained for **87** (77%).

Synthesis of compound **96** proceeded in good yield from **91** and **95** (65%) and it was effectively detosylated using concentrated sulfuric acid. The formation of the hydrobromide salt of the resulting sulfate salt by addition of concentrated HBr (48%) most probably occurred, but attempts to isolate this species were unsuccessful as it was also extremely hygroscopic and dissolved on collection into the sinter funnel. This was disappointing as derivatives of compound **63**, such as **66**, may have been prepared from

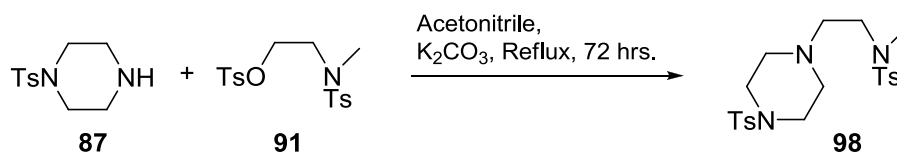
an isolable hydrobromide salt, adding to the intended ligand library. Nonetheless, immediate addition of the Eschweiler-Clarke reagents to the sulfate salt produced **63** cleanly, in good yield (67%).



Scheme 24. Synthetic route to compound **63**



Another route to compound **66** was attempted by synthesis of precursor **98**. The synthesis of **98** is outlined in Scheme 25 and was produced in good yield (80%). Crystals suitable for single crystal X-ray diffraction were obtained in order to study its geometry in the solid form.



Scheme 25. Synthesis of compound **98** in this work

As observed for compound **67**, the piperazine ring is in the thermodynamically favoured chair conformation. Both substituents of the piperazine nitrogen atoms are in the equatorial plane. The methyl substituents of the two *p*-toluenesulfonyl groups are positioned 90° to each other and both of the aromatic rings lie in a plane perpendicular to the piperazine ring (Figures 6 and 7). The N-S bond lengths of 1.6385(18) Å (N(1)-S(1)) and 1.6336(17) Å (N(3)-S(2)) are typical of those found in sulfonamides (1.60-1.63 Å).¹⁴ This indicates the delocalisation of the nitrogen lone pair and partial double bond character of the N-S bond. Further, the sum of the bond angles around the sulfonamide nitrogen atoms is tending towards planarity (346° and 349° for N(1) and N(3) respectively), away from the trigonal pyramidal expected for an *sp*³ nitrogen (such as N(2) where the sum of bond angles is 330°). Selected bond lengths and angles are given in Table 6.

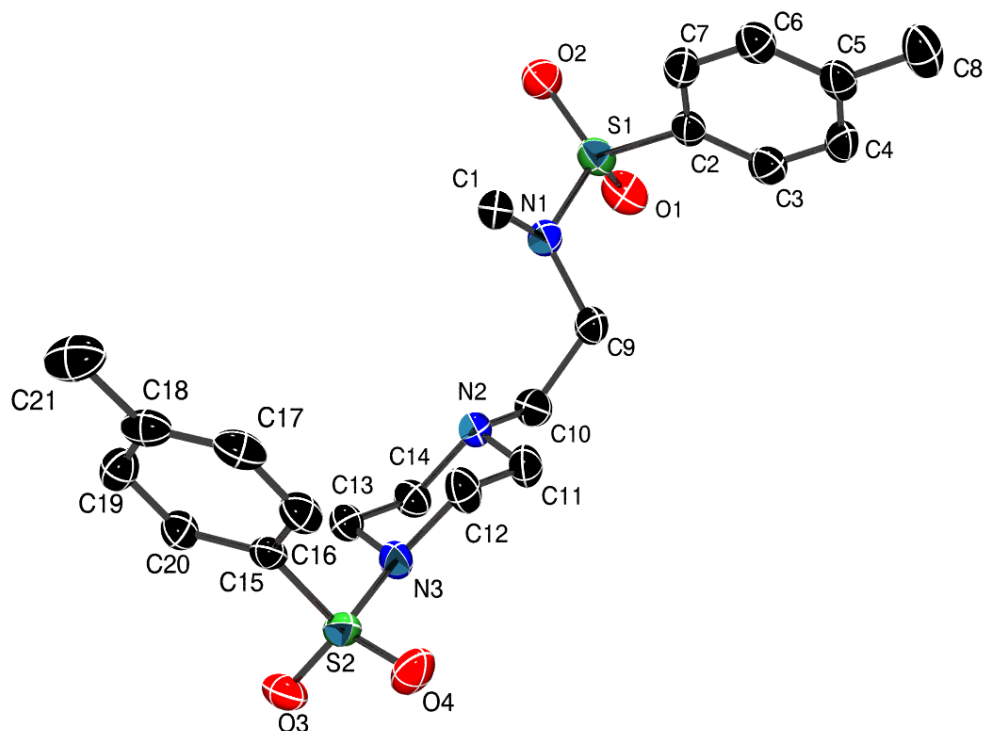


Figure 6. ORTEP⁸ plot of the single crystal X-ray structure of **98** with 50% probability displacement ellipsoids

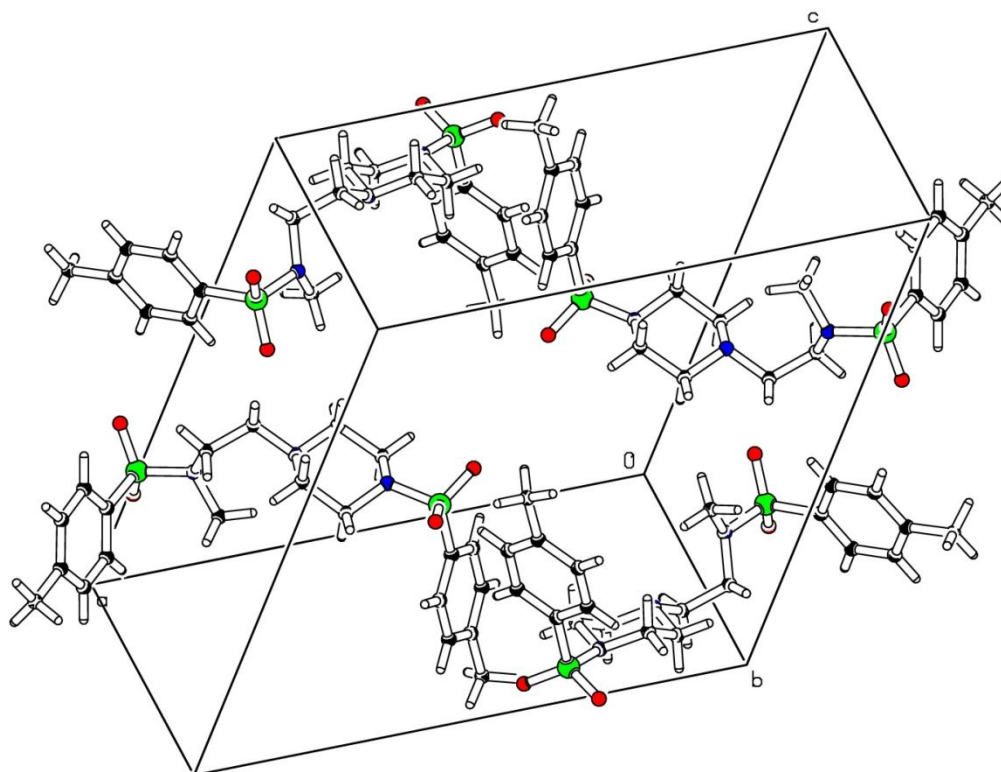


Figure 7. A SHELX¹⁵ representation of a fragment of the crystal lattice for compound **98**, showing the packing arrangement of the molecules in the unit cell

Table 6. Selected bond lengths (Å) and angles (°) for compound **98** with e.s.ds

Bond	Length (Å)	Bond	Angle (°)
N(1)-S(1)	1.6385(18)	C(1)-N(1)-C(9)	115.37(16)
N(3)-S(2)	1.6337(17)	C(1)-N(1)-S(1)	114.96(14)
C(1)-N(1)	1.477(3)	C(9)-N(1)-S(1)	115.46(14)
C(9)-C(10)	1.520(3)	C(13)-N(3)-S(2)	119.18(14)
C(10)-N(2)	1.466(3)	C(12)-N(3)-S(2)	117.24(14)
C(11)-N(2)	1.473(3)	C(13)-N(3)-C(12)	112.34(16)
C(11)-C(12)	1.517(3)	C(14)-N(2)-C(10)	110.24(16)
O(1)-S(1)	1.4310(18)	C(14)-N(2)-C(11)	108.89(17)
C(2)-S(1)	1.769(2)	C(10)-N(2)-C(11)	110.52(17)
C(15)-S(2)	1.763(2)	C(3)-C(2)-S(1)	121.18(18)
C(2)-C(3)	1.386(3)	C(2)-C(3)-C(4)	118.7(2)
C(3)-C(4)	1.398(3)	C(5)-C(4)-C(3)	122.0(2)
C(4)-C(5)	1.381(4)	C(4)-C(5)-C(8)	121.9(2)
C(5)-C(8)	1.501(3)	N(2)-C(10)-C(9)	115.05(18)

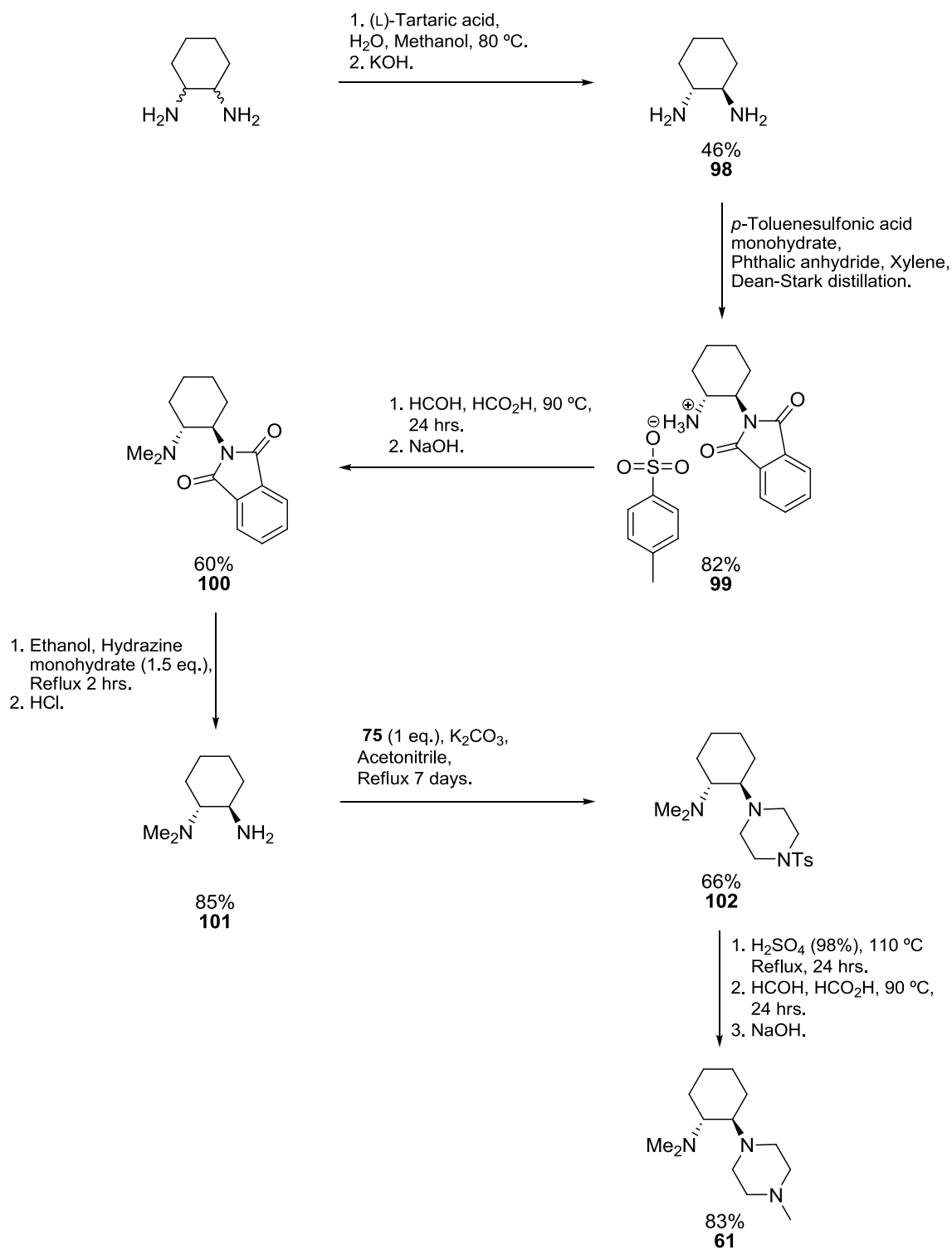
Unfortunately, detosylation, followed by the attempted formation and isolation of the hydrobromide salt was again unsuccessful. This prevented subsequent derivatisation to compound **66**.

2.6 Synthesis of compound **61**

Synthesis of a chiral derivative (**61**) (Scheme 26) of ligand **60** was undertaken for particular use in the testing for asymmetric epoxidation catalysis. In order to achieve this, the diaminocyclohexane backbone was chosen as the source of asymmetry (*vide supra*, 1.12). Resolution of a single enantiomer of *trans*-1,2-diaminocyclohexane was achieved through the use of an enantiomerically pure tartaric acid and the formation of diastereoisomeric salts.¹⁶ Using this method, the diastereoisomeric salt of *R,R*-diaminocyclohexane conveniently crystallises out of solution and can be collected. The free amine, **98**, can then be liberated using potassium hydroxide.

In order to access compound **61**, unsymmetrical derivatisation of the diaminocyclohexane backbone was necessary. A convenient and efficient way of mono-protecting the diaminocyclohexane backbone has been reported by Kaik and Gawronski¹⁷ and leads to the formation of compound **99** (the *p*-toluene sulfonate salt **99** precipitates out of solution in a clean and high yielding reaction) in a single step from the enantiomerically pure amine **98**. Monophthaloylation is explained to occur over derivatisation of both the amine functionalities due to the steric effect of the phthaloyl group on the vicinal amine functionality preventing its reaction with a further equivalent of phthalic anhydride. Furthermore, formation of the salt from *p*-toluenesulfonic acid, ensures precipitation of **99** out of solution preventing further reaction. In this work, compound **99** was obtained in 82% yield which was less than that reported (96%), but nonetheless it proved to be an efficient reaction.

Compound **100** was synthesised using the Eschweiler-Clarke protocol directly from the salt **99** as described by Kaik and Gawronski. The yield of 60% was lower than that reported (86%). This may be due to the necessary change in solvent system for crystallisation where the reported use of a benzene-*n*-hexane system was not viable due to the carcinogenic nature of benzene. Instead an ethanol-diethyl ether system was found to work reasonably well.



Scheme 26. Synthetic route to compound **61**

Deprotection of the phthaloyl group in **100** was effected using the protocol described by Kaik and Gawronski. Using hydrazine hydrate (monohydrate) followed by treatment with hydrochloric acid (0.5 M), and neutralisation with sodium hydroxide furnishing the chiral amine **101** in 85% yield.

With the *R,R*-isomer, **101** in-hand, derivatisation of its primary amine was undertaken using the electrophile **75**, in an analogous cyclisation to that used to form compound **76**. The cyclisation worked well, forming the previously unreported compound **102** in 66% yield after recrystallisation from an acetone-water solvent system.

Crystals that formed were of suitable quality for single crystal X-ray diffraction analysis and a structure of the novel compound **102** was obtained (Figures 8 and 9). As expected both the diaminocyclohexane backbone and the piperazine rings are in the thermodynamically favoured chair conformation. Both of the amine groups on the cyclohexane backbone are in the equatorial positions, as are both bulky substituents of the piperazine nitrogen atoms. The diaminocyclohexane ring lies in a plane perpendicular to that of the piperazine ring which lies in a plane perpendicular to the aromatic ring of the *p*-toluenesulfonyl group. As for compound **98**, the N-S bond length of 1.6352(14) Å is that expected for a sulfonamide and the sum of the bond angles around N(3) is 345 °, which is deviating from the trigonal pyramidal expected for an sp^3 nitrogen (such as N(1) where the sum of the bond angles are 336 °). The bond lengths and angles are as expected and a selection are presented in Table 7.

Compound **61** was synthesised by removal of the sulfonamide protecting group using concentrated sulfuric acid followed by precipitation of the sulfate salt by addition of the acidic reaction mixture to diethyl ether. After the diethyl ether was decanted, the Eschweiler-Clarke reagents were immediately added producing the per-methylated compound **61** in sufficient purity and excellent yield (83%).

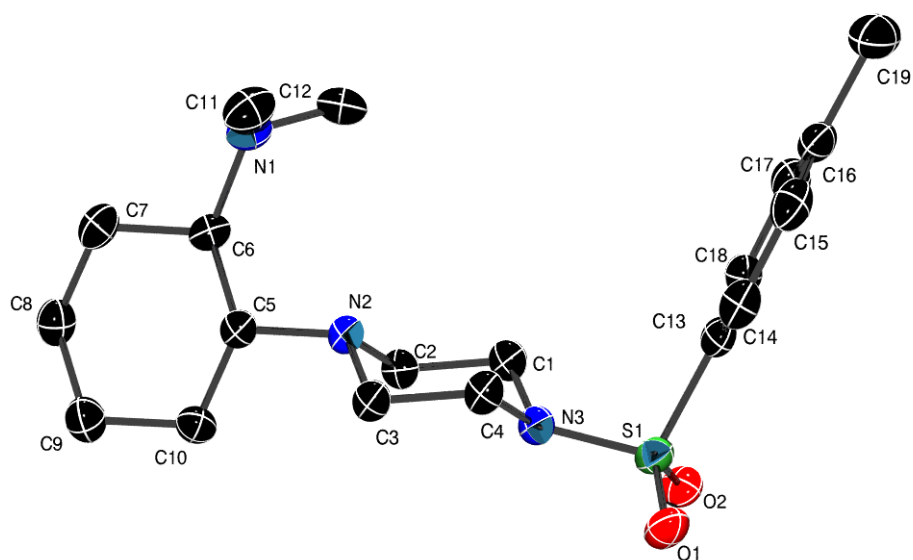


Figure 8. ORTEP⁸ plot of the single crystal X-ray structure of **102** with 50% probability displacement ellipsoids

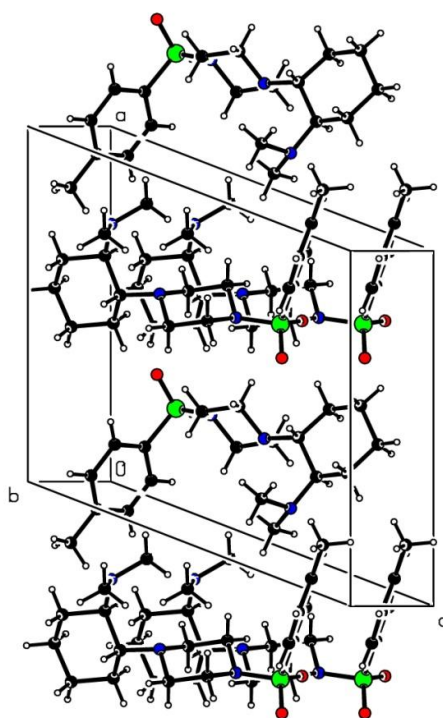


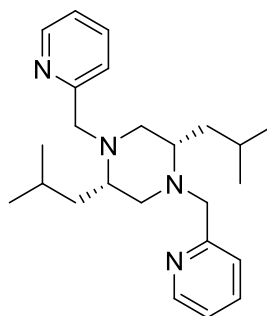
Figure 9. A SHELX¹⁵ plot representing a fragment of the crystal lattice for compound **102**, showing the packing arrangement of the molecules in the unit cell

Table 7. Selected bond lengths (Å) and angles (°) for compound **102** with e.s.ds

Bond	Lengths (Å)	Bond	Angle (°)
N(3)-S(1)	1.6352(14)	C(1)-N(3)-C(4)	111.37(13)
C(1)-N(3)	1.468(2)	C(1)-N(3)-S(1)	116.82(10)
C(1)-C(2)	1.514(2)	C(4)-N(3)-S(1)	116.95(11)
C(2)-N(2)	1.456(2)	C(2)-N(2)-C(3)	109.80(13)
C(5)-N(2)	1.478(2)	C(2)-N(2)-C(5)	113.95(13)
C(5)-C(6)	1.540(2)	C(3)-N(2)-C(5)	112.15(12)
C(6)-C(7)	1.531(2)	C(12)-N(1)-C(11)	110.81(15)
O(1)-S(1)	1.4240(13)	C(12)-N(1)-C(6)	115.34(14)
C(13)-S(1)	1.7544(18)	C(11)-N(1)-C(6)	114.80(15)
C(13)-C(14)	1.385(2)	N(3)-C(1)-C(2)	108.58(13)
C(14)-C(15)	1.388(3)	C(7)-C(6)-C(5)	108.20(14)
C(15)-C(16)	1.386(3)	O(1)-S(1)-O(2)	120.17(8)
C(16)-C(19)	1.509(3)	O(1)-S(1)-N(3)	106.78(7)

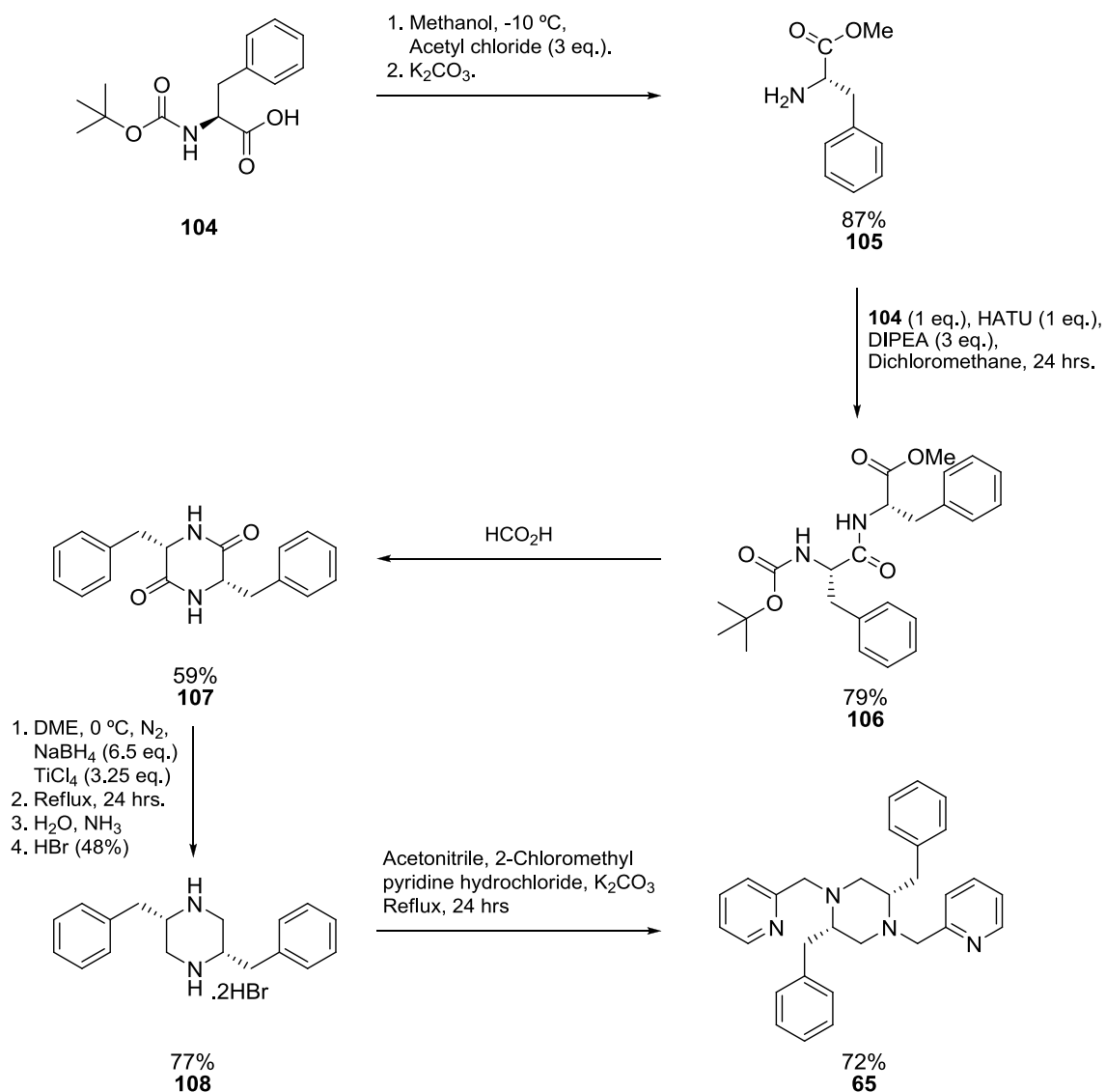
2.7 Synthesis of compound **65**

The synthesis of another asymmetric ligand, **65**, was planned based on ligand **103**¹⁸ where the stereogenic centres would be positioned in the 2,5-positions of the piperazine ring. The planned synthesis for **65** is outlined in Scheme 27 and mirrors the synthesis of **103** utilising an elegant synthesis first proposed by Nitecki *et al.*¹⁹

**103**

Starting with enantiomerically pure amino acids, the synthesis facilitates the simultaneous formation of the piperazine backbone with the stereogenic centres of the starting amino acids placed in the 2,5-positions.

Conversion of **104** to **105** was achieved cleanly in a very efficient reaction where the choice of the methanol solvent was important. Reaction of the acid chloride with methanol produced hydrochloric acid (3 equivalents) as a by-product in a controlled manner removing the Boc-protecting group and also the catalytic amount of acid required in the esterification of the carboxylic acid functional group. Finally, the remaining hydrochloric acid furnishes the hydrochloride salt which was conveniently collected.



Scheme 27. Synthetic route used to produce **65**

The free amine was liberated by treatment with base producing **105** in high yield (87%). The coupling of **104** and **105** was facilitated by the coupling agent HATU again in a

high yielding reaction (79%) in the production of **106**. The diketopiperazine **107** was accessed by treatment with formic acid in moderately good yield (59%). The complete reduction of **107** was accomplished using sodium borohydride in the presence of a Lewis acid, titanium tetrachloride, in good yield (77%). The product was obtained as a thick brown oil which was converted to the hydrobromide salt **108** for ease of handling. Derivatisation of the piperazine nitrogens in order to produce **65** was undertaken using conditions already described as exemplified in the synthesis of **67** from its precursor **77**. Using this procedure, **65** was synthesised in good yield (77%).

2.8 Conclusions

The synthesis of the ligands described has been a challenging part of the project. However, all of the ligands originally planned for synthesis were successfully prepared except **66**. Use of the *p*-toluenesulfonyl chloride protecting group proved to be highly beneficial in this synthetic work despite its drawbacks (*vide supra*). It no doubt aided the numerous purification steps by facilitating crystallisation or solidification of many compounds, both novel and also those previously reported. In doing so, much time was saved especially in the purification of new compounds such as **97** and **102**.

The synthesis of compound **62** has been described without the need for involved purification steps. This is certainly an improvement on the best reported method where a number distillation steps were required.^{4b} Furthermore, an improved yield for **62** was obtained compared to this synthesis. Some insight into the cyclisation mechanism in the formation of a precursor to **62** (compound **76**) was gained through the detection of a reaction intermediate (**82**) by using mass spectrometry. The slow crystallisation of salt **77** (a precursor to **62**) from water in order to obtain a highly pure form of this compound, eventually proved beneficial as it also served as a precursor to **67**, **68** and **69**.

The favoured route to compound **60**, developed during this work opens the possibility for the synthesis of derivatives. Although many variants of **60** were not pursued during this work (owing to time constraints) compound **63** is essentially a derivative, synthesised using the same strategy. Furthermore, if either **60** or **63** show any activity in catalytic oxidation, the synthetic routes used in their preparation will allow tuning of their activity through the preparation of derivatives in the future. A chiral derivative of

60 (61) was successfully prepared along with another chiral compound **65**. These ligands open the possibility of asymmetric induction in the planned alkene epoxidation screening.

With a small selection of piperazine based ligands in hand, testing for their efficacy in oxidation processes (bleaching and alkene epoxidation) will allow evaluation of these ligands in terms of the structural features which are found to be beneficial in terms of oxidation catalysis.

2.9 References

1. M. L. Hair and W. Hertl, *J. Phys. Chem.*, 1970, **74**, 91-94.
2. (a) B. Nyasse, L. Grehn and U. Ragnarsson, *Chem. Commun.*, 1997, 1017-1018; (b) G. Sabitha, B. V. Subba Reddy, S. Abraham and J. S. Yadav, *Tetrahedron Lett.*, 1999, **40**, 1569-1570.
3. (a) H. T. Clarke, H. B. Gillespie and S. Z. Weisshaus, *J. Am. Chem. Soc.*, 1933, **55**, 4571-4587; (b) W. Eschweiler, *Chem. Ber.*, 1905, **38**, 880-892.
4. (a) G. Caliendo, R. Di Carlo, G. Greco, R. Meli, E. Novellino, E. Perissutti and V. Santagada, *Eur. J. Med. Chem.*, 1995, **30**, 77-84; (b) F. G. Mann and F. C. Baker, *J. Chem. Soc.*, 1957, 1881-1899; (c) H. L. Yale, A. I. Cohen and F. Sowinski, *J. Med. Chem.*, 1963, **6**, 347-350.
5. J. Huang, Z. Zhou and T. H. Chan, *Synthesis*, 2009, 2341-2344.
6. (a) J. E. Baldwin, *J. Chem. Soc., Chem. Commun.*, 1976, 734-736; (b) J. E. Baldwin, J. Cutting, W. Dupont, L. Kruse, L. Silberman and R. C. Thomas, *J. Chem. Soc., Chem. Commun.*, 1976, 736-738; (c) J. E. Baldwin and M. J. Lusch, *Tetrahedron*, 1982, **38**, 2939-2947; (d) J. E. Baldwin, R. C. Thomas, L. Kruse and L. Silberman, *J. Org. Chem.*, 1977, **42**, 3846-3852; (e) C. D. Johnson, *Acc. Chem. Res.*, 1993, **26**, 476-482.
7. J. Ratilainen, K. Airola, R. Fröhlich, M. Nieger and K. Rissanen, *Polyhedron*, 1999, **18**, 2265-2273.
8. L.J. Farrugia, ORTEP-3 for Windows, *J. Appl. Cryst.*, 1997, **30**, 565.
9. A. L. Spek, PLATON: A Multipurpose Crystallographic Tool, Utrecht University, Utrecht, The Netherlands, 1998.
10. H. W. Stewart, R. J. Turner, J. J. Denton, S. Kushner, L. M. Brancone, W. L. McEwen, R. I. Hewitt and Y. Subbarow, *J. Org. Chem.*, 1948, **13**, 134-143.

11. S. H. Pine and B. L. Sanchez, *J. Org. Chem.*, 1971, **36**, 829-832.
12. J. Mlynarski, J. Jankowska and B. Rakiel, *Tetrahedron: Asymmetry*, 2005, **16**, 1521-1526.
13. (a) C. Couturier, J. Blanchet, T. Schlama and J. Zhu, *Org. Lett.*, 2006, **8**, 2183-2186; (b) P. O'Brien and T. D. Towers, *J. Org. Chem.*, 2002, **67**, 304-307.
14. K. F. Sibbons, Ph.D. Thesis, University of London, 2008.
15. G. M. Sheldrick, *Acta. Crystallogr., Sect. A*, 2008, **64**, 112-122.
16. F. Galsbøl, P. Steenbøl and S. Sørensen, *Acta. Chem. Scand.*, 1972, 3605-3611.
17. M. Kaik and J. Gawroński, *Tetrahedron: Assymetry*, 2003, **14**, 1559-1563.
18. M. Ostermeier, C. Limberg, C. Herwig and B. Ziemer, *Z. Anorg. Allg. Chem.*, 2009, **635**, 1823-1830.
19. D. E. Nitecki, B. Halpern and J. W. Westley, *J. Org. Chem.*, 1968, **33**, 862-864.

Chapter 3. Results and Discussion

3.1 General remarks

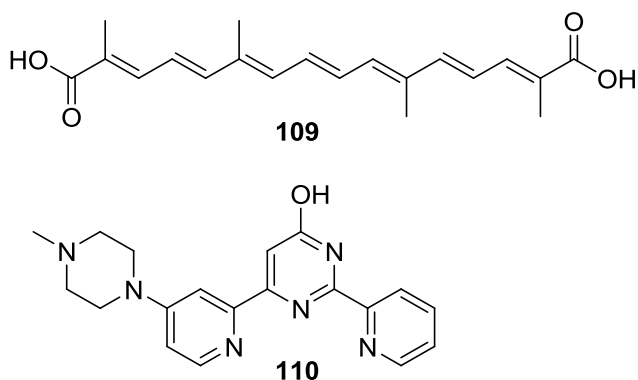
The testing of ligands for their efficacy as bleaching catalysts was carried out using methods provided by my industrial sponsors (Warwick International Ltd.). The primary screening test could be carried out without any specialist equipment (*vide infra*, 4.34) and ligands were tested as they were prepared throughout the study. Ligands which demonstrated promise in the primary screening test were carried forward for testing in the initial stain removal test (wash-test), which essentially replicates typical European laundry washing conditions. Specialist equipment was required for this test which was only available at the company site (*vide infra*, 4.35). As a consequence, not all of the ligands prepared were evaluated using this test.

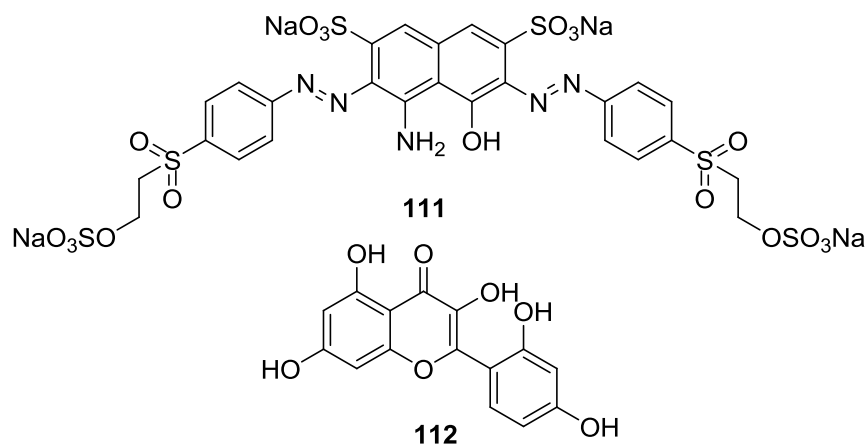
All of the ligands prepared were tested for their efficacy in alkene epoxidation using a method developed in the course of this work. Finding conditions which facilitate the epoxidation reaction and allow the survival of the epoxide product proved to be a challenge and required much developmental work. Despite this, an efficient method in this regard was eventually found and allowed the testing of the ligands (*vide infra*, 4.36).

3.2 The primary screening test

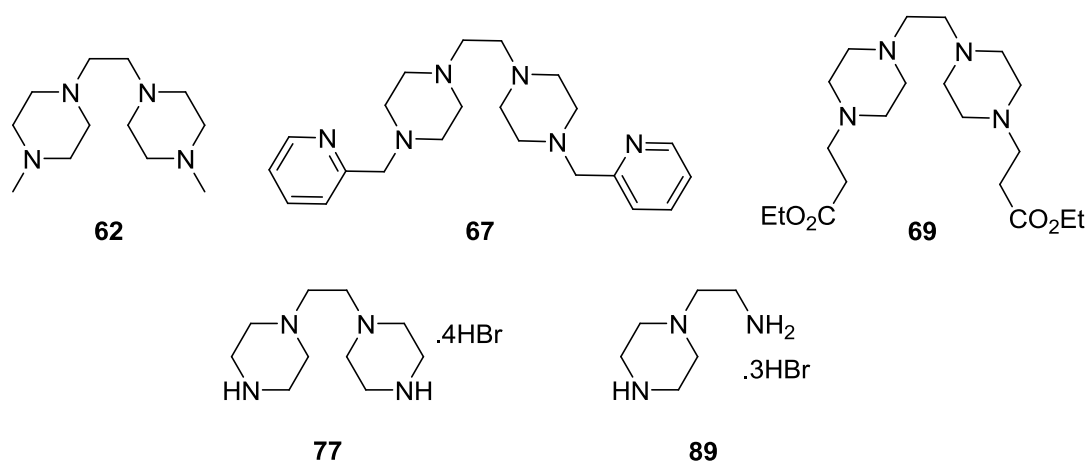
As any potential bleaching catalyst must show activity under the conditions of the wash-test, the screening test to identify such species must replicate these conditions as closely as possible. The wash-test was carried out on a litre scale, and as work on this scale would be impractical for the screening test, it was scaled down 10-fold. However, in the primary screening test, a catalyst concentration of 1×10^{-5} M was used but in the wash-test this concentration was approximately halved (4.6×10^{-6} M, equivalent to 50 ppm manganese level). This was to allow the detection of less active systems in the primary screening test. Also, the wash-test was carried out at 40 °C and the primary screening test was run at ambient temperature. This was for the sake of practicality and to allow the screening test to be carried out on a reasonable timescale.¹

Furthermore, a fast method of testing the efficacy of a potential catalytic system needed to be in place in order to increase the chances of finding a successful hit. A system which assumed *in situ* catalyst formation by combination of the test ligand and a series of metal salts was put in place in order to achieve this. Such a system avoided the lengthy process of preparing complexes of particular metal-ligand combinations. This strategy was used in both the primary screening test and the wash-test. Peracetic acid was appropriate for the screening test as it was formed in the wash-test from hydrogen peroxide and **3** (TAED). A suitable stain mimic was a more complex issue as stains are chemically varied. A wide range of dyes representing all the major dye classes were tested and crocetin (**109**) (extracted from saffron, see 4.34) was chosen as the most suitable model dye substrate as it gave a reliable and repeatable indication of catalytic bleaching activity. However, it must be stressed that crocetin is very different in its chemical nature to many other dye and stain molecules, for example polyphenols, found in tea and red wine. Indeed, examples of the same catalyst showing excellent bleaching activity with one type of substrate, then little or no activity with others are known.² This is exemplified by the fact that the iron(II) complex of a bispyridyl pyrimidine ligand (**110**), in alkaline media exhibited excellent bleaching with a textile dye, R Bk005 (**111**), however, the catalyst activity was drastically reduced with the substrate Morin (**112**), a polyphenol. Further, when the metal ion was changed to manganese(II) the reactivity was inverted for the same substrates. Another point which must be noted from the outset is that in a real wash-test, the bleach catalysis occurs with stains on fabrics, whereas in the screening test the stains are in solution.





The ligands under evaluation for catalytic activity (**62**, **67**, **69**, **77**, **89**) were combined with a series of metal salts, VCl_3 , $MnCl_2 \cdot 4H_2O$, $FeCl_3$, $CoCl_2 \cdot 6H_2O$ and $CuSO_4 \cdot 5H_2O$. Again it is important to stress that any potential bleaching catalyst was assumed to form *in situ*.



The activity of a particular metal-ligand combination was compared to a series of standards, for a qualitative assessment of activity in the bleaching of **109** using peracetic acid as the oxidant. The first standard contained a carbonate buffer (pH = 10, see 4.34), IEC-A detergent solution containing sequestrant and crocetin dye. Standard two contained carbonate buffer, IEC-A detergent solution containing sequestrant, metal salt, dye and peracetic acid. Finally, the third standard contained the same composition as standard two, where the metal salt was $CoCl_2 \cdot 6H_2O$ and another component, the ligand 1,10-phenanthroline. The test was monitored by following the decrease in intensity of the yellow crocetin colour over time, by eye. Standard one allowed the elimination of colour depletion (oxidation of **109**) by aerial oxidation. The second standard evaluated the effect of metal ion oxidation

and/or any oxidation due to species formed by interaction of the metal salt with the oxidant. The final standard was a guide to the potency of a test metal-ligand combination. The cobalt, 1,10-phenanthroline combination forms a potent bleaching catalyst for the bleaching of **109**. A metal, ligand combination which performed better than standard two was considered as active and one which performed comparably to standard three was considered to be an excellent candidate for further development.

In order to test the influence of metal to ligand ratio on potential bleaching activity the test was carried out on a 1:1 and 1:2 metal to ligand ratio. The results indicated that the different metal to ligand ratio did have an influence on bleaching activity using the same ligand. Ligand **77** showed activity in combination with $\text{CoCl}_2 \cdot 6\text{H}_2\text{O}$ with a 1:1 metal to ligand ratio, however no activity using a 1:2 ratio. This suggests a change in coordination around the cobalt metal centre (compared to a 1:1 metal to ligand ratio) had resulted in the formation of a catalytically inactive species using a 1:2 metal to ligand ratio. The catalytic activity exhibited by ligand **77** was greater than the bleaching shown by the metal salt on its own, but significantly lower than that exhibited by standard three. However, this still indicated catalytic activity and ligand **77** in combination with $\text{CoCl}_2 \cdot 6\text{H}_2\text{O}$ was a good candidate for further testing using the wash-test. Unfortunately, all other metal-ligand combinations tested exhibited no significant activity over standard 2 using either a 1:1 or 1:2 metal to ligand ratio. However, in order to test the validity of the screening test, it was decided that **67**, **69** and **89** would also be tested in the wash-test in combination with $\text{CoCl}_2 \cdot 6\text{H}_2\text{O}$. Also, as no differences in activity were observed with ligands **67**, **69** and **89** with the 1:2 metal to ligand stoichiometry, the wash-test was carried out using the 1:1 ratio.

A possible explanation for the inactivity shown by ligand **62** even though ligand **77**, which was structurally very similar and did show activity using the same metal salt, may be due to the increased solubility of ligand **77** over **62**. Despite this, the observed catalytic activity is contrary to a related observation from the work of De Vos where the attempted alkene epoxidation involving **16** with secondary nitrogen donors proceeded with non-productive hydrogen peroxide decomposition only. Alkene epoxidation took place using the analogous ligand **7**, with its tertiary nitrogen donors under otherwise similar conditions (*vide supra*, 1.6). Ligand **69** was

expected to undergo an *in situ* saponification, under the basic conditions of the screening test, providing carboxylate pendant arms which have been shown to be beneficial in catalytic oxidation processes (*vide supra*, 1.18). The inactivity of **69** was initially thought to be a result of the failure of the expected ester saponification reaction under the conditions of the screening test or within the timescale permitted. However, support for the saponification of **69** and related compound **68**, under similar conditions during alkene epoxidation exists (*vide infra*, 3.13). A possible reason for the inactivity of **67**, **69** and to some extent ligand **89** came to light during the testing of these ligands during alkene epoxidation. Ligands **67** and **69** demonstrated a significant and complex counterion dependency in their catalytic activity during alkene epoxidation (*vide infra*, 3.13) using different manganese salts. Such a counterion dependency on catalytic activity may be at play in these cobalt systems using ligands **67** and **69** and possibly other metal-ligand combinations during catalytic bleaching experiments. Indeed, it may be an explanation for the lack of catalytic bleaching activity when using **67** and **69** as only cobalt(II) chloride was utilised in the screening test.

3.3 Initial stain removal test (Wash-test)

Assessment of stain removal by the ligand systems identified by the screening test to be potential bleaching catalysts were carried out using the wash-test (*vide infra*, 4.35). The ligand system under evaluation was assessed for stain removal ability against a blank, containing only hydrogen peroxide introduced as **1**, another blank containing **1** and **3** and finally a system with **1**, **3** and catalyst **6** at a 50 ppm manganese level. The stains were in the form of standardised cotton swatches with various stain types. Assessment of stain removal was carried out by measuring the % brightness using a spectrophotometer of the unwashed and washed stained swatches. Comparison of stain removal data are valid for a series of ligand systems where the wash-test was performed at the same time with the same batch of stained swatches. However, comparison between different wash-tests and batches of swatches is not possible, as the variations between the stained swatches is large. A difference of 3% in stain removal between bleaching systems may be considered significant.

As expected, the % stain removal achieved using catalyst **6** was the greatest with

most dyes, with the system containing **1** and **3** showing a smaller enhancement in stain removal ability compared to catalyst **6**, but both showing better stain removal ability than the system containing **1** only. However, as Figure 10 shows, ligand **77** in combination with $\text{CoCl}_2 \cdot 6\text{H}_2\text{O}$ did not repeat the stain bleaching ability exhibited during the screening test under the conditions of the wash-test. The lack of activity observed for **69** and **89** during the screening test was repeated in the wash-test, demonstrating to some extent, the validity of the primary screening test. Similarly, ligand **67** did not show any catalytic bleaching activity with any of the stain types. The only exception being ligand **67** with red wine, which exhibited better activity than the blank containing **1**, but performed worse than the blank containing **1** and **3**. This interesting result was considered worthy of further investigation, especially as the ligand did not show any activity in the screening test using the same metal salt.

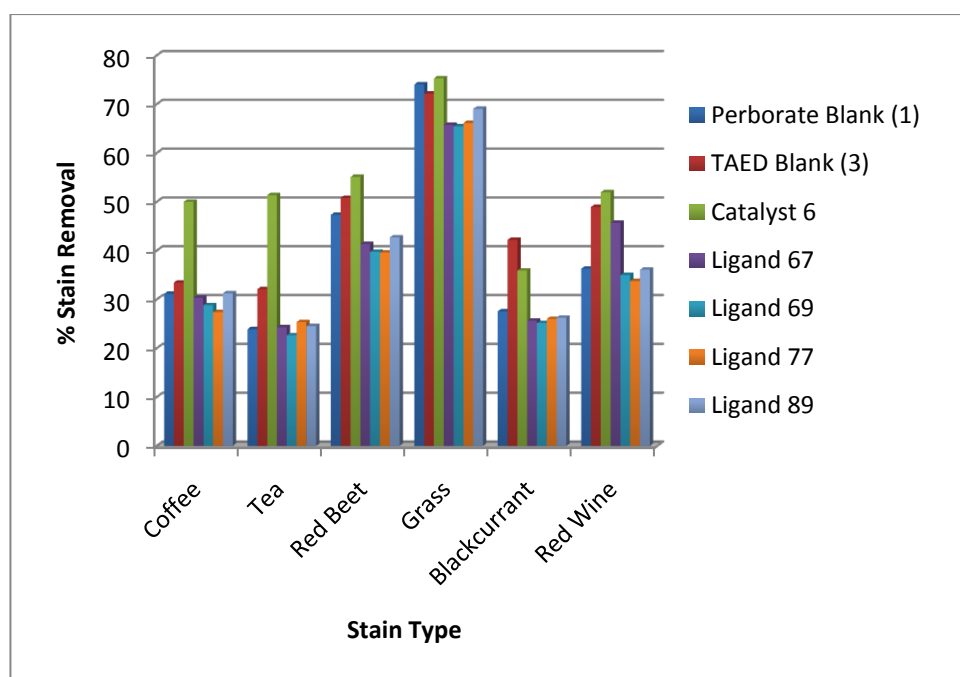


Figure 10. Bleaching activity in the wash-test using the terg-o-tometer. $\text{CoCl}_2 \cdot 6\text{H}_2\text{O}$ was added in combination with each ligand using a 1:1 ratio (with a catalyst loading of $4.6 \times 10^{-6} \text{ mol dm}^{-3}$)

3.4 Investigation into the catalytic activity of cobalt complexes of ligands **62** and **67**

Ligand **67**, in combination with $\text{CoCl}_2 \cdot 6\text{H}_2\text{O}$ showed some bleaching activity in the wash-test with red wine stained swatches. In order to investigate this further, attempts at

synthesising authentic complexes of this ligand, in combination with the cobalt salt, $\text{CoCl}_2 \cdot 6\text{H}_2\text{O}$, were undertaken. In view of this promising result, similar effort towards an authentic complex was attempted for ligand **62**. This exhibited no activity in the screening test yet it differs from ligand **67** only by its substitution on both terminal nitrogens of the bis-piperazine system.

Attempts to synthesise a cobalt complex from an equimolar mixture of ligand **67** and $\text{CoCl}_2 \cdot 6\text{H}_2\text{O}$ in methanol resulted in the production of a blue precipitate within 1 hour, which was isolated. This had poor solubility in most solvents except DMSO, DMF and water and single crystals could not be obtained despite trying a number of crystallisation methods. Similar attempts to synthesise a cobalt complex from ligand **62** did not produce a precipitate even after 48 hours, however, a blue-green powder was obtained on evaporation of the methanol solvent. Its solubility was found to be similar to the complex of ligand **67**. Washing this powder repeatedly with diethyl ether resulted in the formation of a blue powder, reminiscent of the product formed using ligand **67**.

Both of these powders were tested in the screening test (Figures 11 and 12), against the respective ligands and cobalt(II) salt combinations. Both exhibited higher activity compared to their respective metal-ligand combinations in the bleaching of **109**. With these encouraging results, attempts to characterise these powders were undertaken.

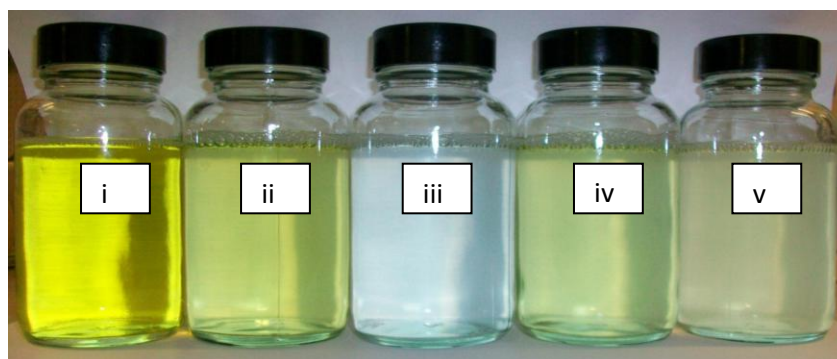


Figure 11. Screening test after 20 minutes, testing ligand **67** and the product of its attempted complexation. (i) Contains detergent and saffron solution; (ii) the same as bottle (i) but contains $\text{CoCl}_2 \cdot 6\text{H}_2\text{O}$ and oxidant (36-40% peracetic acid); (iii) the same as (ii) only it contains the ligand 1,10-phenanthroline in a 1:1 ratio to the cobalt salt; (iv) the same as (iii) only ligand **67** is substituted for 1,10-phenanthroline.; (v) the powder resulting from the complexation of ligand **67** with $\text{CoCl}_2 \cdot 6\text{H}_2\text{O}$

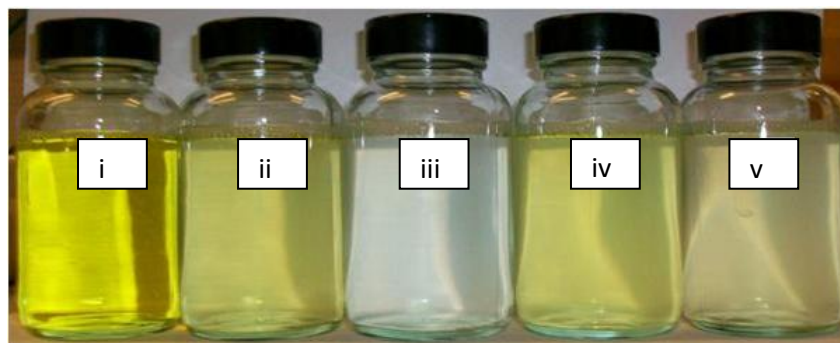
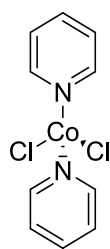


Figure 12. Screening test after 20 minutes, testing ligand **62** and its respective complex. (i) Contains detergent and saffron solution; (ii) the same as bottle (i) but contains $\text{CoCl}_2 \cdot 6\text{H}_2\text{O}$ and oxidant (36-40% peracetic acid); (iii) the same as (ii) only it contains the ligand 1,10-phenanthroline in a 1:1 ratio to the cobalt salt; (iv) the same as (iii) only ligand **62** is substituted for 1,10-phenanthroline.; (v) the powder resulting from the complexation of ligand **62** with $\text{CoCl}_2 \cdot 6\text{H}_2\text{O}$

3.5 A complex of ligand **67**

Analysis of the blue powder produced from **67** by mass spectrometry indicated a complex consistent with the formulation $[\text{MLCl}_2]$ had formed (m/z 510.1476 correlates with the molecular ion $[\text{M}+\text{H}]^+$). However, this gives no indication of the coordination geometry of the cobalt complex.

The IR spectrum resulting from the product of complexation of ligand **67** to $\text{CoCl}_2 \cdot 6\text{H}_2\text{O}$ is particularly diagnostic. The vibrational spectrum of pyridine has been extensively studied³ and in its various metal complexes, two bands at 604 cm^{-1} and 420 cm^{-1} , in the far infrared region, are known to undergo significant shifts to higher frequencies. These bands in pyridine are attributed to in-plane (604 cm^{-1}) and out-of-plane (420 cm^{-1}) ring deformations (bending). On coordination of the pyridine nitrogen to a metal centre, the band at 604 cm^{-1} underwent shifts with magnitudes which were sensitive to and indicative of the geometry around the metal centre.⁴ Complex **113** exemplifies the findings of this IR study.⁴ It is known to exist in a tetrahedral form as well as a chloro-bridged octahedral polymeric state.



113

A shift of the uncoordinated pyridine band at 604 cm^{-1} to 642 cm^{-1} and 631 cm^{-1} was observed for the tetrahedral and octahedral forms respectively. With a pyridine moiety in ligand **67**, it was envisaged that such a shift of the corresponding band in the 600 cm^{-1} region would occur if coordination of the pyridine moiety to the cobalt metal centre was taking place.

Furthermore, it was also anticipated that an insight into the coordination geometry of the cobalt complex of ligand **67** may be gained by comparison of the magnitude of such a shift with the existing data for complex **113**. In order to make such a comparison, the validity and reproducibility of the originally reported IR study needed to be tested with the instrument at our disposal (*vide infra*, 4.1). To achieve this, complex **113** in both its tetrahedral and polymeric octahedral forms were prepared and their respective IR spectra recorded (Figure 13).

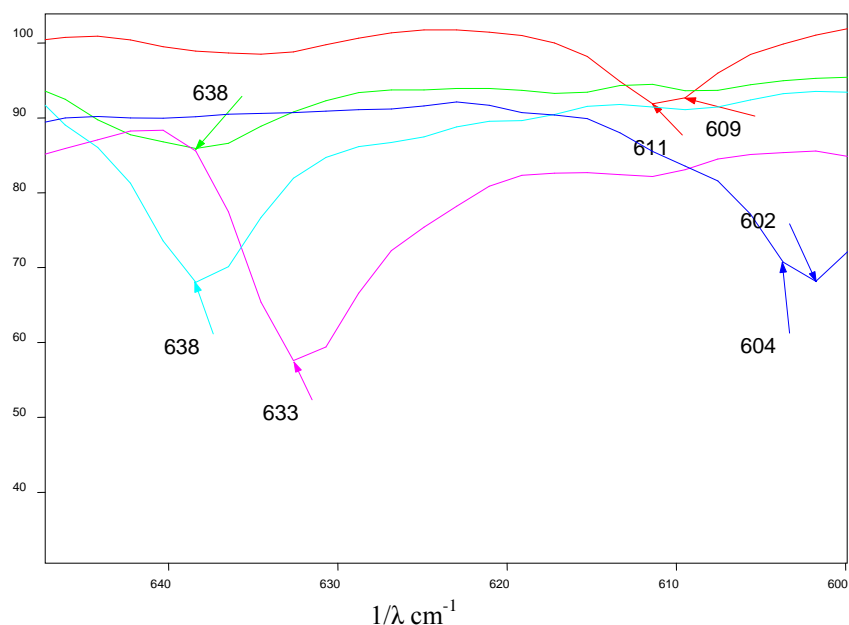


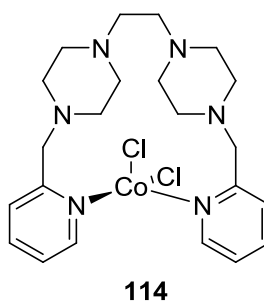
Figure 13. An overlay of the far infra-red spectra of pyridine (blue), complex **113** (light blue), the octahedral polymeric form of **113** (magenta), ligand **67** (red) and the complex of ligand **67** (green)

In the present study, an uncoordinated pyridine band at 604 cm^{-1} was found to shift to 638 cm^{-1} and 633 cm^{-1} for the tetrahedral and octahedral forms respectively (which is in close agreement to 642 cm^{-1} and 631 cm^{-1} quoted previously for the tetrahedral and octahedral forms respectively). Having prepared **113** in both its tetrahedral and octahedral forms and confirmed the reported measurements empirically, a tentative assignment of the coordination geometry for the cobalt complex of ligand **67** will be possible using this methodology.

The corresponding band for the uncoordinated pyridine moiety in ligand **67** was seen at a slightly higher wavenumber compared to pyridine and was observed at 609 cm^{-1} . However, the shape of this band was comparable to the corresponding band for pyridine. This absorption was shifted to 638 cm^{-1} for the blue powder produced from the complexation of ligand **67** to cobalt(II). The same type of shift was observed for complex **113** in its tetrahedral form, in terms of position and shape of the band. This demonstrated that the pyridine moiety was involved in complexation to the metal centre. Also, the magnitude of the shift was comparable to shifts observed for tetrahedral complexes such as **113**.

3.6 Summary for a cobalt complex of ligand **67**

Analysis of the blue powder by mass spectrometry indicates a molecular ion consistent with a $[\text{MLCl}_2]$ species. A shift of the pyridine ring vibration to higher wavenumbers on coordination of the pyridine ring to metals supports coordination of the pyridine moiety of the ligand as opposed to coordination through the tertiary nitrogens. Also, the magnitude of this shift is comparable to the tetrahedral form of **113** as opposed to its octahedral form. This supports the blue powder resulting from the reaction of ligand **67** and $\text{CoCl}_2 \cdot 6\text{H}_2\text{O}$ being a complex of tetrahedral (or pseudo-tetrahedral) geometry with a ligand set consisting of one ligand **67** coordinating through the two pyridine rings, possibly forming a bidentate-chelate complex with two chloro ligands completing the coordination sphere as depicted in **114**. However the possibility of monomeric units forming dimers and polymers still remains, due to the potential for the chloride ligands to bridge between metal centres.



However, without an X-ray structure it is impossible to confirm the structure and attempts to obtain single crystals of this complex have been unsuccessful.

3.7 A UV-Vis study of complex **114** and the 1:1 complex of ligand **62** with $\text{CoCl}_2 \cdot 6\text{H}_2\text{O}$

A consequence of **114** displaying appreciable solubility only in coordinating solvents such as DMSO was that the coordination geometry of the solid may not be maintained once dissolved in the solvent. This meant that study of its structure in solution was problematical.

Indeed, **114** on dissolution in DMSO produced a UV-Vis spectrum (Figure 14) remarkably reminiscent of that of $\text{CoCl}_2 \cdot 6\text{H}_2\text{O}$ dissolved in DMSO in the visible region (500-750 nm). This suggests that the coordination in a certain amount of **114** is altered on dissolution in DMSO to a species which is also formed once $\text{CoCl}_2 \cdot 6\text{H}_2\text{O}$ is dissolved in the same solvent (within the time-frame that **114** was dissolved in the solvent and measurement of its UV-Vis spectrum taken of 2-3 hours). However, intense features in the spectrum for **114** in the UV-region (with a shoulder which tails into the visible region) are absent in the spectrum for $\text{CoCl}_2 \cdot 6\text{H}_2\text{O}$. The intensity of these features excludes the possibility that they are due to *d-d* transitions. Furthermore, the absence of these bands in the spectrum (Figure 14) for the product of complexation between ligand **62** and $\text{CoCl}_2 \cdot 6\text{H}_2\text{O}$ (which lacks the pyridine moiety) supports that these absorptions are probably linked to the pyridine moieties found in ligand **67**. Some light as to whether these intense UV-absorptions are due to free ligand **67** in solution or the result of a charge transfer interaction ($\pi-\pi^*$) between cobalt and coordinated pyridine moieties (found in ligand **67**) is shed by the difference in intensity of this band compared to the intensity of a similar band found for ligand **67** in DMSO solution (see Appendix 2). This band for **114** in DMSO solution is significantly more intense than the

corresponding band for ligand **67** (dissolved in DMSO) suggesting the features found for **114** in the UV-region are due to a charge transfer interaction.

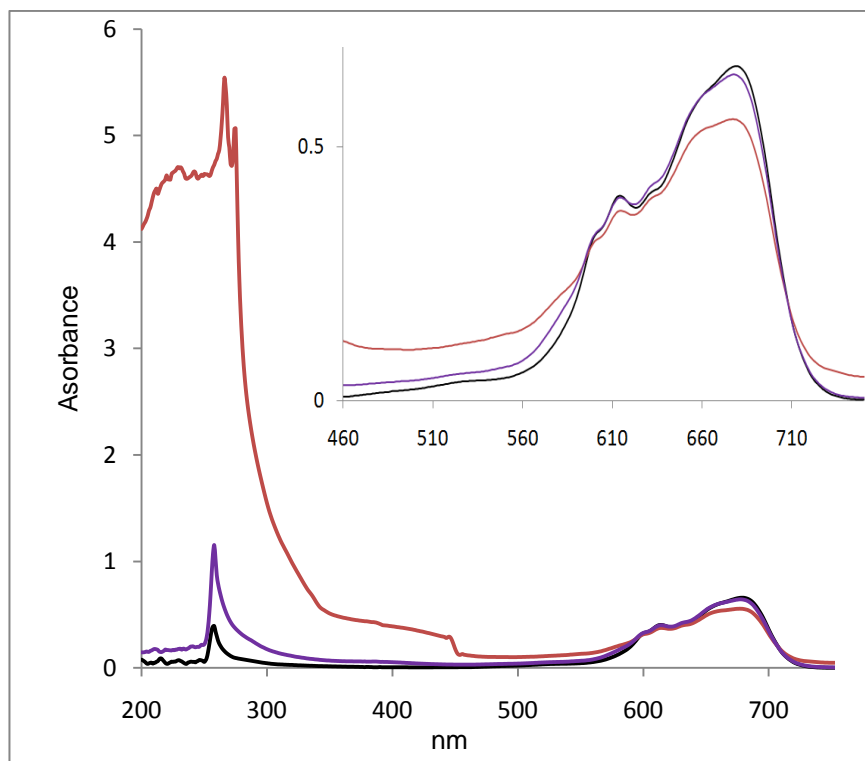


Figure 14. UV-Vis spectra for the DMSO solutions of $\text{CoCl}_2 \cdot 6\text{H}_2\text{O}$ (black), the product of complexation between ligand **62** and $\text{CoCl}_2 \cdot 6\text{H}_2\text{O}$ (purple) and **114** (red). Measurements were carried out using a 1 cm cell at a concentration of $3.37 \times 10^{-3} \text{ mol dm}^{-3}$ in all cases

Also, further support for a charge transfer interaction comes from the solvatochromism displayed by a similar band for the related complex **113** dissolved in DMSO and dichloromethane (*vide infra*). This information suggests the presence of a species due to **114** with the pyridine moieties in ligand **67**, still coordinated to the cobalt metal centre.

In order to show that tetrahedral complexes such as **114** (see section 3.6) undergo changes to their coordination geometry once dissolved in DMSO (within the time frame that the complex was dissolved in DMSO and its UV-Vis measurement taken) the UV-Vis spectra of a similar authentic complex, **113** (Figure 15), was studied in both DMSO and dichloromethane solutions. Indeed, two very different bands are observed for **113** in the visible region, in terms of shape, intensity and energies for the two spectra recorded in either DMSO or dichloromethane. The spectrum recorded in DMSO is very similar in the visible region (500-750 nm) to the DMSO spectra recorded for $\text{CoCl}_2 \cdot 6\text{H}_2\text{O}$, **114**

and the product of complexation between **62** and $\text{CoCl}_2 \cdot 6\text{H}_2\text{O}$. Also, the spectra for **113** in different solvents show solvatochromism in the band observed in the UV-region (compare with the pyridine spectra recorded in DMSO and dichloromethane, which shows that in both solvents the UV-bands are the same in terms of energy and intensity, but significantly less intense than the UV-bands for **113** in either DMSO or dichloromethane, appendix 3), indicating that these bands are due to a charge transfer interaction. A similar band found in the DMSO spectrum for **114** gives further support that such a band is due to a charge transfer absorption (*vide supra*).

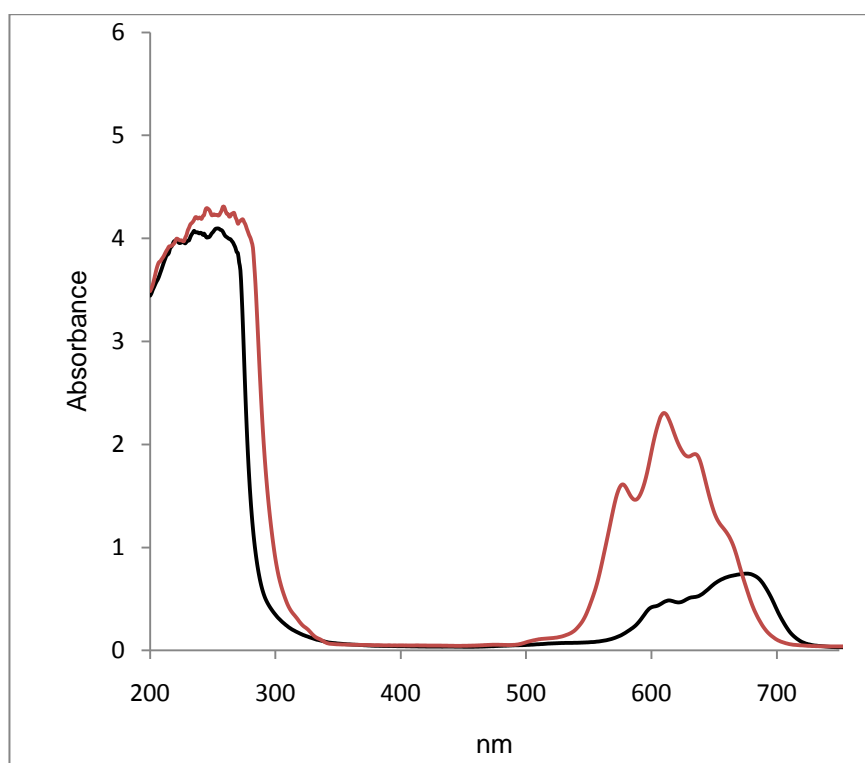


Figure 15. UV-Vis spectra for **113** dissolved in DMSO (black) and **113** dissolved in dichloromethane (red). Measurements were carried out using a 1 cm cell at a concentration of $3.37 \times 10^{-3} \text{ mol dm}^{-3}$ in both cases

This brought into question as to the types of species in DMSO solution responsible for the common absorption band observed in the visible region (500-750 nm) for $\text{CoCl}_2 \cdot 6\text{H}_2\text{O}$, **114** and the product of complexation between **62** and $\text{CoCl}_2 \cdot 6\text{H}_2\text{O}$. For the salt $\text{CoCl}_2 \cdot 6\text{H}_2\text{O}$ dissolved in DMSO, it is possible that a species of the type $[\text{Co}(\text{DMSO})_x]^{2+}[\text{CoCl}_4]^{2-}$ (where $x = 2-6$) was forming owing to the stability of the $[\text{CoCl}_4]^{2-}$ dianion and the apparent coordinating ability of DMSO. Similarly, for **114** and the product of complexation between **62** and $\text{CoCl}_2 \cdot 6\text{H}_2\text{O}$, a species of the type

$[[\text{Co}(\text{L})_x(\text{DMSO})_y]^{2+}[\text{CoCl}_4]^{2-}]$ (where L = **67** or **62**, x = 1 or 2 and y = 2-4) is tentatively suggested. It is likely that the dicationic cobalt species of the suggested structures in DMSO solution were octahedral and this would explain the lack of observed *d-d* transitions due to the cation in the presence of a tetrahedral $[\text{CoCl}_4]^{2-}$ anion (the centrosymmetric nature of the octahedral geometry means that *d-d* transitions are far less intense compared to the tetrahedral geometry which lacks an inversion centre). Also, support for a cationic species suggested for **114** in DMSO with ligand **67** still coordinated has already been presented (*vide supra*). However, it must be stressed that in solid form, support for the 1:1 complex between ligand **67** and $\text{CoCl}_2 \cdot 6\text{H}_2\text{O}$ (**114**) being tetrahedral in nature exists (see section 3.6).

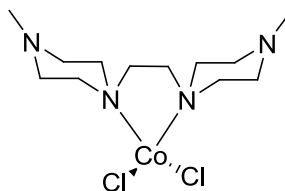
With these considerations and assuming the common band in the visible region (500-750 nm) for $\text{CoCl}_2 \cdot 6\text{H}_2\text{O}$, **114**, **113** and the product of complexation between **62** and $\text{CoCl}_2 \cdot 6\text{H}_2\text{O}$ observed in DMSO solutions are due to the $[\text{CoCl}_4]^{2-}$ anion, these spectra may be interpreted as follows: In general, for tetrahedral cobalt(II), three absorption bands are expected in its UV-Vis spectrum. The lower energy absorptions correlating to ${}^4\text{A}_2 \rightarrow {}^4\text{T}_2$ (F) and ${}^4\text{A}_2 \rightarrow {}^4\text{T}_1$ (F) were not observed and should appear in the infrared region. However, strong absorptions at higher energies, in the visible region are in agreement with the observed blue colour of the DMSO solutions of $\text{CoCl}_2 \cdot 6\text{H}_2\text{O}$, **114**, **113** and the product of complexation between **62** and $\text{CoCl}_2 \cdot 6\text{H}_2\text{O}$. This band, correlating to the ${}^4\text{A}_2 \rightarrow {}^4\text{T}_1$ (P) transition had an absorption maxima at 677 nm in all four cases (extinction coefficients (ϵ) 195, 165, 221 and 191 $\text{dm}^3 \text{mol}^{-1} \text{cm}^{-1}$ for the DMSO solutions of $\text{CoCl}_2 \cdot 6\text{H}_2\text{O}$, **114**, **113** and the product of complexation between **62** and $\text{CoCl}_2 \cdot 6\text{H}_2\text{O}$ respectively). The intensities support a tetrahedral geometry in all cases as opposed to a centrosymmetric octahedral geometry for which weaker absorptions would be expected. The extinction coefficients fall well within the range of 10^2 to $2 \times 10^3 \text{ dm}^3 \text{mol}^{-1} \text{cm}^{-1}$ quoted previously⁵ for the tetrahedral geometry. Also observed in the same band are absorptions at higher energies which correlate with spin forbidden quartet to doublet transitions.

3.8 Cobalt complexes of ligand **62**

The blue powder produced from the 1:1 complexation reaction between ligand **62** and $\text{CoCl}_2 \cdot 6\text{H}_2\text{O}$ was shown by high resolution mass spectrometry to form a molecular ion consistent with a species of stoichiometry $[\text{MLCl}_2]$ (the ion at m/z 355.0865 correlates

with the molecular ion $[M]^+$). Given its identical appearance to **114** it may not be completely unreasonable to suggest a tetrahedral geometry for such a species (see section 3.6).

However, as ligand **62** does not have a pendant pyridine moiety, its ligand set must differ to that suggested in **114**. Also, given the mass spectrometry data and assuming a tetrahedral geometry (*vide supra*), coordination through all four tertiary nitrogen donors is unlikely. A possible coordination sphere is one with two tertiary nitrogen donors and two chloride donors forming a neutral complex and this is in agreement with the mass spectrometry data. Support for this comes from the observed coordination mode of 1,4-dimethylpiperazine to cobalt(II) under similar conditions. It was reported to take place through one of the tertiary nitrogens with the piperazine ring remaining in the thermodynamically favoured chair conformation.⁶ Based on this information, it is tentatively suggested that **115** represents the complex formed from ligand **62** and $\text{CoCl}_2 \cdot 6\text{H}_2\text{O}$. However, without a crystal structure it would be difficult to say with certainty. Again, as with **114**, the potential for such a complex to form dimeric or polymeric structures still remains.



115

As described earlier (Section 3.4), in preparation of a cobalt complex of ligand **62**, a blue-green powder was obtained as the crude product. Washing this repeatedly using diethyl ether produces a blue powder. Evaporation of the diethyl ether from the washings revealed a small amount of ligand **62** as determined by ^1H NMR spectroscopy. The amount of ligand **62** (10 wt% of total yield) collected from the washings suggested that much of the ligand had been converted to a complex. The properties of this complex are described above. However, the crude blue-green powder obtained from the initial reactions involving the attempted complexation of ligand **62** was not washed using diethyl ether. Instead, after very many failed recrystallisation attempts to obtain single crystals, a final recrystallisation was tried using glacial acetic acid as the solvent. A small quantity of single crystals suitable for X-ray diffraction

were isolated and an X-ray structure obtained. The crystal structure reveals the presence of the $[\text{CoCl}_4]^{2-}$ anion in the unit cell accompanied by ligand **62** which is doubly protonated and acting as the cation. It would appear then that the unreacted ligand **62** and $\text{CoCl}_2 \cdot 6\text{H}_2\text{O}$ had formed this species (**116**) in the presence of acid from the crude reaction mixture. Similar synthesis using various bis-protonated piperazine as the counterion has been demonstrated for the $[\text{CoCl}_4]^{2-}$ anion previously.⁷

The single crystal X-ray structure of **116** confirms the expected double chair conformation for the ligand as the thermodynamically favoured form in the absence of appropriate coordination to the metal centre of complex (Figure 16).

The protonation of both methylated nitrogens of the ligand is confirmed by the significant lengthening of the C-N bonds of the protonated nitrogens as compared to the non-protonated ring nitrogens (Table 8). The mean C-N bond length around N(1) and N(2) are 1.490(5) Å and 1.464(5)Å respectively supporting the fact that N(1) is protonated and N(2) is not.

Table 8. Selected bond lengths (Å) and angles (°) for **116** with e.s.ds

Bond	Lengths (Å)	Bond	Angle (°)
C(1)-N(1)	1.488(5)	C(1)-N(1)-C(2)	111.7(3)
C(2)-N(1)	1.490(5)	C(1)-N(1)-C(5)	113.2(3)
C(5)-N(1)	1.491(5)	C(2)-N(1)-C(5)	109.2(3)
C(3)-N(2)	1.468(5)	C(4)-N(2)-C(3)	108.2(3)
C(4)-N(2)	1.457(5)	C(6)-N(2)-C(3)	111.8(3)
C(6)-N(2)	1.467(5)	C(6)-N(2)-C(3)	111.8(3)
C(2)-C(3)	1.503(6)	N(2)-C(4)-C(5)	111.0(4)
Cl(1)-Co(1)	2.2629(13)	Cl(2)-Co(1)-Cl(1)	107.29(5)

A chloride ligand bound to a metal centre is known⁸ to accept hydrogen bonds well. For **116** three centred hydrogen bonding is observed (Figure 17), with the average distance between the hydrogen bond donor (N(1)) and acceptor (Cl) being 3.365(4) Å (Table 9). This figure is in good agreement with the average for this distance reported by Dadon and Bernstein.⁹ They determined this average from a CSD search for compounds displaying three centred hydrogen bonds with chloride acceptors and nitrogen or oxygen donors.

Table 9. Bond distances and angles involving hydrogen bonding for complex **116**

D-H...A	d(D-H)	d(H...A)	d(D...A)	<(DHA)
N(1)-H(1)---Cl(1)	0.91	2.67	3.357(4)	132.8
N(1)-H(1)---Cl(2)	0.91	2.65	3.372(4)	137.0

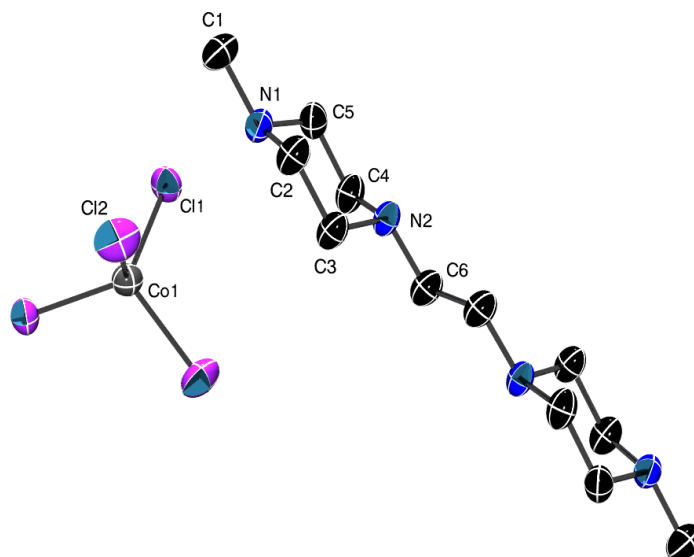


Figure 16. ORTEP¹⁰ plot of the single crystal X-ray structure of **116** with 50% probability displacement ellipsoids

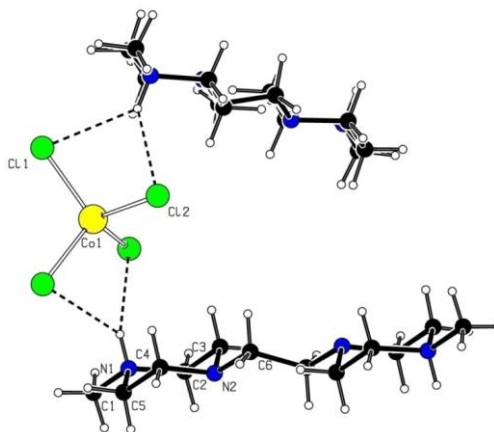


Figure 17. A Platon¹¹ plot showing hydrogen bonding network for **116**

3.9 Magnetic moment measurements for **114** and **115**

The solution magnetic moments of **114** and **115** were measured using the Evans NMR method¹² which showed that both complexes were paramagnetic. The procedure

involved the use of a coaxial tube containing a known concentration of complexes **114** or **115** which were dissolved (freshly prepared) in a stock solution of *t*-butyl alcohol and deuterated DMSO (2:1 respectively). The coaxial tube was then inserted into a high precision NMR tube containing the stock solution. A proton NMR spectrum was then obtained in the usual way (using an instrument with an operating frequency of 270 MHz, see 4.1). The molar susceptibility can be determined from equation 5, using the chemical shift difference that occurs between the methyl protons of *t*-butyl alcohol in the presence of the paramagnetic species compared to the chemical shift observed in its absence at 298 K. The magnetic moment can be evaluated using the value obtained for magnetic susceptibility from the equation 6.

$$\chi_m = \frac{3 \cdot \Delta f}{1000 \cdot f \cdot c} \quad \text{Equation 5}$$

$$\mu_{eff} = 798 \sqrt{T \cdot \chi_m} \quad \text{Equation 6}$$

Where χ_m is the molar susceptibility of the sample in $\text{m}^3 \text{mol}^{-1}$; Δf is the difference in the chemical shift of a set of protons in Hz; f is the frequency of operation of the spectrometer in Hz; c is the concentration of the sample in mol dm^{-3} ; and T is the temperature in K . The concentrations of the samples were calculated based upon the molecular weights determined from the proposed structures for the respective samples as discussed above. The measured magnetic moment for complexes **114** and **115** are 5.78 and 4.41 μ_B respectively. As the calculated spin-only magnetic moment for a high spin d^7 tetrahedral system within weak field limits is 3.87 μ_B , these values would suggest a significant orbital contribution to the magnetic moment due to spin-orbit coupling.¹³ Accordingly, typical magnetic moment of tetrahedral (or pseudo-tetrahedral) cobalt complexes fall within the range of 4.3-5.2 μ_B and are assigned as high spin.¹⁴ Although the measured magnetic moment for complex **114** is slightly outside this range, a recent example of a divalent cobalt complex with an N_2Cl_2 donor set, with two sp^2 hybridised nitrogen atoms, has been reported to have a μ_{eff} of 6.48 μ_B .¹⁵

3.10 Summary of the catalytic bleaching results

The development of a bleaching catalyst is a challenging area of research. The array of chemically diverse stain molecules make it unlikely that any one catalytic species will

be able to bleach them all. The issue of dye damage and fabric degradation further complicate the situation, requiring a catalyst to be selective only for stains, which is a challenge as many dyes are similar in chemical structure to molecules constituting stains. The specific conditions under which a catalyst must operate is a further constraint. The need for an environmentally benign catalyst able to utilise hydrogen peroxide is also a key requirement. With all this in mind, it is easier to understand why there are no bleaching catalysts in current commercial formulations despite the many advantages they promise over existing technology. Unfortunately, the current work towards a bleaching catalyst did not identify any metal-ligand combinations which exhibit catalytic activity comparable to or even approaching that of **6** in the wash-test. However, the preformed cobalt complexes of **62** and **67** demonstrated some catalytic activity during the primary screening test although these complexes have not been tested in the wash-test. Furthermore, using a variety of spectroscopic techniques, an insight into the coordination chemistry of these complexes has been gained during this study.

The catalytic activity observed for the cobalt complexes of ligands **62** and **67** during the screening test was greater than the cobalt systems generated *in situ* from the same ligands. This highlights a possible weakness of this method of testing and suggests that other preformed complexes of other metal salts using the same ligands may have some potential. Moreover, complexes of other metal-ligand combinations may show potential as bleaching catalysts. This emphasises the difficulty in identifying active metal-ligand combinations in an efficient manner. The *in situ* method of catalyst generation was favoured in order to identify active systems rapidly. Clearly, this approach has drawbacks in that it produced false negative results for ligands **62** and **67** as described above, possibly because under the conditions of the test, complexes failed to form. Despite this, making authentic complexes of all metal-ligand combinations would have been unrealistic. On a practical level, the current screening test, although not ideal, is possibly still the best method of identifying active bleaching catalysts.

3.11 Epoxidation catalysis

The utility of certain systems found to be active in bleaching catalysis have also demonstrated their efficacy in epoxidation catalysis, for example the manganese-ligand **7** systems (*vide supra*, 1.5 and 1.6). In this respect, some of the ligands and complexes

already tested for catalytic bleaching ability (and others) were intended for testing in epoxidation catalysis.

Both the reactivity and selectivity in catalytic epoxidation reactions show a strong sensitivity to reaction conditions,¹⁶ the catalytic system and the substrate. Owing to these complex set of parameters which need to be taken into consideration, the discovery of a new catalytic epoxidation system requires much time and effort and undeniably, a certain amount of serendipity must be involved.

As for the initial screening test used for the identification of potential bleaching catalysts, operational simplicity and speed was of importance in order to maximise the chances of finding an active catalytic epoxidation system. As a result, a method developed in the course of this research (see 4.36, Method A), involved the screening of systems at ambient temperature with the reactions carried out in air. Furthermore, in order to identify and develop less active systems, under the conditions used, a relatively high catalyst loading of 5 mol% (relative to alkene) was used in this study. Peracetic acid (36-40 wt% in acetic acid) was utilised as the oxidant in this work for the sake of continuity. This oxidant was utilised in both the screening test and the wash-test (formed *in situ*) during the catalytic bleaching studies.

3.12 Epoxidation using complex 114 and 115

Complex **114** and **115** have shown promise in the initial screening test for catalytic bleaching activity and as a result were tested for their potential in epoxidation. Owing to the poor solubility of these complexes in the reaction solvent (acetonitrile), a modified method to that used in the general epoxidation reactions was used (see 4.36, Method B).

Complex **114** and **115** exhibited no significant catalytic enhancement in the oxidation of *p*-chlorostyrene compared to the free-metal (Table 10, entries 1-3). In fact, **114** actually inhibited the oxidation of the substrate compared to the free-metal (Entry 1). The catalytic activity after three hours was minimal for **114** and **115** with no further significant conversion of the substrate taking place. The epoxide selectivity for both **114** and **115** was low and for both systems, the epoxide product was completely consumed within 18 hours. This suggested the involvement of complexes **114** and **115** in the conversion of the epoxide product. Such a possibility was considered as under the

reaction conditions (Method B), the epoxide of *p*-chlorostyrene was found to survive for at least 18 hours. This was not entirely surprising as the ability of cobalt complexes to act as a Lewis acid and effect the ring opening of epoxides is well known.¹⁷

Table 10. Epoxidation of *p*-chlorostyrene using **114** and **115**

Entry	Catalyst	Conversion %	Epoxide (%)	Epoxide Selectivity %
1	114	26	5	20
2	115	35	13	37
3	CoCl ₂ ·6H ₂ O	34	15	45

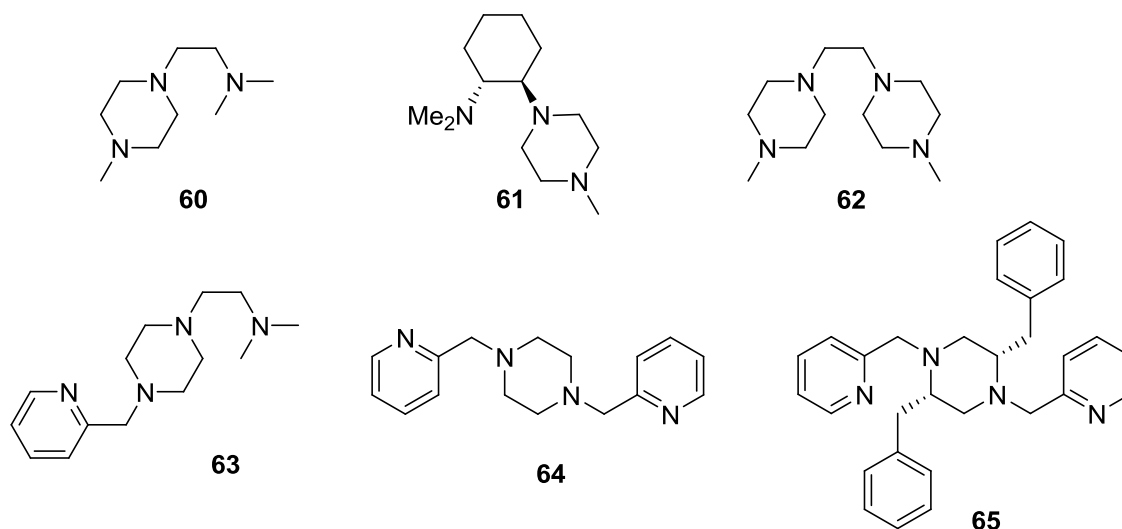
Conditions: As described in Method B

3.13 Epoxidation involving manganese systems of ligands incorporating the piperazine backbone

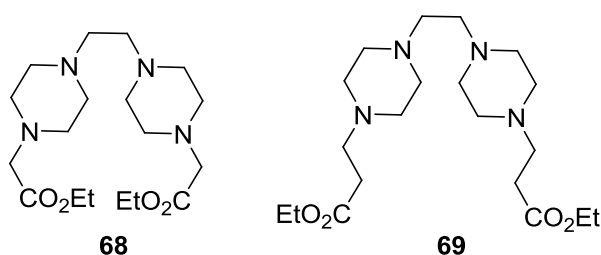
Owing to time constraints, preparation of authentic manganese complexes of any ligand systems prepared was not possible. Therefore, in order to test these ligands for their efficacy in catalytic epoxidation reactions, the *in situ* formation of a catalytic system was assumed as in the strategy employed by De Vos in their work towards a manganese-based epoxidation system.¹⁸ Using manganese(II) sulfate or triflate as the metal source and ligands **60-65** in a 1:1 ratio (5 mol% catalyst loading), no significant catalytic enhancement was observed for the epoxidation of *p*-chlorostyrene using acetonitrile as the reaction solvent (Method A) after three hours. This showed that all the potentially tri- and tetra-dentate donor ligands were ineffective in catalysing the epoxidation reaction, at least under the conditions employed. This was disappointing as much effort went into the synthesis of these ligands, some of which are novel compounds.

However, a number of interesting observations were made during the screening of these ligands. Although the degree of conversion (~10%) of *p*-chlorostyrene for ligands **60-65** (using both manganese(II) sulfate and triflate) were similar to the background conversion observed for the free-metal, epoxide was only seen for the tri-dentate donor ligands, **60** and **61**. Epoxide was not observed for any other manganese systems involving the tetra-dentate donor ligands, the free-metal or the peracetic acid conversions of *p*-chlorostyrene. Also, the observed selectivity for the epoxide was high

for both **60** and **61** with a 92% and 70% selectivity observed after three hours for the respective ligands. Furthermore, for ligand **60**, the majority (65%) of the epoxide was still present after 33 hours. This is significant as it demonstrates that if produced, the epoxide survives under the conditions of the reaction.



As both ligands **68** and **69** were in the precursor ester form to the desired carboxylate derivatives, a modification of the method was required in order to facilitate the *in situ* saponification (*vide supra*, 1.18) and potential coordination to a metal centre (this *in situ* saponification was assumed to take place under the basic conditions of the screening test, which was used in the screening for catalytic bleaching activity). Therefore, a modification to the general epoxidation method and conditions was required for these particular ligands and involved the addition of a volume of pH 11 sodium hydroxide buffer (Method B). The respective ligands were stirred for half an hour in this buffer after which time the methodology followed was the same as that used for all other systems (Method A). In order to keep the reaction volume the same in both methodologies, the volume of acetonitrile was appropriately reduced for the modified method which facilitated the screening of ligands **68** and **69**.



Using this methodology and manganese(II) sulfate, both ligands **68** and **69** exhibited catalytic enhancement compared to the background reaction in the epoxidation of *p*-chlorostyrene after three hours (Table 11, entries 1 and 2 versus entry 5) using peracetic acid as the oxidant. The epoxide selectivity was very high for the system involving ligand **68** (92%) and slightly lower for ligand **69** (70%), but still good. The yield for the system utilising ligand **69** (41%) was ~10% less compared to ligand **68** (53%). Both of these systems including ligands **68** and **69** have shown much potential for their application in epoxidation catalysis. Especially as promising results have been obtained at this early stage, optimisation of these systems may increase the activity of these systems and even selectivity for the ligand **69** system. The success of the *in situ* saponification to form the carboxylate arm is to some extent demonstrated by the catalytic activity of ligands **68** and **69**. Without the success of the saponification reaction, a coordinating pendant arm would not be present in ligands **68** and **69**. The importance of a coordinating arm is demonstrated by the lack of catalytic activity using ligand **62**. Furthermore, epoxidation of *p*-chlorostyrene involving ligand **69** and manganese(II) sulfate under the standard epoxidation methodology (Method A, with no pH 11 buffer) exhibited no catalytic activity.

Table 11. The epoxidation of *p*-chlorostyrene

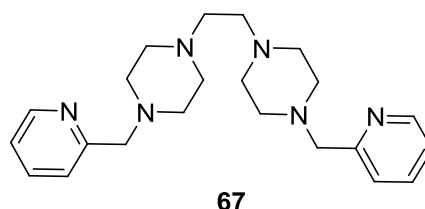
Entry	Ligand	Mn salt	Conversion		Epoxide		Epoxide selectivity (%)	Time /mins
			%	TON	%	TON		
1	68 [†]	MnSO ₄ .H ₂ O	53	12	48	11	92	180
2	69 [†]	MnSO ₄ .H ₂ O	41	10	29	7	70	180
4	67 [‡]	Mn(OTf) ₂	>99	20	57	11	57	30
5	-	MnSO ₄ .H ₂ O	10	2	0	0	0	180
6	-	Mn(OTf) ₂	5	1	0	0	0	180

Conditions: As described in [‡]Method A and [†]Method B. For the ligand **67**-manganese(II) triflate system an external standard was used during the HPLC analysis of the reaction

Using ligands **68** and **69** in combination with manganese(II) triflate, no significant catalytic activity was observed for the epoxidation of *p*-chlorostyrene compared to the background reaction after three hours. Therefore, a five-fold increase in catalytic activity was observed for the manganese(II) sulfate-ligand **68** system compared to the system using manganese(II) triflate within the same time frame. This shows a

significant counterion effect on the catalytic systems involving ligands **68** and **69** with manganese(II) salts. The influence of different counterions on the catalytic epoxidation activity of an otherwise identical catalyst has been noted by De Vos.¹⁹ In terms of the screening test for catalytic bleaching, both ligands **68** and **69** did not show any activity. The counterion dependency observed in the catalytic epoxidation reactions may have been the reason for this as manganese(II) chloride was used for the bleaching test. Furthermore, the catalytic activity observed with the particular manganese salt vindicates the use of the *in situ* saponification strategy used in the bleaching and wash-tests.

The manganese(II) sulfate-ligand **67** system exhibited no significant catalytic activity in the epoxidation of *p*-chlorostyrene compared to the background reaction (using the general epoxidation method, A). However, changing to manganese(II) triflate as the manganese source resulted in a dramatic increase in the catalytic activity (Entry 4). Again, like the systems involving ligands **68** and **69**, a counterion effect on the catalytic activity is observed. However, for ligand **67**, the active system involves the triflate anion and the inactive system is the one including the sulfate counterion. It appears there is an inversion in counterion dependency on the catalytic activity involving ligands **68** and **69** compared to that observed for the ligand **67** system.



A >99% conversion was observed using the manganese(II) triflate-ligand **67** system, within 30 minutes, this represents a doubling of the catalytic activity compared to the manganese(II) sulfate-ligand **68** system within a fraction of the time. However, the epoxide selectivity using the ligand **67** system was found to be lower (57%) compared to the manganese(II) sulfate-ligand **68** system. It is interesting to note that this difference in selectivity may be due to the presence of the required buffer in the reaction involving ligands **68** and **69** and its omission in the reaction involving ligand **67**.

Despite this, the manganese(II)-ligand **67** system is an extremely promising one. If amenable to optimisation, there exists the possibility of accessing a whole new class of

epoxidation catalysts incorporating the piperazine moiety. It is noteworthy that ligand **67** was inactive in the screening for catalytic bleaching activity (*vide supra*). The apparent counterion dependency on the oxidative activity of the ligand **67** systems may have been the reason for the observed inactivity, as a manganese(II) chloride salt was utilised in the screening test for bleaching (as for ligands **68** and **69**).

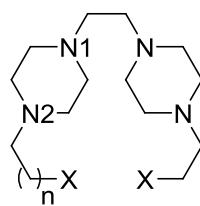
An interesting observation was the ability of the manganese(II)-ligand **67** system to completely consume the naphthalene internal standard used to quantify the epoxidation reactions, within the 30 minute run-time of the reaction. Further investigation into the exact nature of this conversion along with the product/s produced needs to be carried out. Apart from requiring an external standard to quantify the epoxidation reaction, the significance of this observation may be greater. Enzymes are capable of oxidising unfunctionalised aromatic compounds such as cytochrome P-450²⁰ and Rieske dioxygenases.²¹ Efforts to mimic the activity of these enzymes using transition metal complexes in an efficient manner is an active area of research. Such bio-mimetic catalysts would find utility amongst other areas in organic synthesis. In view of this, the apparent ability of the manganese(II)-ligand **67** system to oxidise naphthalene is significant.

3.14 The nature of the piperazine ligands involved in catalytic alkene epoxidation

The identity of the counterion for catalytic activity appeared to be of paramount importance for those ligands showing efficacy in catalysing the epoxidation reaction (**67-69**). Furthermore, particular ligand and counterion combinations appeared to be necessary for catalytic activity. Ligands **68** and **69** only exhibited activity with manganese(II) sulfate and ligand **67** was only active in combination with manganese(II) triflate. The intriguing counterion effect on the catalytic epoxidation involving ligand **67-69** requires further inquiry. In view of this, the preparation of authentic manganese complexes of these ligands needs to be undertaken and structural studies carried out in both the solid state and in liquid medium. Such studies may afford insight into the reasons for the observed counterion influence on the catalytic epoxidation activity.

Despite this complex counterion dependency in these piperazine based ligands, analysis of the structural features which demonstrated catalytic activity and comparison of these

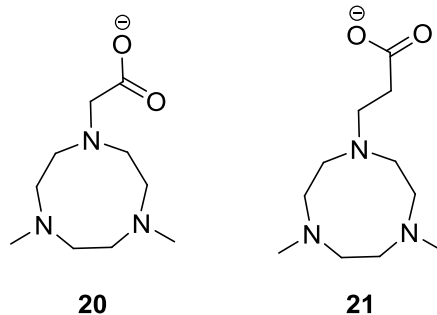
with the systems which did not, brought to light some interesting patterns. The lack of catalytic activity using ligands **60**, **61** and **63-65** in combination with either manganese(II) sulfate or triflate and the presence of catalytic activity using ligands **67-69** in combination with particular manganese salts suggested the importance of the bis-piperazine moiety for the presence of catalytic epoxidation activity. Furthermore, the importance of a pendant arm appended to N2 with a donor atom on the terminal carbon appeared to be necessary for catalytic activity (see **117**).



117

$n = 1$ or 2
 $X = O, N$

This is supported by and may explain the absence of catalytic activity for ligand **62**, despite having the bis-piperazine moiety. More specifically, the length of the pendant arms appeared to be important for the degree of catalytic activity. Ligands **67** and **68** which exhibited the highest catalytic activity (>99% and 53% conversion respectively) of the active systems both have a 2 carbon spacer between N2 and the donor atom. A longer carbon chain appeared to lower catalytic activity as exemplified by ligand **69** which has a 3 carbon spacer and exhibited a lower catalytic activity compared to ligand **68** (24% and 53% respectively) This is contrary to the findings of Shul'pin and co-workers (albeit in a different ligand system), where a longer pendant carboxylate arm in ligand **21** resulted in a higher catalytic epoxidation activity compared to ligand **20**.²² Finally, the nature of the donor atom seemed to be important in the magnitude of the catalytic activity, exemplified by the carboxylate oxygen donors of **68** and **69** which demonstrated lower catalytic activity compared to the pyridine nitrogen donor of ligand **67**. However, it must be noted that this final point is somewhat complicated by the inverted counterion dependency in the observed catalytic activity involving ligands **68** and **69** versus ligand **67**.



The higher epoxide selectivity observed for systems including ligands **68** and **69** compared to the system utilising ligand **67** may simply have been due to the less acidic conditions necessary in the epoxidation using ligands **68** and **69**. The more acidic conditions under which the ligand **67** system was operational may have promoted ring opening reactions of the epoxide product, thus lowering epoxide selectivity.

3.15 Conclusions

The majority of the piperazine ligands discussed displayed inactivity in alkene epoxidation (under the condition utilised). Despite this, these ligands have provided a means of evaluating the structural features which impart catalytic alkene epoxidation in these systems by comparison with active ligands. The inclusion of pendant carboxylate groups (assumed to form *in situ*) and the pendant pyridine moieties in ligand design has been justified. Ligands containing these features (**67**, **68** and **69**) are the only systems which displayed catalytic epoxidation activity. The observed consumption of naphthalene by the ligand **67**-manganese(II) triflate system is a very interesting observation and suggests the potential use of this system in the oxidation of aromatic substrates. The catalytic alkene epoxidation work carried out during this study has yielded some positive results and a number of interesting observations. The systems in question needs to be better understood and developed, in this respect, further study of these systems is required.

3.16 References

1. K. Shastri, E. W. C. Cheng, M. Motevalli, J. Schofield, J. S. Wilkinson and M. Watkinson, *Green Chem.*, 2007, **9**, 996-1007.
2. T. Wieprecht, M. Hazenkamp, H. Rohwer, G. Schlingloff and J. Xia, *C. R. Chimie*, 2007, **10**, 326-340.

3. N. S. Gill, R. H. Nuttall, D. E. Scaife and D. W. A. Sharp, *J. Inorg. Nucl. Chem.*, 1961, **18**, 79-87.
4. R. J. H. Clark and C. S. Williams, *Inorg. Chem.*, 1965, **4**, 350-357.
5. A. B. P. Lever, in *Inorganic Electronic Spectroscopy*, Elsevier, New York, 2nd edn., 1984.
6. D. A. Clemente, A. Marzotto, G. Valle and C. J. Visonà, *Polyhedron*, 1999, **18**, 2749-2757.
7. X. J. Zhao, M. Du, Y. Wang and X. H. Bu, *J. Mol. Struct.*, 2004, **692**, 155-161.
8. J. C. M. Rivas and L. Brammer, *Coord. Chem. Rev.*, 1999, **183**, 43-80.
9. H. Dadon and J. Bernstein, *Inorg. Chem.*, 1997, **36**, 2898-2900.
10. L.J. Farrugia, ORTEP-3 for Windows, *J. Appl. Cryst.*, 1997, **30**, 565.
11. A. L. Spek, PLATON: A Multipurpose Crystallographic Tool, Utrecht University, Utrecht, The Netherlands, 1998.
12. D. F. Evans, *J. Chem. Soc.*, 1959, 2003-2005.
13. R. H. Holm and F. A. Cotton, *J. Chem. Phys.*, 1959, **31**, 788-792.
14. D. M. Jenkins, A. J. Di Bilio, M. J. Allen, T. A. Betley and J. C. Peters, *J. Am. Chem. Soc.*, 2002, **124**, 15336-15350.
15. L. Wang, C. Zhang and Z. X. Wang, *Eur. J. Inorg. Chem.*, 2007, **17**, 2477-2487.
16. K. P. Ho, W. L. Wong, K. M. Lam, C. P. Lai, T. H. Chan and K. Y. Wong, *Chem. Eur. J.*, 2008, **14**, 7988-7996.
17. L. P. C. Nielsen, C. P. Stevenson, D. G. Blackmond and E. N. Jacobsen, *J. Am. Chem. Soc.*, 2004, **126**, 1360-1362.
18. D. E. De Vos and T. Bein, *J. Organomet. Chem.*, 1996, **520**, 195-200.
19. D. De Vos and T. Bein, *Chem. Commun.*, 1996, 917-918.
20. S. V. Barkanova and O. L. Kaliya, *J. Porphyrins Phthalocyanines*, 1999, **3**, 180-187.
21. Y. Feng, C. Y. Ke, G. Xue and L. Que Jr., *Chem. Commun.*, 2009, 50-52.
22. V. B. Romakh, B. Therrien, G. Süss-Fink and G. B. Shul'pin, *Inorg. Chem.*, 2007, **46**, 1315-1331.

Chapter 4: Experimental

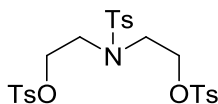
4.1 General remarks

All reagents were used as supplied from Alfa Aesar, Sigma-Aldrich or VWR unless otherwise stated. Manganese(II) triflate was obtained from Solchemar Fine Chemicals and was used without further purification. Dry acetonitrile was prepared by distillation over calcium hydride in an atmosphere of nitrogen. Tetrahydrofuran was dried by refluxing over sodium metal and benzophenone ketyl in an atmosphere of nitrogen prior to collection. Thin layer chromatography (tlc) was carried out on either VWR silica gel 60 F₂₅₄ plates or Merck neutral aluminium oxide 60 F₂₅₄ 150 plates. Flash column chromatography was carried out on either silica gel 60 (230-400 mesh) (VWR) or on neutral aluminium oxide 90 (70-230 mesh) (Merck Chemicals).

Melting point measurements were recorded on an electrothermal melting point apparatus and are uncorrected. Optical rotation measurements were made on a Jasco P1010 polarimeter ($\lambda = 589$ nm) with samples prepared in solvents and in concentrations as indicated, rotations are given in degrees. Elemental analysis was carried out at the chemistry department of University College London. UV-Visible spectra were recorded on a Hewlett-Packard 8453 diode array UV-Vis spectrophotometer. Infrared spectra were recorded directly as either solids or neat liquids on a Bruker Tensor 37 FTIR Spectrometer using a PIKE MIRacle ATR accessory or on a Shimadzu FTIR 8300 spectrometer as KBr discs or between NaCl plates (film). Nuclear magnetic resonance (NMR) were recorded on a JEOL JNM-EX270 (δ_H 270 MHz, δ_C 67.0 MHz), a Bruker AV 400 (δ_H 400.2 MHz, δ_C 100.6 MHz) and a Bruker AMX 400 (δ_H 400.1 MHz, δ_C 100.6 MHz) using solutions of deuterated solvents as indicated. Coupling constants (J) are given in Hz. Low resolution mass spectrometry and accurate mass analyses were carried out at the EPSRC National Mass Spectrometry Service Centre, University of Wales, Swansea. ESI measurements were made using a Waters ZQ-4000 instrument (Polyethyleneimine was added as the reference compound which was introduced in an ammonium acetate buffer). EI and CI analysis were carried out using either a Micromass Quattro II or a Finnigan MAT 95XP instrument. For EI, heptacosafuorotributylamine or perfluorokerosene was used as the reference compound

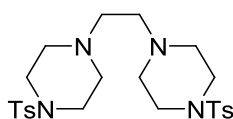
with analyses carried out at 70 eV. For CI, methane or ammonia were used as the ionisation source using heptacosafuorotributylamine as the reference compound.

4.2 (4-Methyl-*N*-(2-(*p*-toluenesulfonyloxy)ethyl)phenylsulfonamido)ethyl-4-methylbenzenesulfonate (**75**)



The synthesis of **75** has been reported previously,¹ however an improved yield can be obtained using the following method: To a cooled solution (0 °C) of diethanolamine (10.00 g, 95.11 mmol) dissolved in dichloromethane (50 cm³) was added, dropwise, a solution of *p*-toluenesulfonyl chloride (54.39 g, 285.3 mmol) dissolved in dichloromethane (90 cm³). After the addition was complete, the formation of a colourless precipitate was observed, which redissolved after the addition of triethylamine (53.00 g, 523.8 mmol) dissolved in dichloromethane (20 cm³) was completed. After stirring at 0 °C for a further half hour a colourless precipitate reappeared. The reaction vessel was allowed to reach ambient temperature and the dichloromethane was removed under reduced pressure, leaving an colourless oily solid. This was triturated with water (250 cm³), overnight, producing a solid which was collected and recrystallised from hot ethanol (1 L), yielding **75** as a crystalline colourless solid (43.68 g, 81%). mp 144-145 °C (ethanol); $\tilde{\nu}_{\text{max}}/\text{cm}^{-1}$ 1597, 1353, 1158, 975, 812; δ_{H} (400 MHz; CDCl₃; Me₄Si) 7.76 (4H, ap. d, *J* 8.4), 7.62 (2H, ap. d, *J* 8.4), 7.36 (4H, ap. d, *J* 8.4), 7.30 (2H, ap. d, *J* 8.4), 4.12 (4H, t, *J* 6.0), 3.38 (4H, t, *J* 6.0), 2.48-2.36 (9H, m); δ_{C} (100 MHz; CDCl₃; Me₄Si), 145.4, 144.3, 135.5, 132.6, 130.2, 130.1, 128.1, 127.4, 68.4, 48.6, 21.8, 21.7.

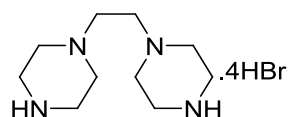
4.3 1,2-bis(4-Methylbenzenesulfonylpiperazin-4-yl)ethane (**76**)²



A solution of ethylenediamine (1.06 g, 17.6 mmol) in dry acetonitrile (100 cm³) and potassium carbonate (9.74 g, 70.6 mmol) were stirred under an atmosphere of dry

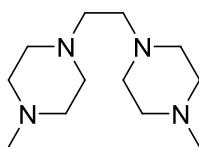
nitrogen. A solution of **75** (20.02 g, 35.27 mmol), dissolved in the minimum volume of dry acetonitrile was then added and the reaction mixture heated at reflux with stirring for 5 days. The organic solvent was removed under reduced pressure leaving a colourless solid. This was dissolved in water and extracted with dichloromethane (5 x 100 cm³). The combined organic extracts were dried using MgSO₄ with the subsequent removal of the solvent *in vacuo* yielding **76** as a colourless solid (7.89 g, 88%). mp 257-259 °C (dichloromethane); $\tilde{\nu}_{\max}/\text{cm}^{-1}$ 3032, 2824, 1346, 1167, 826; δ_H (400 MHz; CDCl₃; Me₄Si) 7.60 (4H, ap. d, *J* 8.2), 7.30 (4H, ap. d, *J* 8.2), 2.96 (8H, br. s), 2.61-2.45 (8H, m) 2.41 (10H, br. s); δ_C (100 MHz; CDCl₃; Me₄Si), 143.8, 132.2, 129.8, 128.0, 55.5, 52.7, 46.0, 21.6. *m/z* (ESI) 507.2089 (M+H⁺. C₂₄H₃₅N₄O₄S₂⁺ requires 507.2094).

4.4 1,2-bis(Piperazin-1-yl)ethane tetrahydrobromide salt (**77**)



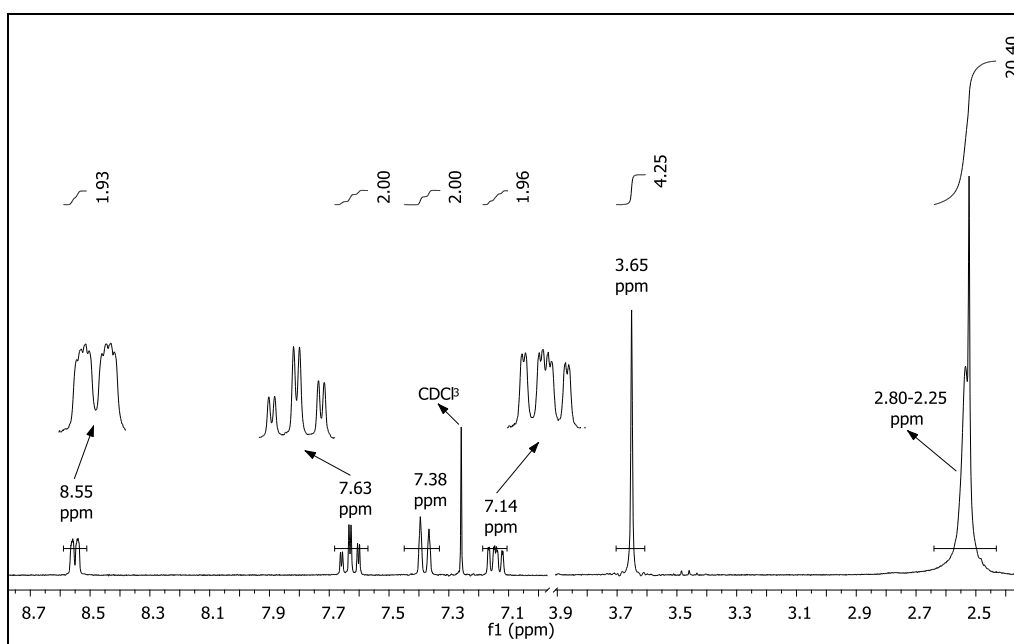
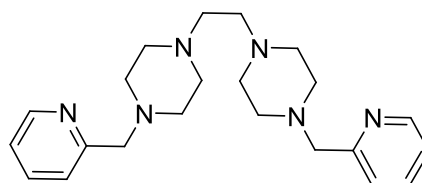
77 is a known³ compound but an improved method for its synthesis is as follows: To **76** (5.34 g, 10.5 mmol) was added concentrated sulfuric acid (98%) (35 cm³) and the mixture was then stirred until a clear solution formed. This was then heated to 110 °C and stirred under a nitrogen atmosphere at this temperature for 24 hours. The mixture was cooled to ambient temperature and the resulting solution added dropwise to ice-cold diethyl ether (100 cm³) without allowing the temperature to rise above 10 °C, resulting in the formation of a colourless precipitate. The diethyl ether was then carefully decanted and concentrated HBr in water (48%) (35 cm³) was added immediately. Stirring this solution for 30 minutes resulted in the formation of the tetrahydrobromide salt. The product was collected by filtration and was washed with ice-cold diethyl ether (3 x 30 cm³) then air dried to give **77** as a colourless solid (5.29 g, 96%). mp decomposes >270 °C; (Found: C, 20.7; H, 5.4; N, 9.4. calcd. for C₁₀H₂₆N₄Br₄ + 4H₂O: C, 20.2; H, 5.8; N, 9.4%); $\tilde{\nu}_{\max}/\text{cm}^{-1}$ 2923, 2361, 1435; δ_H (270 MHz; D₂O) 3.65-3.54 (8H, m), 3.54-3.42 (12H, m); δ_C (67.9 MHz; D₂O), 50.9, 49.5, 41.3; *m/z* (ESI) 199.1917 (M-4HBr+H⁺. C₁₀H₂₃N₄⁺ requires 199.1917).

4.5 1,2-bis(4-Methylpiperazin-1-yl)ethane (**62**)³⁻⁴



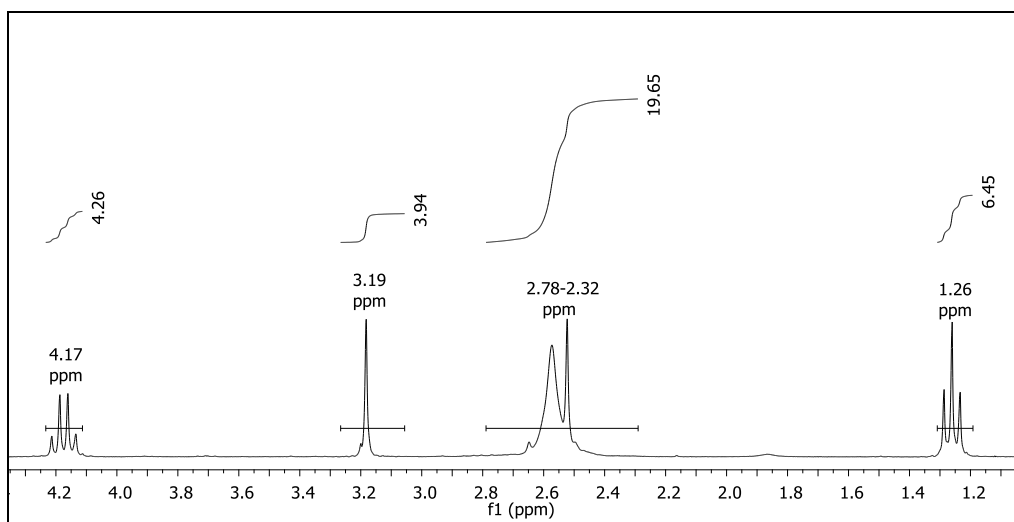
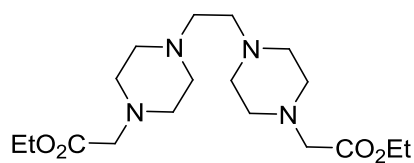
N-Methylation of **77** was accomplished using the Eschweiler-Clarke methodology.⁵ To **77** (1.03 g, 1.97 mmol) was added formic acid (97%) (6 cm³), formaldehyde (37%) (5 cm³) and distilled water (0.5 cm³) and the resultant mixture stirred and heated under reflux for 24 hours. The mixture was then cooled and transferred to ice-cold distilled water (15 cm³). This mixture was basified using a saturated solution of sodium hydroxide (~pH 12), keeping the temperature below 25 °C. The resulting basic solution was extracted using dichloromethane (5 x 100 cm³) and the combined organic extracts were dried using MgSO₄. The organic solvent was removed under reduced pressure producing **62** as a waxy colourless solid (0.38 g, 86%). mp 39-41 °C (dichloromethane); $\tilde{\nu}_{\max}/\text{cm}^{-1}$ 2936, 1451, 1377; δ_H (400 MHz; CDCl₃; Me₄Si) 2.77-2.30 (20H, m), 2.27 (6H, s); δ_C (100 MHz; CDCl₃; Me₄Si), 56.1, 55.3, 53.8, 46.2; m/z (ESI) 227.2230 (M+H⁺. C₁₂H₂₇N₄⁺ requires 227.2230).

4.6 1,2-bis(4-(Pyridin-2-ylmethyl)piperazin-1-yl)ethane (**67**)



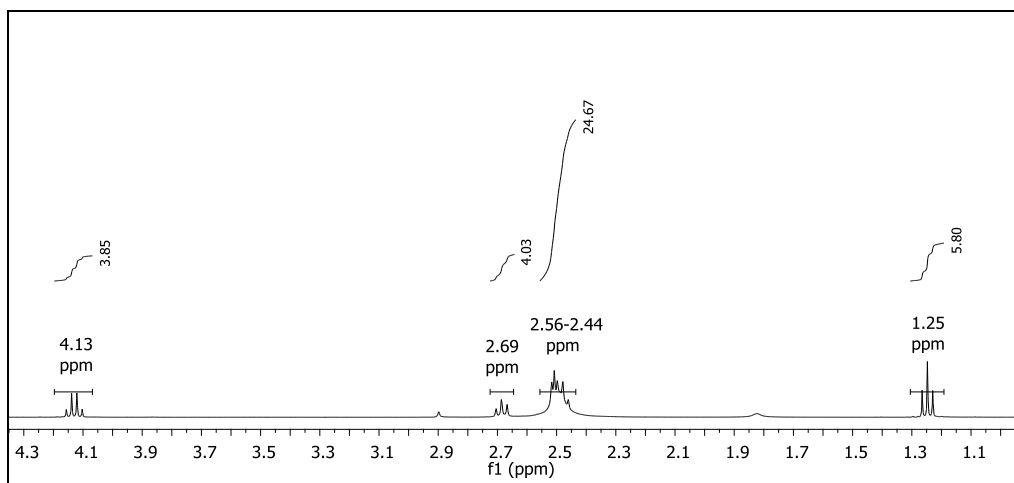
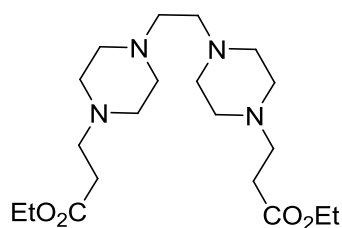
To **77** (2.00 g, 3.83 mmol), 2-chloromethylpyridine hydrochloride (1.28 g, 7.80 mmol) and potassium carbonate (8.47 g, 61.3 mmol) was added dry acetonitrile (150 cm³). This mixture was stirred and heated at reflux for 72 hours under an inert N₂ atmosphere. The resulting cloudy solution was allowed to settle before the majority of the organic solvent was decanted and the residue reduced *in vacuo* to an oily solid. This was extracted using chloroform (3 x 100 cm³) and the combined organic extracts dried using MgSO₄. The chloroform was removed under reduced pressure to produce an orange oil. The crude material was triturated with boiling diethyl ether (minimum volume) to produce an oily brown precipitate which was removed by hot filtration. The resulting filtrate was allowed to cool resulting in the formation of **67** as yellow crystals (1.26 g, 85%). mp 109-111 °C (diethyl ether); $\tilde{\nu}_{\max}/\text{cm}^{-1}$ 2815, 1589, 1568, 1448, 1434, 1375, 757, 609; δ_{H} (270 MHz; CDCl₃; Me₄Si) 8.55 (2H, ddd, *J* 5.0, 1.7, 0.7), 7.63 (2H, td, *J* 7.5, 1.7), 7.38 (2H, ap. d, *J* 7.6), 7.14 (2H, ddd, *J* 7.5, 4.9, 1.0), 3.65 (4H, br. s), 2.80-2.25 (20H, m); δ_{C} (67.9 MHz; CDCl₃; Me₄Si), 158.6, 149.4, 136.4, 123.3, 122.0, 64.7, 56.1, 53.7, 53.3; *m/z* (ESI) 381.2759 (M+H⁺. C₂₂H₃₃N₆⁺ requires 381.2761).

4.7 Diethyl-2,2'-(4,4'-(ethane-1,2-diyl)bis(piperazine-4,1-diyl))diacetate (**68**)



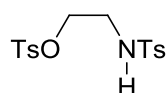
To **77** (2.00 g, 3.83 mmol), ethylbromoacetate (1.28 g, 7.66 mmol) and potassium carbonate (4.79 g, 34.6 mmol) was added acetonitrile (100 cm³) and the mixture heated at reflux with stirring for 48 hours. The resulting cloudy solution was filtered and the solvent then removed from the filtrate under reduced pressure producing a solid. To this was added distilled water and the mixture extracted using dichloromethane (5 x 75 cm³). The combined organic extracts were dried using MgSO₄ before the solvent was removed under reduced pressure to give **68** as a waxy colourless solid (0.81, 57%). mp 86-87 °C (dichloromethane); $\tilde{\nu}_{\max}(\text{film})/\text{cm}^{-1}$ 2978, 2818, 1747, 1334, 1298; δ_{H} (270 MHz; CDCl₃; Me₄Si) 4.17 (4H, q, *J* 7.1), 3.19 (4H, s), 2.78-2.32 (20H, m), 1.26 (6H, t, *J* 7.1); δ_{C} (67.9 MHz; CDCl₃; Me₄Si) 170.4, 60.7, 59.7, 56.0, 53.5, 53.2, 14.4; *m/z* (ESI) 371.2656 (M+H⁺. C₁₈H₃₅N₄O₄⁺ requires 371.2653).

4.8 Diethyl 3,3'-(4,4'-(ethane-1,2-diyl)bis(piperazine-4,1-diyl))dipropionate (**69**)



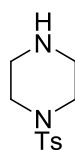
To **77** (2.00 g, 3.83 mmol), ethyl-3-bromopropionate (1.39 g, 7.68 mmol) and potassium carbonate (4.76 g, 34.4 mmol) was added acetonitrile (100 cm³) and the mixture heated at reflux with stirring for 36 hours. The resulting cloudy solution was filtered and the solvent then removed from the filtrate under reduced pressure producing a solid. To this was added distilled water and the mixture extracted using dichloromethane (5 x 75 cm³). The combined organic extracts were dried using MgSO₄ before the solvent was removed under reduced pressure to give **69** as a waxy colourless solid (0.97 g, 63%). mp 61-62 °C (dichloromethane); $\tilde{\nu}_{\max}(\text{film})/\text{cm}^{-1}$ 2945, 2804, 1728, 1383, 119; δ_{H} (400 MHz; CDCl₃; Me₄Si) 4.13 (4H, q, *J* 7.1), 2.69 (4H, t, *J* 6.8), 2.56-2.44 (24H, m), 1.25 (6H, t, *J* 7.1); δ_{C} (100 MHz; CDCl₃; Me₄Si) 172.6, 60.5, 56.0, 53.7, 53.0, 51.6, 32.5, 14.4; *m/z* (ESI) 399.2981 (M+H⁺. C₂₀H₃₉N₄O₄⁺ requires 399.2966).

4.9 2-(4-Methylphenylsulfonamido)ethyl-4-methylbenzenesulfonate (**86**)



Compound **86** has been prepared previously,⁶ however the following is an improved synthesis using dichloromethane instead of pyridine as the reaction solvent: Ethanolamine (5.00 g, 81.9 mmol) dissolved in dichloromethane (300 cm³) was cooled to -5 °C. To this was added *p*-toluenesulfonyl chloride (31.21 g, 163.7 mmol) dissolved in dichloromethane (600 cm³), dropwise, over a period of 30 minutes, keeping the temperature at -5 °C. The mixture was allowed to stir at ca. -5 °C for a further hour, after which time a precipitate was observed. The addition of triethylamine (33.13 g, 327.4 mmol) followed and the mixture was stirred at ambient temperature for a further hour. The volume of the reaction mixture was reduced *in vacuo* to approximately a third of its original volume and this was added to a saturated brine solution (300 cm³). The mixture was extracted using dichloromethane (5 x 150 cm³) and the combined organic layers were dried using MgSO₄. Dichloromethane was removed under reduced pressure, producing a colourless oil. Trituration of this oil with distilled water (500 cm³), overnight, produced a white solid. This was purified by column chromatography on silica gel using diethyl ether and *n*-hexane as the solvent system (70:30 respectively), giving **86** as colourless, needle-like crystals (21.12 g, 70%). mp 92-93° C (diethyl ether/*n*-hexane); $\tilde{\nu}_{\max}/\text{cm}^{-1}$ 2940, 1599, 1420, 1365, 1153, 809; δ_{H} (400 MHz; CDCl₃; Me₄Si) 7.77-7.67 (4H, m), 7.37-7.24 (4H, m), 4.97 (1H, ap. t, *J* 6.4), 4.04 (2H, t, *J* 5.3), 3.21 (2H, td, *J* 6.4, 5.3), 2.45 (3H, s), 2.42 (3H, s); δ_{C} (100 MHz; CDCl₃; Me₄Si) 145.5, 143.9, 136.7, 132.4, 130.2, 130.0, 128.1, 127.1, 68.8, 42.3. 21.8, 21.7; *m/z* (EI) 369.0694 (M⁺. C₁₆H₁₉NO₅S₂⁺ requires 369.0699).

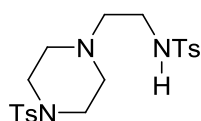
4.10 1-(4-Methylphenylsulfonamido)piperazine (**87**)⁷



Anhydrous piperazine (45.18 g, 524.0 mmol) dissolved in dichloromethane (600 cm³) was stirred and cooled to -5 °C. To this solution was added *p*-toluenesulfonyl chloride (5.00 g, 26.2 mmol) dissolved in dichloromethane (200 cm³), dropwise, over a period of 2 hours, and the temperature was kept below 0 °C resulting in the formation of a white precipitate. The resulting mixture was allowed to warm to room temperature and stirred for a further 30 minutes. The cloudy solution was then filtered and the filtrate washed using a saturated brine solution (1L). The organic layer was dried using MgSO₄ and the

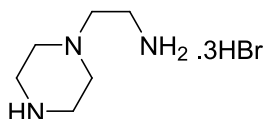
solvent removed under reduced pressure, leaving **87** as a white solid (4.55 g, 72%). mp 99-100 °C (dichloromethane); $\tilde{\nu}_{\max}(\text{film})/\text{cm}^{-1}$ 3050, 2920, 2851, 1338, 1167, 816; δ_H (400 MHz; CDCl₃; Me₄Si) 7.62 (2H, ap. d, *J* 8.1), 7.31 (2H, ap. d, *J* 8.1), 2.99-2.87 (8H, m), 2.42 (3H, s), 1.48 (1H, br. s); δ_C (100 MHz; CDCl₃; Me₄Si) 143.7, 132.6, 129.7, 127.8, 47.0, 45.5, 21.6; *m/z* (ESI) 241.1008 (M+H⁺. C₁₁H₁₇N₂O₂S⁺ requires 241.1005).

4.11 4-Methyl-*N*-(2-(4-methylbenzenesulfonylpiperazin-1yl)ethyl)-benzenesulfonamide (**88**)⁸



To a mixture of **86** (5.42 g, 14.7 mmol), **87** (3.53 g, 14.7 mmol) and potassium carbonate (4.06 g, 29.4 mmol) was added dry acetonitrile (80 cm³). The mixture was heated at reflux under dry nitrogen for 48 hours, after which time it was cooled down to ambient temperature. Acetonitrile was removed under reduced pressure and the resulting oily solid extracted using dichloromethane (5 x 100 cm³). The combined organic extracts were dried using MgSO₄ and reduced *in vacuo* to give an oily solid as the crude product. This was recrystallised from acetonitrile to give **88** as a crystalline colourless solid (4.23 g, 66%). mp 149-151 °C (acetonitrile); $\tilde{\nu}_{\max}(\text{film})/\text{cm}^{-1}$ 3263, 1596, 1326, 1148, 810; δ_H (400 MHz; CDCl₃; Me₄Si) 7.69-7.50 (4H, m), 7.31 (2H, ap. d, *J* 8.3) 7.26-7.16 (2H, m), 4.84 (1H, m), 3.09-2.69 (6H, m), 2.46-2.21 (12H, m); δ_C (100 MHz; CDCl₃; Me₄Si) 144.2, 143.7, 136.6, 132.1, 129.9, 129.8, 127.9, 127.2, 55.4, 51.6, 46.1, 39.1, 21.8, 21.7; *m/z* (ESI) 438.1519 (M+H⁺. C₂₀H₂₈N₃O₄S₂⁺ requires 438.1516).

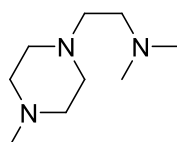
4.12 1-(2-Aminoethyl)piperazine trihydrobromide salt (**89**)



Compound **88** (1.19 g, 2.72 mmol) was dissolved in concentrated H₂SO₄ (98%) (30 cm³) and the mixture then heated to 110 °C under an inert nitrogen atmosphere for 72 hours. The resulting brown liquid was cooled to room temperature and slowly added

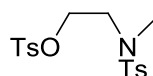
dropwise to ice-cold diethyl ether (70 cm³), without allowing the temperature to exceed 15 °C. The diethyl ether was decanted from the resulting precipitate, to which was added concentrated HBr in water (48%) (30 cm³) and the mixture stirred overnight at ambient temperature. The off-white trihydrobromide salt was collected by filtration but found to be extremely hygroscopic. Storing this solid in a desiccator for a week, produced a orange/brown crystalline solid of **89** (0.68 g, 67%). mp decomposes; $\tilde{\nu}_{\text{max}}(\text{film})/\text{cm}^{-1}$ 2988, 1544, 1329, 1000; δ_{H} (400 MHz; D₂O) 3.70-3.40 (m); δ_{C} (100 MHz; D₂O) 53.2, 49.3, 40.8, 33.6; m/z (ESI) 130.1340 (M-3HBr+H⁺. C₆H₁₆N₃⁺ requires 130.1339).

4.13 *N,N*-Dimethyl-2-(4-methylpiperazin-1-yl)ethanamine (**60**)^{3,9}



To **89** (2.00 g, 5.38 mmol) was added formic acid (97%) (26 cm³), formaldehyde (37%) (24 cm³) and distilled water (3 cm³). This mixture was stirred and heated at reflux for 48 hours then cooled to ambient temperature. The mixture was transferred to ice-cold distilled water (40 cm³) and basified using a saturated sodium hydroxide solution to ~pH 12, keeping the temperature below 25 °C. The resulting basic solution was extracted using dichloromethane (4 x 100 cm³) and the combined organic extracts dried using MgSO₄. The solvent was removed under reduced pressure giving **60** as a light yellow oil (0.69 g, 75%). $\tilde{\nu}_{\text{max}}/\text{cm}^{-1}$ 2942, 2799, 1458, 751; δ_{H} (270 MHz; CDCl₃; Me₄Si) 2.59-2.31 (12H, m) 2.30-2.14 (9H, m); δ_{C} (67.9 MHz; CDCl₃; Me₄Si) 57.0, 56.8, 55.1, 53.7, 46.1, 46.0; m/z (ESI) 172.1810 (C₉H₂₂N₃+H⁺. C₉H₂₃N₃⁺ requires 172.1808).

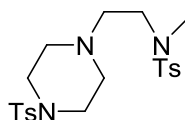
4.14 2-(*N*-4-Dimethylphenylsulfonamido)ethyl-4-methylbenzenesulfonate (**91**)



Compound **91** was prepared by a different method to that described by Michejda *et al.*¹⁰ with an improved yield as follows: 2-(Methylamino)ethanol (10.00 g, 133.1 mmol)

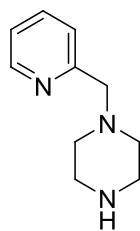
dissolved in dichloromethane (50 cm³) was cooled to below -5 °C. To this was added *p*-toluenesulfonyl chloride (50.77 g, 266.3 mmol) dissolved in dichloromethane (350 cm³), dropwise, over a period of one hour, keeping the temperature below -5 °C. This mixture was allowed to stir at room temperature for a further hour after which time, triethylamine (26.95 g, 266.3 mmol) was added, followed by a further hour of stirring at ambient temperature. The mixture was then reduced *in vacuo* to approximately half its original volume and added to a saturated brine solution (250 cm³) then extracted using dichloromethane (5 x 150 cm³). The combined organic layers were dried using MgSO₄ and the solvent removed under reduced pressure, producing a colourless solid. This was recrystallised from hot ethanol giving **91** as a colourless crystalline solid (42.68 g, 83%). mp 81-82 °C (ethanol); $\tilde{\nu}_{\max}/\text{cm}^{-1}$ 1447, 1356, 1326, 1152, 815; δ_H (400 MHz; CDCl₃; Me₄Si) 7.76 (2H, ap. d, *J* 8.3), 7.62 (2H, ap. d, *J* 8.3), 7.36 (2H, ap. d, *J* 8.0), 7.31 (2H, ap. d, *J* 8.0) 4.16 (2H, t, *J* 5.7), 3.29 (2H, t, *J* 5.7), 2.76 (3H, s) 2.49-2.40 (6H, m); δ_C (100 MHz; CDCl₃; Me₄Si) 145.3, 143.9, 134.4, 132.6, 130.2, 130.0, 128.1, 127.5, 68.8, 49.2, 36.7, 21.8, 21.7; *m/z* (ESI) 401.1198 (M+NH₄⁺. C₁₇H₂₅N₂O₅S₂⁺ requires 401.1199).

4.15 *N*-4-Dimethyl-*N*-(2-(4-tosylpiperazin-1-yl)ethyl)benzenesulfonamide (**98**)



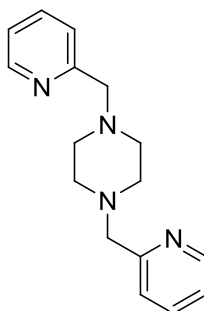
A mixture of **91** (5.63 g, 14.7 mmol), **87** (3.53 g, 14.7 mmol) and potassium carbonate (4.06 g, 29.4 mmol) was heated at reflux in dry acetonitrile (200 cm³) for 72 hours. This was then cooled to room temperature and the solids removed by filtration. The solvent was removed from the resulting filtrate under reduced pressure giving a colourless oil as the crude product. Addition of diethyl ether to the crude oil resulted in the formation of large colourless crystals of **98** (5.31 g, 80%). mp 108-110 °C (diethyl ether); $\tilde{\nu}_{\max}/\text{cm}^{-1}$ 2812, 1452, 1329, 1154, 813; δ_H (400 MHz; CDCl₃; Me₄Si) 7.62 (4H, ap. d, *J* 8.2), 7.35-7.22 (4H, m), 3.10-2.89 (6H, m), 2.69 (3H, s), 2.60-2.46 (6H, m), 2.45-2.35 (6H, m); δ_C (100 MHz; CDCl₃; Me₄Si) 143.9, 143.5, 134.5, 132.4, 129.8, 129.7, 128.0, 127.5, 55.6, 52.3, 47.4, 46.1, 35.4, 21.7, 21.6; *m/z* (ESI) 452.1665 (M+H⁺. C₂₁H₃₀N₃O₄S₂⁺ requires 452.1672).

4.16 1-(Pyridin-2-ylmethyl)piperazine (**95**)¹¹



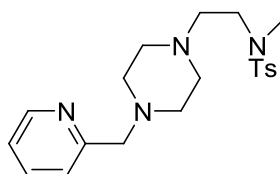
To a stirring solution of anhydrous piperazine (1.00 g, 11.6 mmol) dissolved in acetonitrile was added potassium iodide (0.013 g, 0.078 mmol) and then followed by the dropwise addition of 2-chloromethylpiperazine hydrochloride (0.13 g, 0.80 mmol) dissolved in methanol at room temperature. This mixture was then allowed to stir at ambient temperature overnight. The organic solvents were removed under reduced pressure, leaving a solid residue which was added to distilled water and extracted using dichloromethane (4 x 50 cm³). The combined organic layers were dried using MgSO₄ and the solvent removed under reduced pressure, producing a yellow oil. This was purified by column chromatography on neutral alumina using compositions of dichloromethane and methanol, yielding **95** as a light yellow oil (0.92 g, 66%). $\tilde{\nu}_{\text{max}}/\text{cm}^{-1}$ 2939, 2811, 1590, 1570, 1474, 1433, 756; δ_{H} (400 MHz; CDCl₃; Me₄Si) 8.56-8.51 (1H, m), 7.62 (1H, td, *J* 7.7, 1.7), 7.39 (1H, ap. d, *J* 7.7), 7.17-7.09 (1H, m), 3.62 (2H, s), 2.89 (4H, m), 2.45 (4H, br. s), 1.48 (1H, br. s); δ_{C} (100 MHz; CDCl₃; Me₄Si) 158.7, 149.4, 136.4, 123.4, 122.1, 65.4, 54.9, 46.2; *m/z* (ESI) 178.1330 (M+H⁺. C₁₀H₁₆N₃⁺ requires 178.1339).

4.17 1,4-bis(Pyridin-2-ylmethyl)piperazine (**64**)¹²



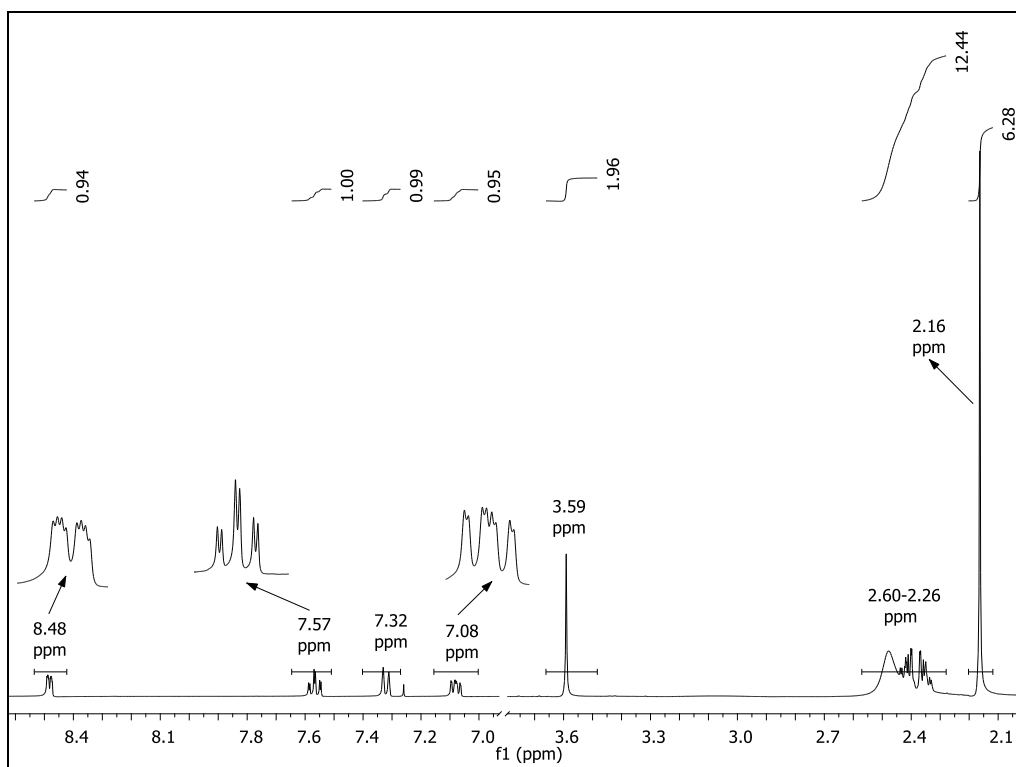
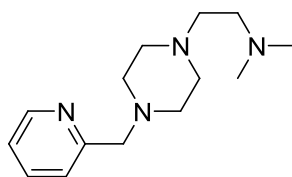
To anhydrous piperazine (2.00 g, 23.2 mmol), 2-chloromethylpyridine hydrochloride (7.62 g, 46.4 mmol) and triethylamine (7.05 g, 69.7 mmol) was added acetonitrile (60 cm³) and the mixture stirred at room temperature for 24 hours. The resulting mixture was added to a saturated brine solution (70 cm³) and extracted with dichloromethane (3 x 100 cm³). The combined organic layers were dried using MgSO₄ and the solvent removed under reduced pressure, producing a yellow oily solid. This was boiled in diethyl ether (100 cm³) which caused a brown precipitate to form which was removed by filtration. The resulting filtrate on standing produced a large crop of crystals which were collected by filtration, giving **64** as large yellow crystals (3.65 g, 59%). 98-100 °C (diethyl ether); $\tilde{\nu}_{\max}/\text{cm}^{-1}$ 2800, 1584, 1420, 1343, 1305, 756; δ_{H} (400 MHz; CDCl₃; Me₄Si) 8.54 (2H, ddd, *J* 4.9, 1.8, 1.0), 7.62 (2H, td, *J* 7.6, 1.8), 7.39 (2H, ap. d, *J* 7.6), 7.13 (2H, ddd, *J* 7.6, 4.9, 1.1) 3.66 (4H, s) 2.56 (8H, br. s); δ_{C} (100 MHz; CDCl₃; Me₄Si) 158.7, 149.4, 136.4, 123.3, 122.1, 64.7, 53.3; *m/z* (ESI) 269.1763 (M+H⁺. C₁₆H₂₁N₄⁺ requires 269.1761).

4.18 *N*-4-Dimethyl-*N*-(2-(4-(pyridin-2-ylmethyl)piperazin-1-yl) ethyl) benzenesulfonamide (**96**)



To **95** (1.15 g, 6.49 mmol), **91** (2.49 g, 6.49 mmol) and potassium carbonate (1.80 g, 13.0 mmol) was added acetonitrile (150 cm³) and the mixture stirred at reflux for 48 hours. The mixture was filtered and the filtrate reduced *in vacuo* leaving a brown oil, which was purified by column chromatography on neutral alumina, using dichloromethane and methanol (99.99:0.01 respectively) as the mobile phase, giving **96** as a colourless crystalline solid (1.63 g, 65%). mp 258-260 °C; $\tilde{\nu}_{\max}/\text{cm}^{-1}$ 2811, 1592, 1337, 1158, 817, 762; δ_{H} (400 MHz; CDCl₃; Me₄Si) 8.55-8.49 (1H, m), 7.67-7.57 (3H, m), 7.35 (1H, ap. d, *J* 7.8), 7.30-7.21 (2H, m), 7.17-7.07 (1H, m), 3.62 (2H, s), 3.10 (2H, m), 2.72 (3H, s), 2.59-2.33 (13H, m); δ_{C} (100 MHz; CDCl₃; Me₄Si) 158.5, 149.4, 143.4, 136.5, 134.8, 129.7, 127.5, 123.4, 122.1, 64.6, 56.5, 56.4, 53.3, 47.6, 35.6, 21.6; *m/z* (ESI) 389.2002 (M+H⁺. C₂₀H₂₉N₄O₂S⁺ requires 389.2006).

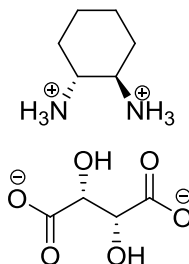
4.19 *N,N*-Dimethyl-2-(4-(pyridin-2-ylmethyl)piperazin-1-yl)ethanamine (**63**)



To **96** (1.03 g, 2.65 mmol) was added concentrated sulfuric acid (98%) (15 cm³) and the mixture heated under an inert atmosphere at 110 °C for 24 hours. The reaction mixture was then cooled to room temperature and added dropwise to ice-cold diethyl ether (50 cm³), resulting in the formation of a white precipitate. The diethyl ether was then carefully decanted leaving a white solid to which was immediately added a pre-mixed solution of formic acid (98%) (5 cm³) and formaldehyde (37%) (10 cm³) and the mixture then heated at reflux for 24 hours. The vessel was allowed to reach room temperature and the reaction mixture added to cold distilled water (30 cm³). This was basified using a saturated sodium hydroxide solution to ~pH 12, keeping the temperature below 25 °C. The resulting basic solution was extracted using dichloromethane (5 x 50 cm³) and the combined organic extracts dried using MgSO₄. Dichloromethane was removed under reduced pressure giving **63** as a light yellow oil (0.44 g, 67%). $\tilde{\nu}_{\max}/\text{cm}^{-1}$ 2809, 1589, 1458, 1157, 758; δ_{H} (400 MHz; CDCl₃; Me₄Si)

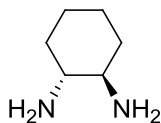
8.48 (1H, ddd, J 4.8, 1.8, 0.9), 7.57 (1H, td, J 7.6, 1.8), 7.32 (1H, ap. d, J 7.6), 7.08 (1H, ddd, J 7.6, 4.8, 1.1), 3.59 (2H, s), 2.60-2.26 (12H, m), 2.16 (6H, s); δ_C (100 MHz; CDCl₃; Me₄Si) 158.5, 149.2, 136.3, 123.2, 122.0, 64.6, 56.9, 56.7, 53.6, 53.2, 45.9; m/z (ESI) 249.2074 (M+H⁺. C₁₄H₂₅N₄⁺ requires 249.2074).

4.20 (1*R*,2*R*)-Cyclohexane-1,2-diammonium (2*R*,3*R*)-2,3-dihydroxytartrate (**118**)¹³



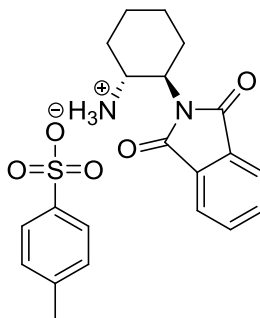
To a mixture of *cis*- and *trans*-1,2-diaminocyclohexane (120 g, 1.05 mol) dissolved in methanol (50 cm³) and distilled water (250 cm³) was added L-(+)-tartaric acid (80 g, 0.53 mol) and glacial acetic acid (31.55 g) and the mixture then heated at reflux (90 °C) for 24 hours and then allowed to cool to ambient temperature. The resulting precipitate which formed was collected by vacuum filtration then washed thoroughly using ice-cold methanol and allowed to air dry, giving **118** as a colourless solid (63.20 g, 37%). All analytical and spectroscopic data were consistent with those reported previously.^{13a}

4.21 (1*R*,2*R*)-Cyclohexane-1,2-diamine (**98**)^{13a}



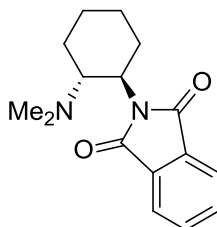
To **118** (62.95 g, 238.2 mmol), dissolved in distilled water (400 cm³) was added a saturated potassium hydroxide solution until the pH reached 10. This solution was extracted using dichloromethane (5 x 200 cm³). The combined organic extracts were dried using MgSO₄ and reduced *in vacuo* to give **98** as a colourless solid (12.43 g, 46%). mp 42-45 °C; $[\alpha]_D^{25}$ -25.3 (*c* 5.0, 1 M HCl); $\tilde{\nu}_{\max}/\text{cm}^{-1}$ 3351, 1590, 1448, 842; δ_H (400 MHz; CDCl₃; Me₄Si) 2.32-2.17 (2H, m), 1.90-1.75 (2H, m), 1.74-1.60 (2H, m), 1.57-1.39 (4H, m), 1.32-1.17 (2H, m), 1.17-0.99 (2H, m); δ_C (100 MHz; CDCl₃; Me₄Si) 57.9, 35.7, 25.6; m/z (EI) 114.1150 (M⁺. C₆H₁₄N₂⁺ requires 114.1152).

4.22 (1*R*,2*R*)-2-(1,3-dioxoisindolin-2-yl)cyclohexanaminium-4-methylbenzenesulfonate (**99**)¹⁴



p-Toluenesulfonic acid monohydrate (8.33 g, 43.8 mmol) dissolved in xylene (225 cm³) was dried using a Dean-Stark trap. To this was added phthalic anhydride (99%) (6.49 g, 43.8 mmol) and **98** (5.00 g, 43.8 mmol) and the resultant mixture was then heated until a homogenous solution was obtained. Further heating resulted in the crystallisation of the product. The reaction vessel was cooled to room temperature and the product collected by filtration, washed with cold *n*-hexane, then allowed to air dry yielding **99** as a colourless solid (14.96 g, 82%). mp 147-152 °C (xylene/*n*-hexane); [α]_D²⁵ -15.5 (*c* 1.0, CHCl₃); $\tilde{\nu}_{\text{max}}/\text{cm}^{-1}$ 2929, 1706, 1539, 1386, 1168, 814, 717; δ_{H} (400 MHz; CDCl₃; Me₄Si) 7.84 (3H, br. s), 7.66-7.50 (2H, m), 7.50-7.41 (2H, m), 7.37 (2H, ap. d, *J* 8.0), 7.00 (2H, ap. d, *J* 8.0), 4.18 (1H, td, *J* 11.7, 3.8), 4.06-3.75 (1H, m), 2.34 (3H, s), 2.23-1.91 (2H, m), 1.83-1.37 (4H, m), 1.34-1.17 (2H, m); δ_{C} (100 MHz; CDCl₃; Me₄Si) 168.7, 141.2, 140.2, 133.5, 132.2, 128.8, 126.0, 123.1, 52.6, 50.9, 30.2, 29.1, 24.6, 23.8, 21.5; *m/z* (ESI) 245.1282 (M⁺-C₇H₇O₃S⁻. C₁₄H₁₇N₂O₂⁺ requires 245.1285).

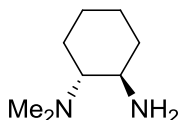
4.23 2-((1*R*,2*R*)-2-(Dimethylamino)cyclohexyl)isoindoline-1,3-dione (**100**)¹⁴



To **99** (26.69 g, 64.05 mmol) was added formaldehyde (37%) (70 cm³) and formic acid (97%) (30 cm³) and the mixture was then heated at reflux, overnight. The resulting

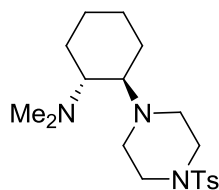
mixture was cooled to room temperature and added dropwise to a cooled, saturated sodium hydroxide solution. The resulting alkaline solution was extracted using dichloromethane (5 x 200 cm³), dried with MgSO₄, and then reduced to a yellow oily solid under reduced pressure. The crude product was recrystallised from hot ethanol and diethyl ether yielding **100** as large yellow crystals (10.53 g, 60%). mp 130-131 °C; $[\alpha]_{\text{D}}^{25}$ -33.0 (*c* 1.0, CHCl₃); $\tilde{\nu}_{\text{max}}/\text{cm}^{-1}$ 2932, 1762, 1702, 1370, 1140, 716; δ_{H} (400 MHz; CDCl₃; Me₄Si) 7.86-7.78 (2H, m), 7.74-7.65 (2H, m), 4.10 (1H, td, *J* 11.7, 3.7), 3.44-3.17 (1H, m), 2.29-2.10 (7H, m), 2.02-1.70 (4H, m), 1.47-1.07 (3H, m); δ_{C} (100 MHz; CDCl₃; Me₄Si) 168.8, 133.7, 132.4, 123.1, 62.3, 52.4, 40.4, 30.4, 25.9, 25.2, 22.9; *m/z* (ESI) 273.1602 (M+H⁺. C₁₆H₂₁N₂O₂⁺ requires 273.1598).

4.24 (1*R*,2*R*)-*N,N*-Dimethylcyclohexane-1,2-diamine (**101**)¹⁴



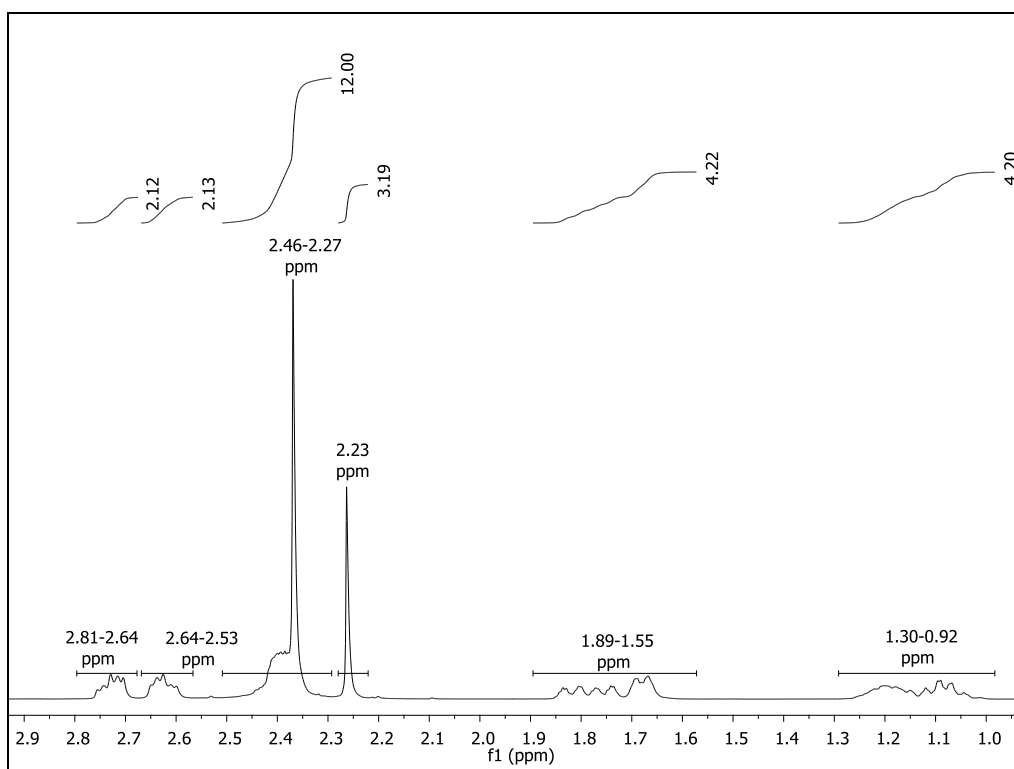
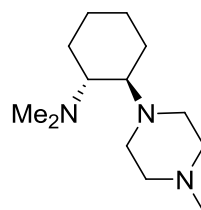
To **100** (4.78 g, 17.6 mmol) dissolved in ethanol (30 cm³) was added hydrazine hydrate (1.5 H₂O) (1.55 g, 26.3 mmol) and the mixture was heated for two hours at reflux. The reaction mixture was cooled to room temperature and added to cold diethyl ether (350 cm³) causing a large amount of a white solid to precipitate. This was separated by filtration and washed with diethyl ether (150 cm³). The resulting filtrate was concentrated *in vacuo*, dissolved in hydrochloric acid (0.5 M, 100 cm³) and the resultant solution stirred for half an hour. The acidic solution was basified using solid potassium carbonate and extracted using dichloromethane (5 x 150 cm³). The combined organic extracts were dried using MgSO₄ and the dichloromethane removed under reduced pressure, giving **101** as a yellow oil (2.11 g, 85%). $[\alpha]_{\text{D}}^{25}$ -32.0 (*c* 1.0, CHCl₃); $\tilde{\nu}_{\text{max}}/\text{cm}^{-1}$ 2925, 2856, 1580, 1449, 1056, 902; δ_{H} (400 MHz; CDCl₃; Me₄Si) 2.49 (1H, td, *J* 10.1, 4.1), 2.15 (6H, s), 2.01-1.80 (2H, m), 1.75-1.63 (2H, m), 1.63-1.49 (3H, m), 1.06-0.89 (4H, m); δ_{C} (100 MHz; CDCl₃; Me₄Si) 69.9, 51.5, 40.2, 35.3, 25.7, 25.1, 20.6; *m/z* (ESI) 143.1541 (M+H⁺. C₈H₂₀N₂⁺ requires 143.1543).

4.25 (1*R*,2*R*)-*N,N*-Dimethyl-2-(4-methylbenzenesulfonylpiperazin-1-yl)cyclohexanamine (**102**)



To **101** (0.590 g, 4.15 mmol) dissolved in acetonitrile (40 cm³), **75** (2.35 g, 4.15 mmol) and potassium carbonate (1.72 g, 12.5 mmol) were added and the mixture then heated at reflux for 7 days. The inorganic solids were then removed by filtration and washed thoroughly with acetonitrile (100 cm³). The filtrate was concentrated under reduced pressure to give a crude oil. This was recrystallised by dissolving in a minimum volume of acetone followed by the addition of distilled water until the first appearance of cloudiness. Allowing this to stand resulted in the formation of large colourless crystals of **102** which were collected by filtration. (0.99 g, 66%). mp 105-108 °C; [α]_D²⁵ -20.0 (*c* 1.0, CHCl₃); $\tilde{\nu}_{\text{max}}/\text{cm}^{-1}$ 2925, 2853, 1451, 1348, 1165, 815, 728; δ_{H} (400 MHz; CDCl₃; Me₄Si) 7.63 (2H, ap. d, *J* 8.2), 7.31 (2H, ap. d, *J* 8.2), 3.07-2.86 (4H, m), 2.83-2.67 (4H, m), 2.41 (3H, s), 2.38-2.28 (2H, m), 2.23 (6H, s), 1.90-1.51 (4H, m), 1.35-0.82 (4H, m); δ_{C} (100 MHz; CDCl₃; Me₄Si) 143.5, 133.1, 129.7, 128.0, 64.6, 63.8, 47.9, 47.0, 40.6, 27.7, 25.9, 25.8, 25.6, 21.7; *m/z* (ESI) 366.2213 (M+H⁺. C₁₉H₃₂N₃O₂S⁺ requires 366.2210).

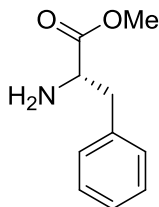
4.26 (1*R*,2*R*)-*N,N*-Dimethyl-2-(4-methylpiperazin-1-yl)cyclohexanamine (**61**)



Compound **102** (1.44 g, 3.94 mmol) was dissolved in sulfuric acid (98%) (15 cm³) and the mixture was heated at 110 °C for 24 hours. The resulting brown solution was cooled and added dropwise to ice-cold diethyl ether, forming an off-white precipitate. The diethyl ether was then decanted and a freshly prepared, premixed solution of formic acid (97%) (5 cm³) and formaldehyde (37%) (15 cm³) immediately added. This solution was then heated at reflux for 24 hours. The resulting acidic mixture was added dropwise to a cooled saturated sodium hydroxide solution. The basic solution was extracted using dichloromethane (3 x 150 cm³), dried using MgSO₄ and the solvent removed under reduced pressure giving **61** as a light yellow oil (0.74 g, 83%). $[\alpha]_{\text{D}}^{25}$ -26.3 (*c* 1.1, CHCl₃); $\tilde{\nu}_{\text{max}}/\text{cm}^{-1}$ 2926, 1450, 1283, 1150, 1014; δ_{H} (400 MHz; CDCl₃; Me₄Si) 2.81-2.64 (2H, m), 2.64-2.53 (2H, m), 2.46-2.27 (12H, m), 2.23 (3H, s), 1.89-1.55 (4H, m),

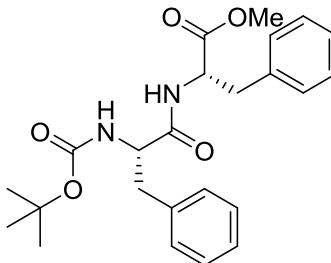
1.30-0.92 (4H, m); δ_C (100 MHz; CDCl_3 ; Me_4Si) 64.9, 63.3, 56.1, 48.3, 46.3, 41.0, 28.4, 26.3, 25.9, 25.8; m/z (ESI) 226.2277 ($\text{M}+\text{H}^+$. $\text{C}_{13}\text{H}_{28}\text{N}_3^+$ requires 226.2278).

4.27 (*S*)-Methyl-2-amino-3-phenylpropanoate (**105**)¹⁵



To **104** (4.00 g, 15.4 mmol) dissolved in methanol (40 cm^3) and cooled to $-10\text{ }^\circ\text{C}$ was added acetyl chloride (3.62 g, 46.11 mmol) and the mixture stirred overnight at ambient temperature. The organic solvents were removed under reduced pressure giving the product ester as a colourless, solid hydrochloride salt. This was dissolved in distilled water (200 cm^3) and basified to pH 10 using potassium carbonate. The resulting free amine was extracted using dichloromethane (5 x 100 cm^3). The combined organic extracts were dried using MgSO_4 and the solvent was removed under reduced pressure giving **105** as a colourless oil (2.35 g, 87%). δ_H (400 MHz; CDCl_3 ; Me_4Si) 7.56-7.05 (5H, m), 3.85-3.64 (4H, m), 3.10 (1H, dd, J 13.5, 5.2), 2.88 (1H, dd, J 13.5, 7.8), 1.46 (2H, br. s); δ_C (100 MHz; CDCl_3 ; Me_4Si) 175.5, 137.3, 129.3, 128.6, 126.9, 55.9, 52.0, 41.2.

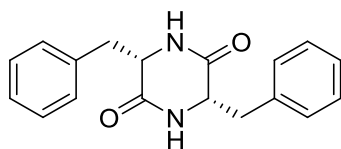
4.28 (*S*)-Methyl-2-((*S*)-2-(*t*-butoxycarbonylamino)-3-phenylpropanamido)-3-phenylpropanoate (**106**)¹⁶



104 (3.48 g, 13.1 mmol), HATU (4.99 g, 13.1 mmol) and diisopropylethyl amine (5.09 g, 39.4 mmol) were dissolved in dichloromethane (100 cm^3) and the resultant solution stirred at room temperature for thirty minutes. To this was added **105** (2.35 g, 13.1

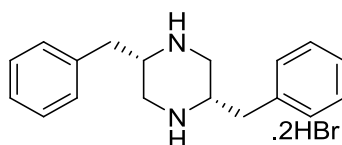
mmol) dissolved in dichloromethane (15 cm³) and the mixture allowed to stir overnight. The dichloromethane solution was then washed with a sodium acetate buffer (pH 4) (150 cm³) and then using a saturated potassium carbonate solution (150 cm³). The organic layer was dried using MgSO₄ and reduced *in vacuo* yielding the **106** as a colourless solid (4.39 g, 79%). mp 120-121 °C (dichloromethane); [α]_D²⁵ -6.0 (*c* 0.67, CH₃OH); $\tilde{\nu}_{\max}/\text{cm}^{-1}$ 3331, 1746, 1700, 1522, 1167, 754, 698; δ_{H} (400 MHz; CDCl₃; Me₄Si) 7.41-7.12 (8H, m), 7.07-6.89 (2H, m), 6.44-6.15 (1H, m), 5.06-4.71 (2H, m), 4.35 (1H, br. s), 3.70 (3H, s), 3.19-2.91 (4H, m), 1.43 (9H, s); δ_{C} (100 MHz; CDCl₃; Me₄Si) 171.5, 170.9, 135.7, 135.8, 129.5, 129.4, 128.8, 128.7, 127.3, 127.1, 80.4, 55.8, 53.4, 52.4, 38.4, 38.1, 28.4; *m/z* (ESI) 427.2228 (M+H⁺. C₂₄H₃₁N₂O₅⁺ requires 427.2227).

4.29 (3*S*,6*S*)-3,6-Dibenzylpiperazine-2,5-dione (**107**)¹⁶



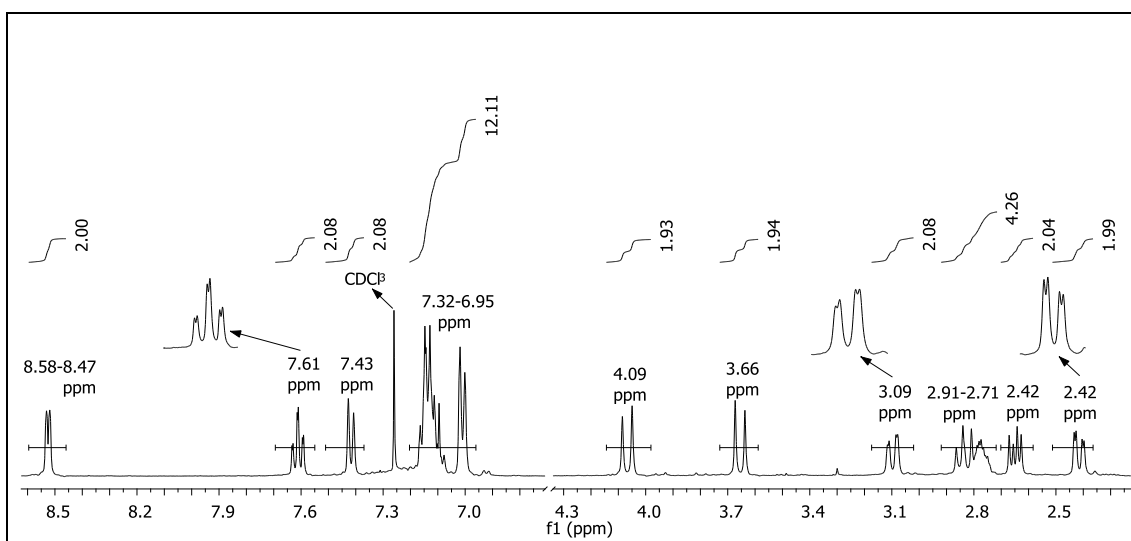
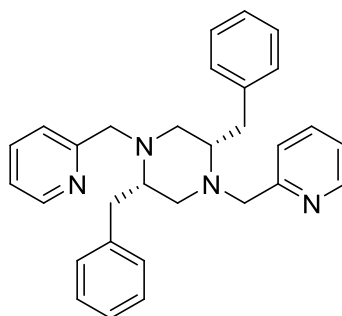
Compound **106** (2.02 g, 4.74 mmol) and formic acid (96%) (20 cm³) were stirred at room temperature for two hours. The resulting acidic solution was reduced in volume under reduced pressure to give a yellow oil. The oil was then recrystallised from a mixture of toluene and 1-butanol, giving a colourless white solid which was air dried, yielding **107** as a colourless fluffy solid (0.82 g, 59%). mp 321-322 °C (toluene/1-butanol); [α]_D²⁵ -160.0 (*c* 0.4, CH₃CO₂H); $\tilde{\nu}_{\max}/\text{cm}^{-1}$ 3203, 1657, 1459, 1338, 698; δ_{H} (400 MHz; TFA-*d*) 7.50-7.34 (6H, m), 7.16 (4H, ap. d, *J* 7.0), 4.61 (2H, dd, *J* 7.4, 3.9), 3.11 (2H, dd, *J* 14.0, 3.9), 2.36 (2H, dd, *J* 14.0, 7.4); δ_{C} (100 MHz; TFA-*d*) 172.8, 140.4, 135.5, 131.8, 131.4, 58.6, 41.6; *m/z* (ESI) 295.1444 (M+H⁺. C₁₈H₁₉N₂O₂⁺ requires 295.1441).

4.30 (2*S*,5*S*)-2,5-dibenzylpiperazine dihydrobromide salt (**108**)



To **107** (0.660 g, 2.24 mmol), dissolved in dimethoxyethane (40 cm³) and under a dry nitrogen atmosphere, was added sodium borohydride (0.550 g, 14.6 mmol) and the mixture was cooled to 0 °C. Titanium tetrachloride (1.38 g, 7.28 mmol) was added dropwise and the mixture allowed to warm to ambient temperature. The mixture was subsequently heated at reflux for 24 hours, after which time it was cooled and carefully added to a distilled water and ice mixture (150 cm³). This was then basified using ammonia solution (28%) to pH 12, causing a white precipitate to form. The mixture was then extracted with dichloromethane (3 x 150 cm³) and the combined organic extracts dried with MgSO₄. The solvent was removed under reduced pressure and the thick, brown oily residue produced dissolved in diethyl ether, which was then cooled to 0 °C, followed by the dropwise addition of HBr (33% in acetic acid) which caused a white precipitate to form. This was collected and washed using diethyl ether giving **108** as a colourless solid (0.74 g, 77%). (mp decomposes >350 °C); $[\alpha]_{\text{D}}^{25}$ 70.6 (*c* 1.0, D₂O); $\tilde{\nu}_{\text{max}}/\text{cm}^{-1}$ 2914, 1454, 967, 735, 697; δ_{H} (400 MHz; D₂O) 7.63-7.34 (10H, m), 4.22-4.04 (2H, m), 3.71-3.50 (4H, m), 3.40-3.22 (4H, m); δ_{C} (100 MHz; D₂O) 133.6, 129.4, 129.3, 128.2, 52.5, 41.3, 34.1; *m/z* (ESI) 267.1857 (M+H⁺. C₁₈H₂₃N₂⁺ requires 267.1783).

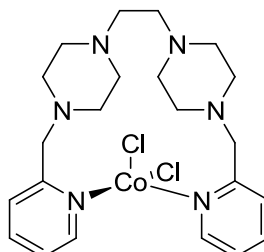
4.31 (2*S*,5*S*)-2,5-Dibenzyl-1,4-bis(pyridin-2-ylmethyl)piperazine (**65**)



To compound **108** (0.770 g, 1.80 mmol), potassium carbonate (2.98 g, 21.6 mmol), 2-chloromethyl pyridine (0.60 g, 3.6 mmol) and potassium iodide (0.03 g, 0.2 mmol) was added acetonitrile (20 cm³) and the mixture heated at reflux for 24 hours. The mixture was cooled to room temperature and the organic solvent removed under reduced pressure. Distilled water was added to the resulting residue and the aqueous solution extracted with dichloromethane (5 x 100 cm³). The combined organic extracts were dried using MgSO₄ and the solvent removed *in vacuo*, giving a red oil. To this was added diethyl ether (150 cm³) and the oil triturated until a solid precipitated. This was removed by filtration and the diethyl ether filtrate concentrated to give a red/orange oil. Further purification by column chromatography on neutral alumina using dichloromethane and methanol (99.999:0.001) as the mobile phase yielded **65** as a light yellow oil (0.22 g, 72%). $[\alpha]_{\text{D}}^{25}$ 40.0 (*c* 0.3, CHCl₃); $\tilde{\nu}_{\text{max}}/\text{cm}^{-1}$ 2815, 1590, 1433, 1165, 732; δ_{H} (400 MHz; CDCl₃; Me₄Si) 8.58-8.47 (2H, m), 7.61 (2H, td, *J* 7.7, 1.7), 7.43 (2H, ap. d, *J* 7.7), 7.32-6.95 (12H, m), 4.09 (2H, d, *J* 14.2), 3.66 (2H, d, *J* 14.2), 3.09 (2H, dd, *J* 12.6, *J* 2.5), 2.91-2.71 (4H, m), 2.64 (2H, dd, *J* 11.7, *J* 5.9), 2.42 (2H, dd, *J*

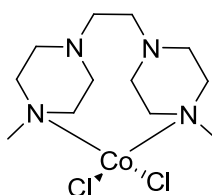
11.7, J 2.9); δ_C (100 MHz; CDCl_3 ; Me_4Si) 159.8, 149.2, 140.2, 136.4, 129.4, 128.3, 125.9, 123.3, 122.0, 61.0, 60.6, 53.6, 34.1; m/z (ESI) 449.2698 ($\text{M}+\text{H}^+$. $\text{C}_{30}\text{H}_{33}\text{N}_4^+$ requires 449.2700).

4.32 Cobalt complex of ligand **67** (**114**)



To a stirring methanolic (10 cm^3) solution of **67** (0.20 g, 0.53 mmol), was added dropwise, $\text{CoCl}_2 \cdot 6\text{H}_2\text{O}$ (0.13 g, 0.54 mmol) dissolved in methanol (5 cm^3) at room temperature. The mixture was heated at reflux with stirring for two hours and the solvent then removed under reduced pressure to produce a blue powder which was collected by filtration and washed with diethyl ether ($5 \times 10\text{ cm}^3$) and then air dried, giving **114** as a blue powder (0.15 g, 54%). mp decomposes $>364\text{ }^\circ\text{C}$; $\tilde{\nu}_{\text{max}}/\text{cm}^{-1}$ 1607, 1574, 1461, 1457, 766, 638; m/z (CI) 510.1467 ($\text{M}+\text{H}^+$. $\text{C}_{22}\text{H}_{33}\text{Cl}_2\text{CoN}_6^+$ requires 510.1470); $\mu_{\text{eff}} = 5.78\ \mu_{\text{B}}$.

4.33 Cobalt complex of ligand **62** (**115**)



To a stirring solution of **3** (0.10 g, 0.45 mmol) in ethanol (5 cm^3), was added dropwise $\text{CoCl}_2 \cdot 6\text{H}_2\text{O}$ (0.11 g, 0.45 mmol) in ethanol (5 cm^3) at room temperature. The mixture was then heated at reflux with stirring for 48 h before the solvent was removed under reduced pressure to produce a blue-green powder. This was collected by filtration and washed with diethyl ether ($5 \times 10\text{ cm}^3$) and then air dried, giving **115** as a blue powder (0.07 g, 47%). mp decomposes $>300\text{ }^\circ\text{C}$; $\tilde{\nu}_{\text{max}}/\text{cm}^{-1}$ 3553, 2963, 2935, 2798, 1456, 1299, 1153; m/z (EI) 355.0865 (M^+ . $\text{C}_{12}\text{H}_{26}\text{Cl}_2\text{CoN}_4^+$

requires 355.0861); $\mu_{\text{eff}} = 4.41 \mu_{\text{B}}$.

4.34 Bleaching catalysis: The primary screening test

A methodology for the primary testing of ligand systems and complexes was devised by Warwick International Ltd. The test was designed to be quick, in order to maximise chances of an initial, positive hit under conditions simulating those found in a typical laundry wash. Other factors considered in the test development included selection of parameters in order to maximise repeatability. The methodology is described as follows:

- A detergent solution was prepared by dissolving IEC-A detergent base (7.50 g) in deionised water (1000 cm³). The mixture was filtered through a sintered funnel under reduced pressure to remove any undissolved solids. Sodium hydroxide (0.66 g) was then added to the solution and the mixture was stirred until the base had dissolved. Only solutions from the same batch were used for one set of tests.
- Ligands were dissolved in deionised water such that their concentrations were 1×10^{-3} M.
- Metal salts used in the test (VCl₃, MnCl₂·4H₂O, FeCl₃, CoCl₂·6H₂O and CuSO₄·5H₂O) were dissolved in deionised water such that their concentrations were 1×10^{-3} M.
- The dye solution was prepared by boiling a commercial 1 g packet of saffron (actually c.a. 0.5 g of saffron) in deionised water (10 cm³) for 5 min. The red/orange liquid was filtered and the saffron strands underwent a second extraction using the same amount of solvent. The filtrates were combined and stored in a refrigerator, in the absence of light. Just before the dye was used, the extract was diluted with 1:1 water: carbonate buffer solution*, making up to 50 cm³ to give the dye solution for testing.

*The carbonate buffer solution was prepared by dissolving sodium hydrogen carbonate (42.0 g) and sodium carbonate (53.0 g) in deionised water (2400 cm³). A few drops of glacial acetic acid were added to adjust the pH to 10.

A set of identical glass jars with screw on tops were numbered and lined up in order. Bottle No.1 was filled with detergent solution (99 cm³). Bottle No.2 was filled with

detergent solution (98 cm³) and metal salt solution (1 cm³). All the remaining bottles were filled with detergent solution (96 cm³), metal salt solution (1 cm³) and the specific ligand solutions (which were assigned to each of the remaining bottles) (2 cm³), including 1,10 phenanthroline as a control. These mixtures were left for 30 min, and the colours of all metal-ligand mixtures noted as this might affect the colours seen on bleaching.

Saffron dye solution (1 cm³) was then added to each bottle and mixed thoroughly. Addition of 36-40 wt% peracetic acid in acetic acid (0.095 cm³) to each bottle, excluding Bottle No. 1 then followed. A stopwatch was started at the same time of the addition of PAA. The tops were then placed on the bottles and the solutions were mixed. The whole set of bottles were monitored at regular intervals and the times of any colour changes of the solutions were noted.

4.35 Bleaching catalysis: Initial stain removal test (Wash-test)

The stain removal tests were carried out at Warwick International Limited using a tergo-tometer machine, Model 72435. Six bleachable stains impregnated on to standardised cotton swatches were selected for these tests (BC2 – coffee stain, BC3 – tea stain for low temperature wash, BC5 – red beet stain, CS8 – grass stain, CS12 – red wine stain, and E114 – blackcurrant stain).

A metal-ligand solution was prepared by mixing the appropriate metal salt and ligand solutions (equivalent to 50 ppm manganese in five grams of formulation) in water at 40 °C (7 L). It was stirred for 30 min before this solution (1 L) was added into each pot. The agitators were set off and a detergent mixture of IEC-A detergent base (4.25 g), uncoated TAED (0.25 g) and PBS (0.50 g) was added followed by two swatches of each stained cloth in each separate pot. The wash was carried out at 40 °C and 150 rpm for 20 min. After the wash cycle, stained swatches were rinsed, ironed and the stain removal results were measured as Z% brightness using a spectraflash-500 spectrophotometer. The stain removal values were plotted in the chart to show the effectiveness of the catalysts.

At the beginning of each day, a blank wash (only IEC-A detergent base (4.25 g) and PBS (1) (0.50 g) in detergent mixture), a TAED (3) wash (using the standard detergent

mixture but no catalyst in washing solution) and a **6** wash were carried out before any metal-ligand systems were tested. The stain removal values of the potential metal-ligand systems were only compared to the three standard washes carried out on the same day.

Table 12. Percentage stain removal values for washes with ligands **67**, **69**, **77** and **89** in combination with $\text{CoCl}_2 \cdot 6\text{H}_2\text{O}$ (1:1) including comparable standard washes

Wash	Coffee	Tea	Red Beet	Grass	Blackcurrant	Red Wine
Perborate Blank (1)	31.2	23.9	47.4	74.1	27.6	36.3
TAED Blank (3)	33.5	32.1	50.8	72.2	42.2	48.9
Catalyst 6	50.0	51.4	55.1	75.3	35.9	51.9
Ligand 67	30.4	24.3	41.4	65.8	25.7	45.7
Ligand 69	28.8	22.7	39.8	65.5	25.2	35.0
Ligand 77	27.4	25.4	39.6	66.2	26.0	33.8
Ligand 89	31.3	24.6	42.7	69.1	26.3	36.1

4.36 Epoxidation catalysis: Method A

The manganese salt (MnSO_4 or $\text{Mn}(\text{CF}_3\text{SO}_3)_2$) (5 mol% to alkene) was added to a stirring solution of ligand (1.1 eq. to manganese salt) dissolved in acetonitrile (8.5 cm^3). This was allowed to stir for 1 hour at room temperature in air after which time *p*-chlorostyrene dissolved in acetonitrile (1 M) (0.5 mmol, 500 μl) was added, followed by the internal standard naphthalene which was dissolved in acetonitrile (0.2 M) (0.1 mmol, 500 μl). A baseline sample[†] was taken at this stage for quantitative analysis of the reaction progress and analysed by HPLC[‡]. The reaction was started by the dropwise addition of peracetic acid (36-40 wt% in acetic acid) (0.95 cm^3) which was added over 30 minutes.

[†] Sampling of the reactions was carried out by removal of a 50 μl aliquot of the reaction mixture which was quenched by dilution in ice-cold acetonitrile (2 cm^3). This sample was then passed through a celite and neutral alumina plug prior to HPLC analysis of the samples.

[‡] The HPLC analyses were performed using a series 200 Perkin Elmer chromatographic system which included an autosampler, a thermostatic column compartment and a UV-Vis detector.

The chromatographic separations were carried out on Chiralpak AS-RH column (amylose tris-((*S*)-methylbenzylcarbamate)) coated on silica gel. The mobile phase composition consisted of acetonitrile/water (50/50, *v/v*) delivered at a flow rate of 0.5 ml min⁻¹ in isocratic elution mode. The column was maintained at 30 °C during analysis and the samples were introduced using a 1 µl injection volume and detections recorded at 228 nm.

Method B

The ligand was stirred in a pH 11 buffer (sodium bicarbonate/sodium hydroxide) (4.5 cm³) for 30 minutes at room temperature prior to the addition of the appropriate manganese salt (MnSO₄ or Mn(CF₃SO₃)₂) and acetonitrile (4 cm³). The procedure followed after this was the same as that described for method A. Also the sampling technique and HPLC analysis was the same as in method A.

4.37 Single crystal X-ray diffraction data

For **67**, **98** and **102** colourless (block) crystals, with approximate dimensions as indicated in Table 13 and 14 were chosen for diffraction study. Data were collected at the temperatures shown below (Table 13 and 14) using a Nonius Kappa CCD area detector diffractometer mounted at the window of a molybdenum rotating anode (50 KV, 85 mA, $\lambda=0.71073$ Å). The crystal-to-detector distance was 30 mm and ϕ and Ω scans (1.0° increments, 20 s exposure time) were carried out to fill the Ewald sphere. Data collection and processing were carried out using DirAx,¹⁷ COLLECT,¹⁸ DENZO¹⁹ and an empirical absorption correction was applied using SADABS.²⁰ The structure was solved by the heavy-atom method using the DIRDIF99²¹ program, refined anisotropically (non-hydrogen atoms) by full-matrix least-squares on F² using the SHELXL-97²² program. The programs ORTEP-3²³ and PLATON²⁴ were used for drawing the molecules.

For **116**, the intensity data were collected on a CAD-4 diffractometer and Mo K α radiation (λ 0.71069 Å) using ω -2 θ scan at 293K. The unit cell parameters were determined by least-squares refinement on 25 automatically centred reflections²⁵ (10.01 $\leq \theta \leq$ 13.93°). All data were corrected for absorption by empirical methods (ψ scan)²⁶

and for Lorentz-polarization effects by XCAD4.²⁷ The structure was solved by Direct method using SHELXS-97²² program, refined anisotropically (non-hydrogen atoms) by full-matrix least-squares on F^2 using SHELXL-97²² program. The H atoms were calculated geometrically and refined with a riding model. The programs ORTEP-3²³ and PLATON²⁴ were used for drawing the molecules.

Table 13. Crystal data and structure refinement for **67** and **98**

	67	98
Empirical formula	C ₂₂ H ₃₂ N ₆	C ₂₁ H ₂₉ N ₃ O ₄ S ₂
Formula weight	380.54	451.59
Temperature/ K	120(2)	293(2)
Wavelength/ Å	0.71073	0.71073
Crystal system	Monoclinic	Monoclinic
Space group	P2 ₁ /c	P2 ₁ /c
Unit cell dimensions	a = 5.8941(3) Å α = 90° b = 13.8775(9) Å β = 94.689(4)° c = 12.7582(7) Å γ = 90°	a = 16.1770(6) Å α = 90° b = 10.1889(3) Å β = 113.655(2)° c = 14.9298(5) Å γ = 90°
Volume/ Å ³	1040.07(10)	2254.05(13)
Z	2	4
Density (Calculated) /mg m ³	1.215	1.331
F(000)	412	960
Absorption coefficient/ mm ⁻¹	0.075	0.268
Crystal size/ mm	0.20 x 0.10 x 0.06	0.37 x 0.23 x 0.15
Theta range/ °	3.34 to 27.68	3.12 to 27.58
Index ranges	-7<=h<=7, -16<=k<=18, -16<=l<=16	-20<=h<=20, -13<=k<=12, -19<=l<=19
Reflections collected	14403	32243
Independent reflections	2403 [R(int) = 0.0926]	5161 [R(int) = 0.0685]
Completeness to theta = 27.68°	98.7%	98.9%
Max. and min. transmission	0.9955 and 0.9851	-
Refinement method	Full-matrix least-squares on F ²	Full-matrix least-squares on F ²
Data/ restraints/ parameters	2403/ 0/ 128	5161/ 0/ 275
Goodness of fit on F ²	1.013	1.001
Final R indices [I>2sigma(I)]	R1 = 0.0617, wR2 = 0.1542	R1 = 0.0493, wR2 = 0.1256
R indices (all data)	R1 = 0.1152, wR2 = 0.1909	R1 = 0.0762, wR2 = 0.1410
Extinction coefficient	0.017(6)	0.0069(19)
Largest diff. peak and hole	0.275 and -0.260 e.Å ⁻³	

Table 14. Crystal data and structure refinement for **102** and **116**

	102	116
Empirical formula	C ₁₉ H ₃₁ N ₃ O ₂ S	C ₁₂ H ₂₈ Cl ₄ Co N ₄
Formula weight	365.53	429.11
Temperature/ K	120(2)	293(2)
Wavelength/ Å	0.71073	0.71073
Crystal system	Monoclinic	Monoclinic
Space group	P2 ₁	A2/n
Unit cell dimensions	a = 12.4967(3) Å	a = 18.276(7) Å
	α = 90°	α = 90°
	b = 6.26130(10) Å	b = 8.7762(10) Å
	β = 108.8990(10)°	β = 101.11(2)°
	c = 13.5289(4) Å	c = 12.529(7) Å
	γ = 90°	γ = 90°
Volume/ Å ³	1001.51(4)	1971.9(14)
Z	2	4
Density (Calculated) /mg m ³	1.212	1.445
F(000)	396	892
Absorption coefficient/ mm ⁻¹	0.178	1.411
Crystal size/ mm	0.42 x 0.40 x 0.32	0.30 x 0.20 x 0.20
Theta range/ °	3.29 to 27.51	2.85 to 26.97
Index ranges	-16 ≤ h ≤ 16, -8 ≤ k ≤ 8,	-23 ≤ h ≤ 22, -3 ≤ k ≤ 11,
	-17 ≤ l ≤ 17	0 ≤ l ≤ 15
Reflections collected	15662	2294
Independent reflections	4579 [R(int) = 0.0421]	2137 [R(int) = 0.0084]
Completeness to theta = 27.68°	99.%	99.4%
Max. and min. transmission	0.9451 and 0.9288	0.7656 and 0.6769
Refinement method	Full-matrix least-squares on F ²	Full-matrix least-squares on F ²
Data/ restraints/ parameters	4579/ 1/ 230	2137/ 0/ 97
Goodness of fit on F ²	1.049	0.913
Final R indices [I > 2σ(I)]	R1 = 0.0382, wR2 = 0.0854	R1 = 0.0512, wR2 = 0.1053
R indices (all data)	R1 = 0.0468, wR2 = 0.0896	R1 = 0.1498, wR2 = 0.1292
Absolute structure parameter	0.03(6)	-
Extinction coefficient	0.040(4)	-
Largest diff. peak and hole	0.215 and -0.250 e.Å ⁻³	0.591 and -0.369 e.Å ⁻³

4.38 References

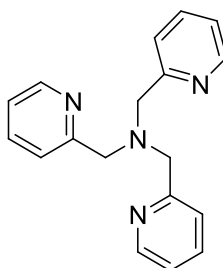
1. G. H. Searle and R. J. Geue, *Aust. J. Chem.*, 1984, **37**, 959-970.
2. S. Fujii, *Nippon Kagaku Kaishi*, 1974, 342-343.
3. F. G. Mann and F. C. Baker, *J. Chem. Soc.*, 1957, 1881-1899.
4. (a) G. Caliendo, R. Di Carlo, G. Greco, R. Meli, E. Novellino, E. Perissutti and V. Santagada, *Eur. J. Med. Chem.*, 1995, **30**, 77-84; (b) H. L. Yale, A. I. Cohen and F. Sowinski, *J. Med. Chem.*, 1963, **6**, 347-350.
5. (a) H. T. Clarke, H. B. Gillespie and S. Z. Weisshaus, *J. Am. Chem. Soc.*, 1933, **55**, 4571-4587; (b) W. Eschweiler, *Chem. Ber.*, 1905, **38**, 880-892.
6. R. Herges, A. Dikmans, U. Jana, F. Köhler, P. G. Jones, I. Dix, T. Frickle and B. König, *Eur. J. Org. Chem.*, 2002, 3004-3014.
7. H. K. Hall Jr., *J. Am. Chem. Soc.*, 1956, **78**, 2570-2572.
8. O. R. Thiel, C. Bernard, T. King, M. Dilmeghani-Seran, T. Bostick, R. D. Larsen and M. M. Faul, *J. Org. Chem.*, 2008, **73**, 3508-3515.
9. H. W. Stewart, R. J. Turner, J. J. Denton, S. Kushner, L. M. Brancone, W. L. McEwen, R. I. Hewitt and Y. Subbarow, *J. Org. Chem.*, 1948, **13**, 134-143.
10. S. R. Koepke, R. Kupper and C. J. Michejda, *J. Org. Chem.*, 1979, **44**, 2718-2722.
11. E. Carceller, M. Merlos, M. Giral, C. Almansa, J. Bartrolí, J. García-Rafanell and J. Forn, *J. Med. Chem.*, 1993, **36**, 2984-2997.
12. H. Tsukube, K. Yamashita, T. Iwachido and M. Zenki, *J. Chem. Soc., Perkin Trans. 1*, 1991, 1661-1665.
13. (a) P. Mucha, G. Mlostoń, M. Jasiński, A. Linden and H. Heimgartner, *Tetrahedron: Asymmetry*, 2008, **19**, 1600-1607; (b) F. Galsbøl, P. Steenbøl and S. Sørensen, *Acta. Chem. Scand.*, 1972, 3605-3611.
14. M. Kaik and J. Gawroński, *Tetrahedron: Asymmetry*, 2003, **14**, 1559-1563.
15. Chao-shan Da, Zhi-jian Han, M. Ni, F. Yang, Da-xue Liu, Yi-feng Zhou and R. Wang, *Tetrahedron: Asymmetry*, 2003, **14**, 659-665.
16. I. O. Donkor and M. L. Sanders, *Bioorg. Med. Chem. Lett.*, 2001, **11**, 2647-2649.
17. A. J. M. Duisenberg, *J. Appl. Crystallogr.*, 1992, **25**, 92-96.
18. R. Hooft and B.V. Nonius, *Collect Data collection and processing user interface: Collect: Data collection software*, 1998.

19. Otwinowski and W. Minor., Denzo Data collection and processing software: Methods in Enzymology, C.W. Carter, Jr and R.M. Sweet, Eds., Academic Press, *Macromolecular Crystallography, Part A*, 1997, **276**, 307-326.
20. Sheldrick, G. M. (2007). SADABS. Version 2007/2. Bruker AXS Inc., Madison, Wisconsin, USA.
21. P. T. Beurskens, G. Beurskens, W. P. Bosman, R. de Gelder, S. Garcia-Granda, R. O. Gould, R. Israel, J. M. M. Smits, DIRDIF99: a program system, Crystallography Laboratory, University of Nijmegen, The Netherlands, 1999.
22. G. M. Sheldrick, *Acta. Crystallogr., Sect. A*, 2008, **64**, 112-122.
23. L. J. Farrugia, ORTEP-3 for Windows, *J. Appl. Cryst.*, 1997, **30**, 565.
24. A. L. Spek, PLATON: A Multipurpose Crystallographic Tool, Utrecht University, Utrecht, The Netherlands, 1998.
25. Enraf-Nonius CAD-4/PC Software. Version 1.5c 1994 Enraf-Nonius, Delft, The Netherlands.
26. A. C. T. North, D. C. Phillips and F.S. Mathews, *Acta Crystallogr., Sect. A*, 1968, **42**, 351-359.
27. Harms, K. XCAD4. Program for data reduction. 1996 Philipps-Universität, Marburg, Germany.

Appendix 1

The following compounds were synthesised in the early stages of the research project and they were also tested using the primary screening test and this represents the work undertaken during the first year of the research. However, this line of enquiry had to be abandoned due to pressure from my industrial sponsors and this was caused by a change in their circumstances. The work described above represents the research carried subsequent to this set-back. The experimental that follows is in draft form and characterisation in most cases is incomplete. Furthermore, the numbering is not consistent with the rest of thesis or throughout this section. However, it is included as a guide of the early work that was carried out.

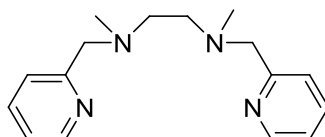
Synthesis of Tris-pyridin-2-ylmethyl-amine (15)



Ligand **15** was synthesised by a literature method which was a modification of a procedure described by Anderegg et al. A solution of (6.41 g, 39.0 mmol) of 2-picolyl chloride hydrochloride in deionized water (16 cm³) was cooled to 0 °C in an ice bath. To this solution was added, with stirring, an aqueous solution of NaOH (7.40 cm³, 5.30 M). Neutralisation results in the free amine appearing as a bright-red emulsion. To this mixture was then added a solution of 2-(aminomethyl)pyridine (2.10 g, 19.0 mmol) in dichloromethane (33 cm³). The mixture was then allowed to warm to room temperature and, over a 48 hour period, a NaOH solution (7.40 cm³, 5.30 M) was added. During addition of the NaOH solution, the pH of the aqueous portion of the reaction mixture was not allowed to exceed 9.5. The crude mixture was then washed with a solution of 15% NaOH, and the organic phase was dried with MgSO₄ and filtered. Removal of the dichloromethane solvent yielded a brown solid mass which was extracted with boiling diethyl ether (3 x 20 cm³). Evaporation of the ether extracts yielded yellow crystals of **15**. The ligand was purified by recrystallization from diethyl ether to give pure **15** as a

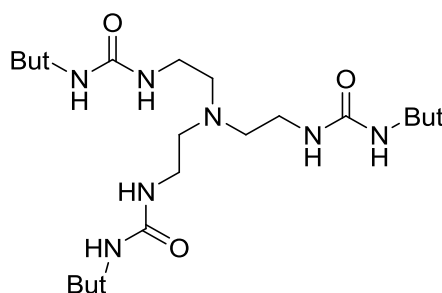
white a crystalline solid (4.30 g, 77%), mp 85-86 °C (diethyl ether); δ_H (270 MHz; CD₃CN; Me₄Si) 8.48-8.45 (3H, m), 7.70 (3H, td, J 7.6, J 1.8), 7.56 (3H, ap. d, J 7.9), 3.79 (6H, s); δ_C (67.9 MHz; CD₃CN) 160.5, 149.9, 137.3, 123.7, 122.9, 60.8.

Synthesis of *N,N'*-Dimethyl-*N,N'*-bis-pyridin-2-ylmethyl-ethane-1,2-diamine (**17**)



Ligand **17** was prepared by a literature method which was a modification of the synthetic route proposed by Toftlund. To an aqueous solution (20 cm³) of *N,N'*-dimethylethane-1,2-diamine (0.90 g, 10 mmol) was added 2-picolyl chloride hydrochloride (3.35 g, 20.4 mmol) dissolved in water (20 cm³). After mixing, 4.50 equivalents of sodium hydroxide (1.83 g, 46.0 mmol) were added. After refluxing for 1 hour at 70 °C, the organic phase was extracted with toluene (5 x 20 cm³) and dried with MgSO₄. The toluene was removed under reduced pressure yielding **17** as a yellow oil (2.76 g, 67%); δ_H (270 MHz; CDCl₃; Me₄Si) 8.45-8.43 (2H, m), 7.54 (2H, td J 7.7, J 1.7), 7.33 (2H, ap. d, J 7.9), 7.07-7.03 (2H, m), 3.60 (4H, s), 2.56 (4H, s), 2.19 (6H, s); δ_C (67.9 MHz; CDCl₃; Me₄Si) 159.5, 149.1, 136.3, 123.0, 121.9, 64.3, 55.6, 43.0.

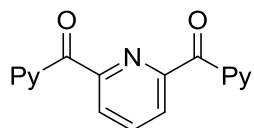
Synthesis **21**.



To a stirring solution of tris(2-aminoethyl)amine (0.78 g, 5.4 mmol) in dry THF (60 cm³) was added dropwise *tert*-butyl-isocyanate (1.60 g, 16.0 mmol). The mixture was then allowed to stir at room temperature for ~1 hour, with the product beginning to precipitate after 0.5 hours. The product was collected on a sintered funnel and washed with diethyl ether (5 x 5 cm³) and allowed to air dry giving the **21** as a white powder

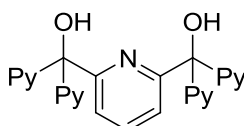
(1.20 g, 51 %), mp (diethyl ether); δ_H (270 MHz; $((CD_3)_2SO)$) 5.73-5.69 (6H, m), 3.05-2.90 (6H, m), 2.42-2.37 (6H, m), 1.21 (27H, s);

Synthesis of (6-(Pyridine-2-carbonyl)-pyridin-2-yl)-pyridin-2-yl-methanone (5)



A THF (anhydrous) solution (200 cm³) of 2-bromopyridine (7.91 g, 50.1 mmol) was cooled to -78 °C and *n*-BuLi (20 cm³, 100.00 mmol (2.5 M in hexane)) was added dropwise keeping the temperature below -55 °C. The dropwise addition of pyridine-2,6-dicarboxylic acid diethyl ester (5.59 g, 25.0 mmol) dissolved in THF (100 cm³) took place thereafter, keeping the temperature at -78 °C. The reaction was quenched using methanol (100 cm³), then allowed to reach R.T, followed by the addition of 10% HCl (200 cm³). The organic solvents were then removed under reduced pressure. The resulting acidic solution was first washed with DCM then basified to pH 12 to 14 using sodium hydroxide pellets. The basic aqueous solution was then extracted using DCM (5 x 100 cm³) and the combined organic extracts were dried using MgSO₄. Removal of the organic solvents under reduced pressure resulted in a brown oily solid. This was titrated in diethyl ether, overnight, yielding **5** as a light brown powder (4.78 g, 66%); mp 135-136 °C; ν_{max}/cm^{-1} 3020, 1675, 1580, 1499; δ_H (270 MHz; CDCl₃; Me₄Si) 8.73 (2H, ap. d, *J* 4.4), 8.30 (2H, ap. d, *J* 7.6), 8.29-8.07 (3H, m) 7.77 (2H, td, *J* 7.7 and 1.7), 7.46-7.41 (2H, m); δ_C (67.9 MHz; CDCl₃; Me₄Si) 191.8, 153.7, 153.4, 149.3, 137.3, 136.5, 127.5, 126.4, 126.2.

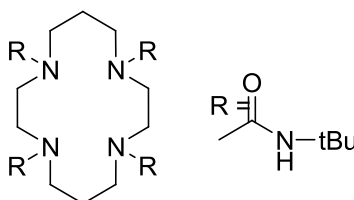
Synthesis(6-(Hydroxy-di-pyridin-2-yl-methyl)-pyridin-2-yl)-di-pyridin-2-yl-methanol (4)



A THF (anhydrous) solution (100 cm³) of 2-bromopyridine (4.15 g 26.3 mmol) was cooled to -78 °C and *n*-BuLi (10.50 cm³, 26.30 mmol (2.5 M in hexane)) was added

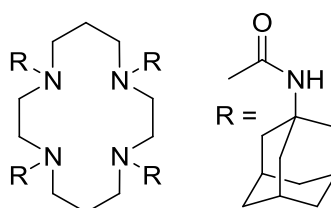
dropwise to keep the temperature below $-55\text{ }^{\circ}\text{C}$. This was followed by the slow addition of a THF solution (25 cm^3) of **5** (3.80 g, 13.1 mmol) at $-78\text{ }^{\circ}\text{C}$. The reaction was then quenched using MeOH (25 cm^3) then allowed to reach R.T followed by the addition of 10% HCl (50 cm^3). The organic solvents were removed and the resulting acidic solution was washed using DCM then basified using sodium hydroxide pellets to pH 12 to 14. This basic solution was extracted using DCM ($5 \times 50\text{ cm}^3$) and the combined organic fractions were dried using MgSO_4 and the solvent was removed under reduced pressure, leaving a yellow crystalline solid as product (2.61 g, 47%); δ_{H} (270 MHz; CDCl_3 ; Me_4Si) 8.50-8.45 (4H, m), 7.71 (2H, s), 7.55-7.34 (9H, m), 7.18-7.09 (6H, m).

Synthesis of 1,4,8,11-tetraaza-Cyclotetradecane-1,4,8,11-tetracarboxylic acid tetrakis-tert-butylamide (7)



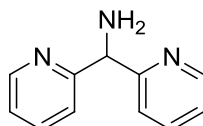
To a stirring solution of cyclam (0.25 g, 1.3 mmol) in dry THF (20 cm^3) was added dropwise *t*-butyl-isocyanate (0.49 g, 5.0 mmol). The mixture was then allowed to stir at room temperature for ~ 1 hour, with the product beginning to precipitate after 0.5 hours. The product was collected on a sintered funnel and washed with diethyl ether ($5 \times 5\text{ cm}^3$) and allowed to air dry giving the product **7** as a white powder (0.67 g, 90%); mp $229\text{-}230\text{ }^{\circ}\text{C}$ (diethyl ether); $\nu_{\text{max}}/\text{cm}^{-1}$ 3352, 3317, 2966, 3074, 1628; δ_{H} (400 MHz; CDCl_3 ; Me_4Si) 4.80 (4H, br s), 3.31 (16H, s), 1.68 (4H, qui, J 7.0), 1.26 (36H, s); δ_{C} (100 MHz; CDCl_3 ; Me_4Si) 157.7, 51.2, 50.4, 47.0, 29.8, 27.8; m/z (ESI) 597.4803 ($\text{M}+\text{H}^+$. $\text{C}_{30}\text{H}_{61}\text{N}_8\text{O}_4^+$ requires 597.4810).

Synthesis of 1,4,8,11-tetraaza-Cyclotetradecane-1,4,8,11-tetracarboxylic acid tetrakis-adamantan-1-ylamide (8)



To a stirring solution of cyclam (0.07 g, 0.35 mmol) in dry THF (10 cm³) was added dropwise 1-adamantyl isocyanate (0.25 g, 1.40 mmol) dissolved in dry THF (10 cm³). The mixture was then allowed to stir at room temperature for ~1 hour, with the product beginning to precipitate shortly after addition of the isocyanate is completed. The product was collected on a sintered funnel and washed with diethyl ether (5 x 5 cm³) and allowed to air dry giving **8** as a white powder (0.28 g, 89%); mp 180 °C, decomposes (diethyl ether); $\nu_{\max}/\text{cm}^{-1}$ 2905, 2847, 1643; δ_H (400 MHz; CDCl₃; Me₄Si) 4.64 (4H, s), 3.35 (16H, s), 2.10-1.82 (36H, m), 1.82-1.54 (28H, m); δ_C (100 MHz; CDCl₃; Me₄Si) 157.1, 51.3, 50.5, 47.0, 42.5, 36.5, 29.6, 27.6; m/z (ESI) 909.6689 (M+H⁺. C₃₀H₆₁N₈O₄⁺ requires 909.6688).

Synthesis of *C,C*-Di-pyridin-2-yl-methylamine (**15**)

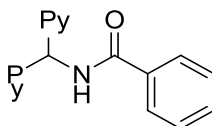


A stirring mixture of **13** (1.88 g, 10.2 mmol), hydroxylamine hydrochloride (0.850 g, 12.3 mmol), sodium bicarbonate (1.03 g, 12.3 mmol), methanol (8 cm³) and distilled water (8 cm³) were allowed to reflux for 0.5 hours. After allowing the vessel to cool to R.T, the methanol was removed under reduced pressure. The remaining aqueous layer was observed to rapidly precipitate out as a pink solid, simultaneously absorbing all the liquid. The pink solid was then transferred to a sintered funnel and washed with water (3 x 50 cm³) and allowed to air dry. The pink solid obtained (1.83 g, 90%), was assumed to be the intermediate oxime (**14**), and was taken to the next transformation without characterisation.

To **14** (1.83 g, 9.10 mmol) was added ammonium hydroxide (25 cm³), methanol (8 cm³) and zinc dust (2.00 g). This was refluxed at 55 to 60 °C for 16 hours. The reaction vessel was allowed to cool to ambient temperature and the organic solvent removed under reduced pressure. The remaining aqueous phase was extracted with DCM (5 x 50 cm³), and the combined organic extracts were dried using MgSO₄ with the solvent removed under reduced pressure, leaving the product amine, **15** as a clear yellow oil (1.29 g, 76%); δ_H (270 MHz; CDCl₃; Me₄Si) 8.49-8.40 (2H, m), 7.50 (2H, td, *J* 7.7, *J*

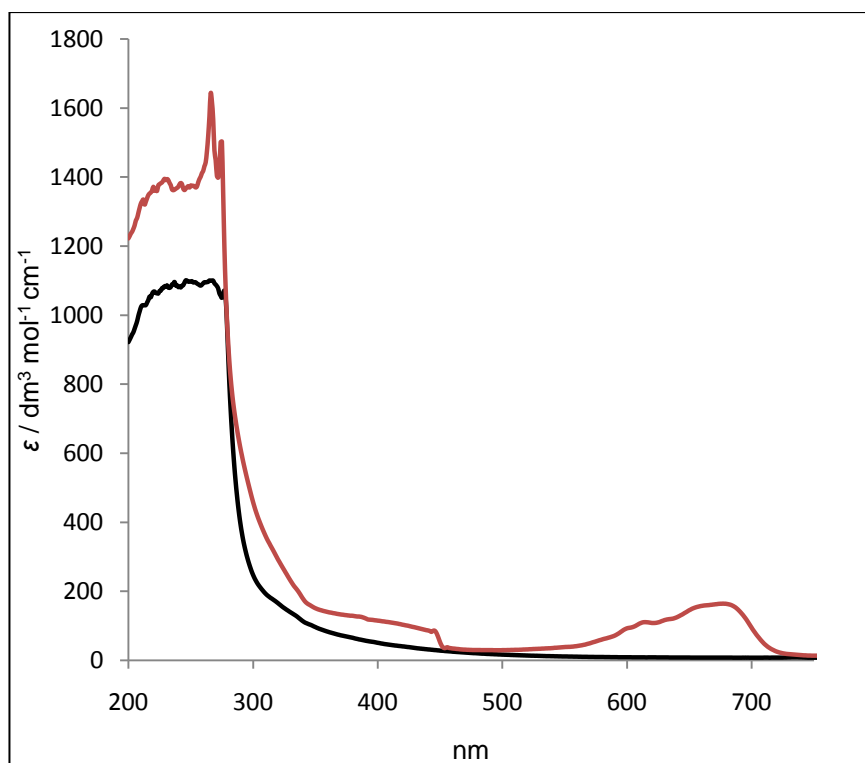
1.7), 7.34-7.22 (2H, m), 7.08-6.93 (2H, m), 5.22 (1H, s), 2.39 (2H, s); δ_C (67.9 MHz; CDCl₃; Me₄Si) 162.8, 149.2, 136.6, 122.1, 121.8, 62.4;

Synthesis of *N*-(Di-pyridin-2-yl-methyl)-benzamide (**10**)

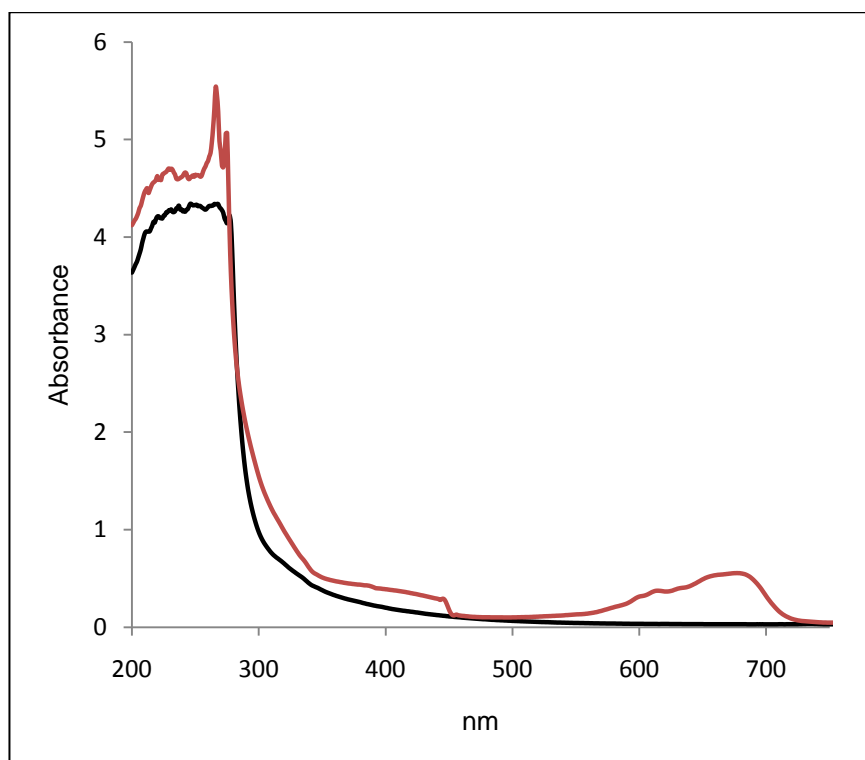


To a stirring solution containing benzoyl chloride (0.69 g, 4.91 mmol) and triethylamine (0.60 g, 5.89 mmol) dissolved in THF (12 cm³) was added, slowly, **15** (0.91 g, 4.9 mmol) dissolved in THF (8 cm³) at 0 °C. This mixture was heated to 60 °C for 0.5 hours, and then cooled back to 0 °C, whereupon the salt Et₃N.HCl precipitated out and was removed by filtration. The THF was then removed under reduced pressure leaving an orange coloured solid, which was redissolved in DCM and washed with sodium hydroxide (saturated solution). The organic layer was then, dried with MgSO₄ and the solvent removed under reduced pressure. The resulting solid was then recrystallised from hot methanol giving the product as a crystalline solid (0.92 g, 65%); $\nu_{\max}/\text{cm}^{-1}$ 3417, 3050, 1659; δ_H (270 MHz; CDCl₃; Me₄Si) 8.82-8.70 (1H, m), 8.59-8.51 (2H, m), 7.98-7.91 (2H, m), 7.64 (2H, td, *J* 7.7, *J* 1.7), 7.55-7.40 (5H, m), 7.20-7.10 (2H, m), 6.40 (1H, d, *J* 6.4); δ_C (67.9 MHz; CDCl₃; Me₄Si), 166.7, 159.0, 149.3, 137.0, 134.3, 131.7, 128.6, 127.4, 122.6, 122.3, 59.4; *m/z* (ESI) 290.1288 (M+H⁺. C₁₈H₁₆N₃O⁺ requires 290.1288).

Appendix 2

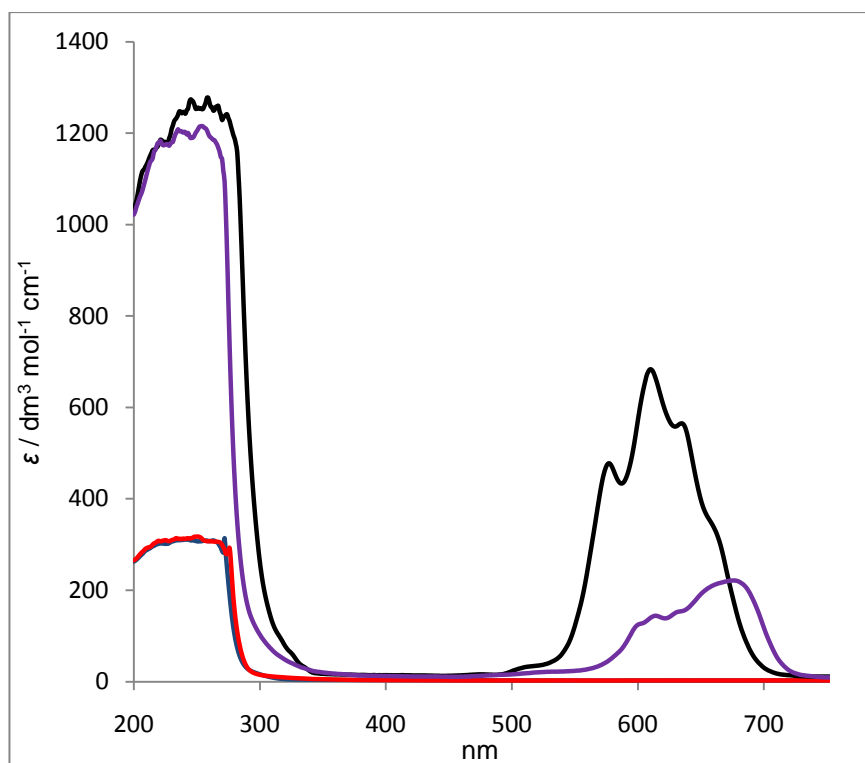


UV-Vis absorption plots (ϵ vs wavelength) for DMSO solutions of ligand **67** (black) and **114** (red) at concentrations of 3.94×10^{-3} and $3.37 \times 10^{-3} \text{ mol dm}^{-3}$ respectively (1 cm cell used)

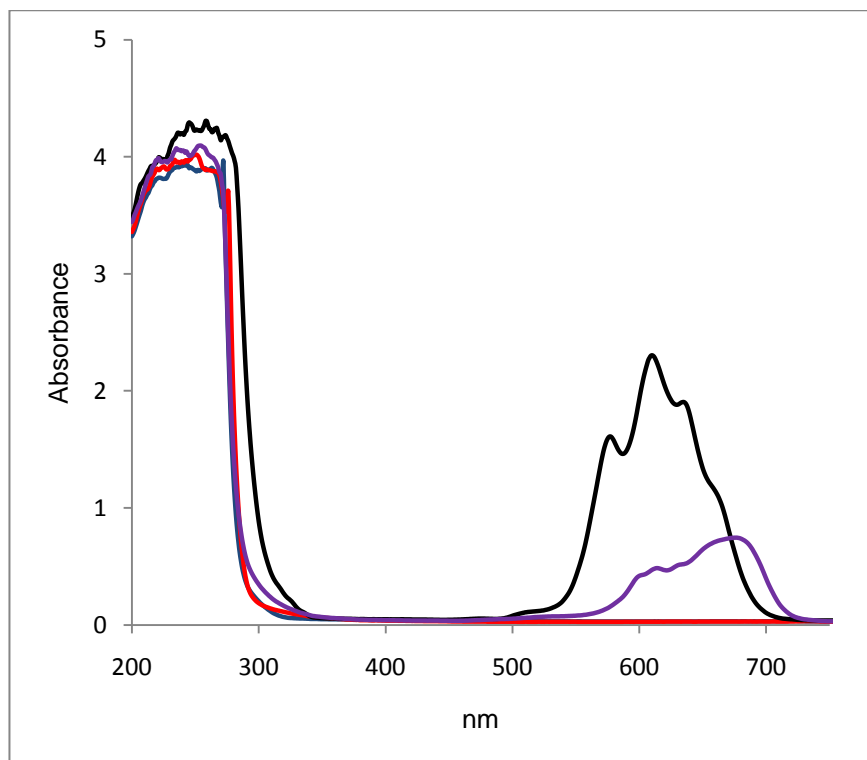


UV-Vis spectra for DMSO solutions of ligand **67** (black) and **114** (red) at concentrations of 3.94×10^{-3} and $3.37 \times 10^{-3} \text{ mol dm}^{-3}$ respectively (1 cm cell used)

Appendix 3



UV-Vis absorption plots (ϵ vs wavelength) for pyridine dissolved in dichloromethane (blue), pyridine dissolved in DMSO (red), **113** dissolved in DMSO (purple) and **113** dissolved in DCM (black) at concentrations of 1.26×10^{-2} , 1.26×10^{-2} , 3.37×10^{-3} and $3.37 \times 10^{-3} \text{ mol dm}^{-3}$ respectively (1 cm cell used)



UV-Vis spectra for pyridine dissolved in dichloromethane (blue), pyridine dissolved in DMSO (red), **113** dissolved in DMSO (purple) and **113** dissolved in dichloromethane (black) at concentrations of 1.26×10^{-2} , 1.26×10^{-2} , 3.37×10^{-3} and 3.37×10^{-3} mol dm⁻³ respectively (1 cm cell used)